The Thesis Committee for Greta Hoe Wells
Certifies that this is the approved version of the following thesis:

Timeline Reconstruction of Holocene Jökulhlaups along the Jökulsá á Fjöllum Channel, Iceland

APPROVED BY
SUPERVISING COMMITTEE:

Supervisor:

Sheryl Luzzadder-Beach

Timothy P. Beach

Daene C. McKinney

Timeline Reconstruction of Holocene Jökulhlaups along the Jökulsá á Fjöllum Channel, Iceland

by

Greta Hoe Wells, B.A.

Thesis

Presented to the Faculty of the Graduate School of

The University of Texas at Austin

in Partial Fulfillment

of the Requirements

for the Degree of

Master of Arts

The University of Texas at Austin

May 2016

Abstract

Timeline Reconstruction of Holocene Jökulhlaups along the Jökulsá á Fjöllum Channel, Iceland

Greta Hoe Wells, M.A.

The University of Texas at Austin, 2016

Supervisor: Sheryl Luzzadder-Beach

The Jökulsá á Fjöllum is Iceland's second longest river, draining from the Vatnajökull ice cap and winding for over 200 km through the eastern highlands before emptying into the Arctic Ocean. Hydrothermal activity and subglacial eruptions beneath Vatnajökull generate enormous quantities of meltwater, which can drain catastrophically in outburst floods, known as jökulhlaups. Jökulhlaups have flowed through the Jökulsá á Fjöllum channel throughout the Holocene, but intense debate exists over their timing and magnitude. While previous studies report a peak flood discharge of 0.9×10^6 m^3 s^{-1}, Howard et al. (2012) found evidence of a peak discharge of 2.2×10^7 m^3 s^{-1}, which would make this the largest known flood on Earth. This project seeks to test Howard et al.'s (2012) hypothesis and, more broadly, to reconstruct a timeline of Holocene jökulhlaups

along the Jökulsá á Fjöllum. First, it reviews current literature and research on Icelandic geology and megafloods; second, it reviews and critiques previous research methods and evidence of Holocene jökulhlaups along the channel, while also presenting new geomorphologic and geochronological evidence from field work in August 2015; and finally, it sets up a framework for future research and explores unanswered questions regarding the history of Holocene jökulhlaups along the Jökulsá á Fjöllum.

Table of Contents

List of Figures

INTRODUCTION

The Jökulsá á Fjöllum river winds through a desolate landscape in northeastern Iceland that has been sculpted by nearly every geologic force. From its source at the Vatnajökull ice cap to its mouth at the Arctic Ocean 206 km later, Iceland's second-longest river slices across the highlands, snaking around mountains and carving through basalt bedrock and lava flows (Figure 1) (Howard et al., 2012).

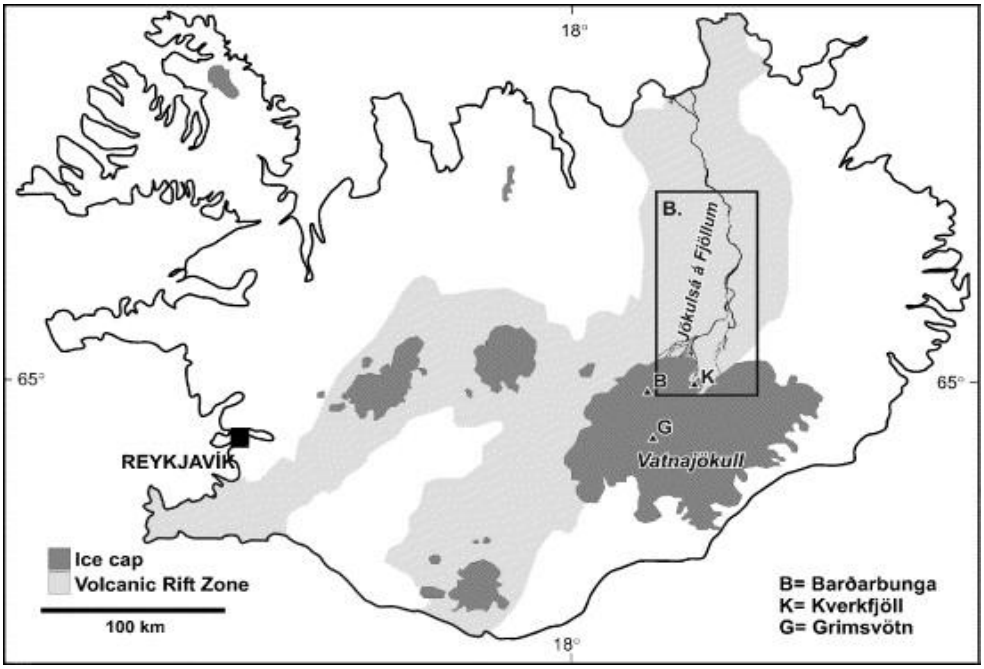

Figure 1. Course of the Jökulsá á Fjöllum from Vatnajökull to the Arctic Ocean (modified from Alho et al., 2005).

Vatnajökull overlies one of Iceland's most tectonically active areas: the meeting point of the Mid-Atlantic Ridge spreading center and a mantle hotspot (Sigmundsson, 2006). This intense volcanic and geothermal activity, as well as the relatively warm climate of the North Atlantic, generates enormous quantities of meltwater, which is often stored in subglacial lakes that form in depressions, such as calderas (Björnsson, 2002; Björnsson and Pálsson, 2008).

When these lakes overflow or their ice dams fail, the water may drain catastrophically in outburst floods, known as jökulhlaups (Björnsson, 2002). Since deglaciation in the early Holocene, jökulhlaups have drained from Vatnajökull through the Jökulsá á Fjöllum channel, leaving behind a landscape of megaflood erosional and depositional features imprinted on antecedent flood, glacial, fluvial, volcanic, and aeolian landforms (Howard et al., 2012).

Several studies have tried to reconstruct a timeline of these jökulhlaups, but they report conflicting results of flood timing and magnitude. Most studies conclude that the largest Holocene jökulhlaup in the Jökulsá á Fjöllum channel had a peak discharge of 0.9×10^6 m^3 s^{-1}, ranking it among the largest floods on Earth (Alho et al., 2005). Howard et al. (2012), however, found evidence suggesting a jökulhlaup with a peak discharge of 2.2×10^7 m^3 s^{-1}, which would make this the largest known flood in Earth history.

Howard et al.'s (2012) claim has been hotly contested on the grounds that Vatnajökull could not have generated a flood this large. Yet this assumption falls into a trap that has ensnared many of science's great ideas over the past centuries. Scientific history has shown us the danger of forcing geologic explanations to conform to existing laws and theories; instead, it has urged us to follow William Morris Davis's advice when trying to decipher the origin of California's Basin and Range features: "…we must ask by what other outrageous process it is proposed to explain them" (Davis, 1926, p. 468).

This is not the first time that jökulhlaups have entered this debate. In the 1920s, University of Chicago geologist J Harlen Bretz postulated that eastern Washington's Channeled Scabland had been sculpted by megafloods, flying in the face of established geologic thought. Though branded as heretical for decades, Bretz's theory ultimately prevailed, championing

Davis's "value of outrageous hypotheses" (Davis, 1926, p. 464; Baker and Bunker, 1985; Baker, 2009b; Howard, unpublished). Carl Sagan (1980) viewed science through a similar lens, arguing that "Extraordinary claims require extraordinary evidence."

This project assesses these extraordinary claims and lines of evidence to test Howard et al.'s (2012) hypothesis of the largest known flood on Earth and, more broadly, to reconstruct a timeline of Holocene jökulhlaups along the Jökulsá á Fjöllum. It is composed of three parts: 1) a review of the literature on Icelandic geology, jökulhlaup dynamics, and megaflood geomorphology; 2) a review and critique of previous research methods and evidence of Holocene jökulhlaups along the Jökulsá á Fjöllum, including new evidence obtained during field work in August 2015; and 3) a framework for future research to reconstruct Holocene jökulhlaup chronology, with a focus on previously unexamined lines of evidence.

The landscape along the Jökulsá á Fjöllum has been shaped by myriad geologic processes, encrypting our interpretation of how it formed. Our goal is to gather evidence and fit all the pieces together in order to solve this puzzle of Holocene landscape evolution; and specifically, to unravel the enigmatic timeline of Holocene jökulhlaups along the Jökulsá á Fjöllum.

PART I: LITERATURE REVIEW

CHAPTER 1: THE GREAT MEGAFLOOD DEBATE

In 1923, University of Chicago geology professor J Harlen Bretz stunned the geological community by proposing that megafloods had sculpted the Channeled Scabland of eastern Washington. Prior to this hypothesis, geologists had attributed its formation to glacial and fluvial processes (Baker, 1981; Baker and Bunker, 1985; Baker, 2009b). Bretz's theory was attacked from all sides by the geological community, who declared: "This heresy must be gently but firmly stamped out" (Baker, 1981, p. 12). Opponents of Bretz's hypothesis decried its apparent departure from uniformitarianism—the theory that natural processes in the past worked in the same ways and at the same rates as in the present. Instead, they argued that Bretz's megaflood hypothesis represented a return to catastrophism—the idea that Earth was formed by catastrophic events such as the biblical flood—which had largely been supplanted by uniformitarianism and whose yoke geology had spent centuries trying to throw off (Baker, 1981; Baker and Bunker, 1985; Baker, 2009b). Bretz (1978, p. 18) succinctly summed up this opposition: "Was not this debacle that had been deduced from the Channel Scabland simply a return, a retreat to catastrophism, to the dark ages of geology? It could not, it must not be tolerated."

Bretz flew in the face of this stiff opposition for the next few decades, gathering further evidence to support his hypothesis, publishing numerous papers, and defending his theory at geologic conferences (Baker, 1981; Baker and Bunker, 1985; Baker, 2009b). As he wrote in 1978: "His apostacy [sic] would not be corrected as advised by the elders. The one-man rebellion was still alive" (Bretz, 1978, p. 18). In the 1940s, J.T. Pardee—a geologist with the

U.S. Geological Survey—reported giant current ripples in the former basin of glacial Lake Missoula, whose extent and volume he had been reconstructing for the past few decades. Pardee hypothesized that this lake drained suddenly, creating enormous waves that sculpted the giant ripples (Pardee, 1942; Baker, 1981; Baker and Bunker, 1985; Baker, 2009b). Bretz connected Pardee's lake with the Channeled Scabland geomorphology, identifying Lake Missoula as the source of the megaflood (Baker, 1981; Baker and Bunker, 1985; Baker, 2009b).

Although this link lent some credence to Bretz's hypothesis among the geological community, his megaflood explanation did not gain widespread acceptance until the 1950s and 1960s, after aerial photographs of eastern Washington revealed giant current ripples that were undetectable from the ground—ironclad evidence supporting a megaflood (Bretz, 1978; Baker, 1981; Baker and Bunker, 1985; Baker, 2009b). Eventually, Bretz's hypothesis was accepted by the very institutions that had so vehemently attacked it a half-century prior. Upon receiving the Penrose Medal—one of the highest honors bestowed by the Geological Society of America—in 1979, Bretz said: "'Perhaps I can be credited with reviving and demystifying legendary catastrophism and challenging a too rigorous uniformitarianism'" (Baker and Bunker, 1985, p. 5).

Bretz's megaflood debate offers insight far beyond the geomorphology of the Channeled Scabland. Bretz drew heavily on T.C. Chamberlin's theory of multiple working hypotheses, concluding that a megaflood was the only process capable of creating the geomorphologic features observed (Baker and Bunker, 1985). He simply stated, "All other hypotheses meet fatal objections" (Bretz, 1923, p. 24). This offers a prime example of the importance of working with multiple hypotheses when conducting research.

The Channeled Scabland debate also highlights the importance of William Morris Davis's "value of outrageous hypotheses" (Davis, 1926, p. 464; Baker and Bunker, 1985). Davis—one of geography's and geology's most distinguished and pioneering figures—cautioned against relying on established laws when interpreting geology, instead urging receptivity to unconventional explanations. He wrote: "…we may be pretty sure that the advances yet to be made in geology will be at first regarded as outrages upon the accumulated convictions of to-day, which we are too prone to regard as geologically sacred" (Davis, 1926, p. 464). Like Chamberlin's multiple working hypotheses, Davis's "value of outrageous hypotheses" is a guiding force in any type of research, extending far beyond eastern Washington's Channeled Scabland.

Baker and Twidale (1991) carried this thread into the present, encouraging researchers to break out of the mold of conventional, established theories. They warned against jumping on "geoideological bandwagons" and cautioned against "…the substitution of elegantly structured methodology and theory for spontaneity, serendipity, and common sense" (Baker and Twidale, 1991, p. 73). They went on to state: "Hope for the reenchantment of Geomorphology lies in a new connectedness to nature that will facilitate the identification of anomalies and the formulation of outrageous hypotheses of causation" (Baker and Twidale, 1991, p. 73), an idea also cited by Howard (unpublished, 2013). Baker and Twidale (1991, p. 96) concluded by imploring, "Hypothesize outrageously, geomorphologists, you have nothing to lose but your paradigms." We must continue to approach geomorphological questions through these methods, bearing the torch lit by pioneering scientists such as Davis, Chamberlin, and Bretz, in order to

decipher the evolution of landscapes worldwide—particularly one clearly formed by extraordinary processes, such as along the Jökulsá á Fjöllum.

CHAPTER 2: GEOLOGY OF ICELAND

GENERAL TOPOGRAPHY

Iceland is a 103,000 km^2 basalt island in the North Atlantic Ocean (Sigmundsson, 2006; Thordarson and Larsen, 2007; Geirsdóttir et al., 2009). The island is part of a 350,000 km^2 basalt plateau, which began to form 24 million years ago (mya) from the dual processes of tectonic spreading and a mantle plume (Thordarson and Larsen, 2007). Iceland occupies an unusual geologic setting, described by Sigurdsson et al. (1995, p. 2) as "…a unique natural laboratory, where virtually all of the major geologic processes are at work."

Now home to 323,000 people, the Norse settled Iceland in 874 AD, though literary evidence exists for settlement beginning in the fifth century, likely by Gaelic monks (Preusser, 1976; Arnalds, 2005a). Ice covers 10 percent of the country and is mostly stored in five ice caps: in ascending size, Drangajökull; Mýrdalsjökull; Hofsjökull; Langjökull; and Vatnajökull—Europe's largest ice cap, covering 8 percent of the country (Björnsson, 2002; Sjöberg et al., 2004; Björnsson and Pálsson, 2008). Iceland is broadly divided into two topographic regions: the coastal lowlands, which skirt the island's coast; and the central highlands, which rise to an elevation of roughly 400 to 1000 m above sea level (masl) and are dotted with mountains climbing to over 1700 masl (Figure 2) (Arnalds, 2008). The highest point in the country is Hvannadalshnúkur—the tip of the Öræfajökull volcano—which rises from Vatnajökull to an elevation of 2110 masl (Hannesdóttir et al., 2015).

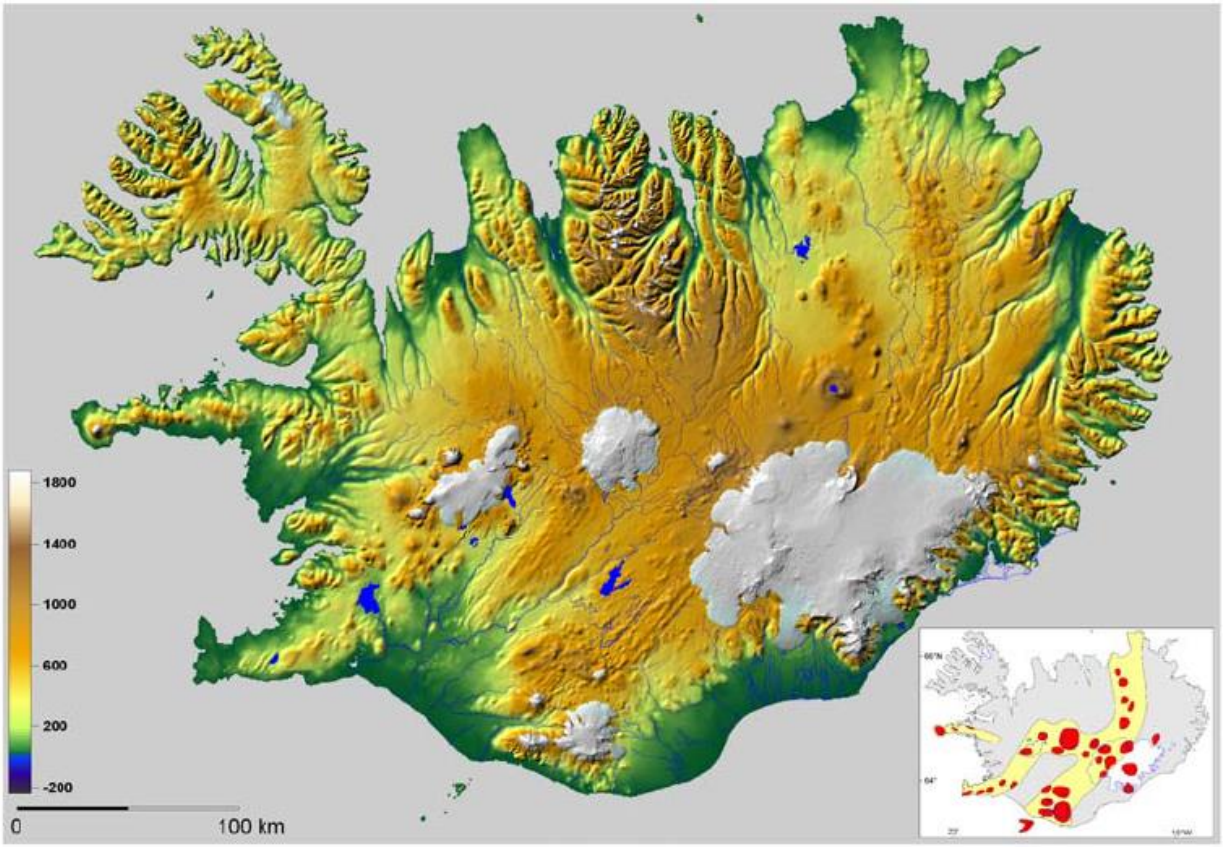

Figure 2. Topographic map of Iceland (vertical elevation in masl). White denotes ice caps. Inlaid map shows volcanic zones in beige and central volcanoes in red (Björnsson and Pálsson, 2008).

TECTONIC SETTING

Iceland is situated over the Mid-Atlantic Ridge—a tectonic spreading center that opened roughly 60 mya—along which the Eurasian and North American plates are separating at a rate of approximately 2 cm per year (Sigurdsson et al., 1995; Sigmundsson, 2006; Sturkell et al., 2006; Árnadóttir et al., 2009). The spreading center cuts diagonally across the middle of the island, trending northeast-southwest and forking into two branches in the south. It is divided into three major components: the Western, Eastern, and Northern Volcanic Zones (Figure 3) (Sigurdsson et al., 1995; Sturkell et al., 2006; Alho et al., 2005; Gudmundsson and Högnadóttir, 2007;

Gudmundsson et al., 2008; Árnadóttir et al., 2009). The Eastern Volcanic Zone (EVZ) has recently been the most active, producing over 80 percent of Iceland's eruptions since deglaciation began on the island around 11,000 years before present (11 ka BP) (Thordarson and Höskuldsson, 2008).

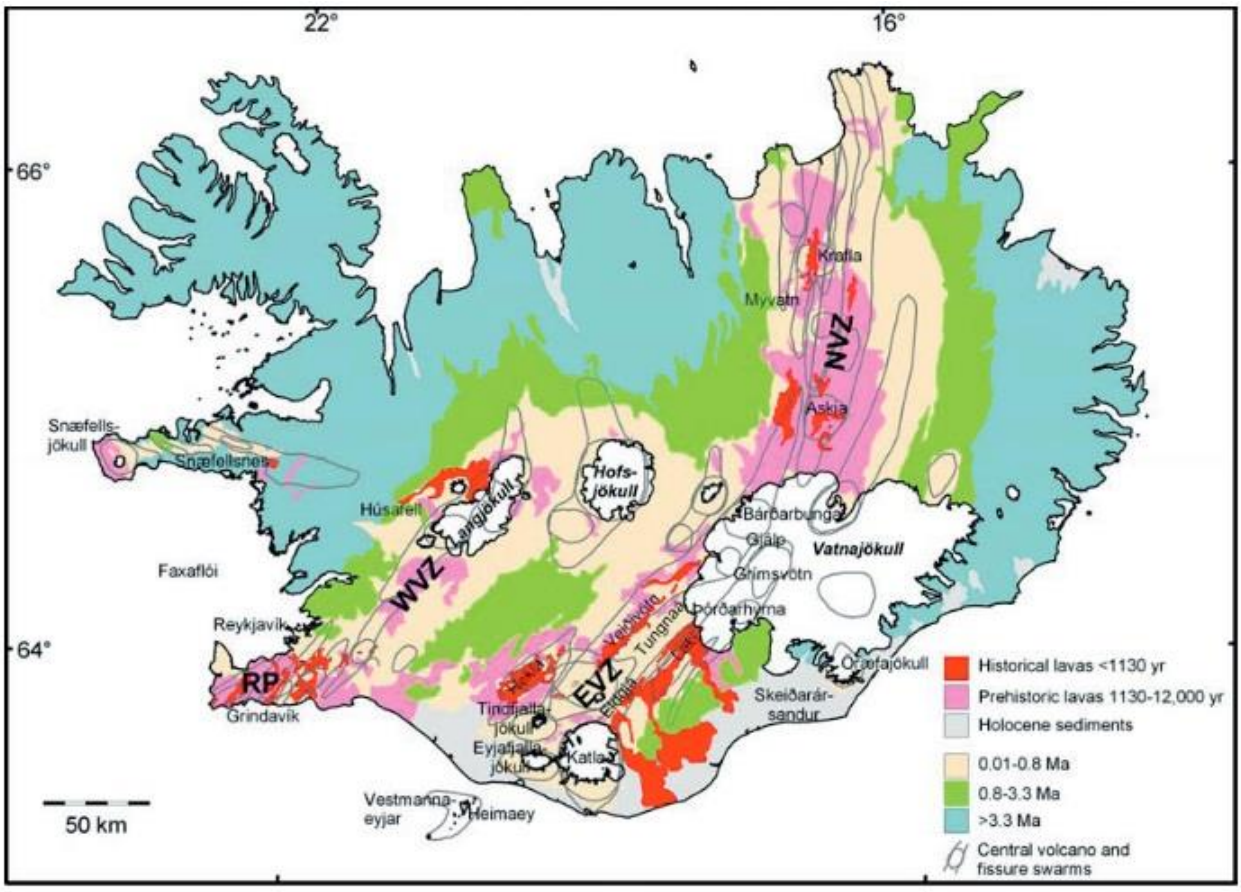

Figure 3. Geology and ice caps of Iceland (Gudmundsson et al., 2008 (modified from Jóhannesson and Sæmundsson, 1998a,b)).

The island also lies over a mantle hotspot, where a plume of extremely hot magma convectively rises from the mantle (Sigmundsson, 2006). The Iceland Mantle Plume—estimated to be 65 million years old—is roughly 2000 km in diameter and is currently centered in the southeastern corner of the island beneath Vatnajökull (Figure 4) (Sigurdsson et al., 1995;

Sigmundsson, 2006; Sturkell et al., 2006; Gudmundsson and Högnadóttir, 2007; Thordarson and Larsen, 2007; Árnadóttir et al., 2009). The island's active tectonic forces are manifest on the surface in myriad ways, including mud pots, geysers, earthquakes, faults, geothermally-heated lakes, hyaloclastites, and volcanoes.

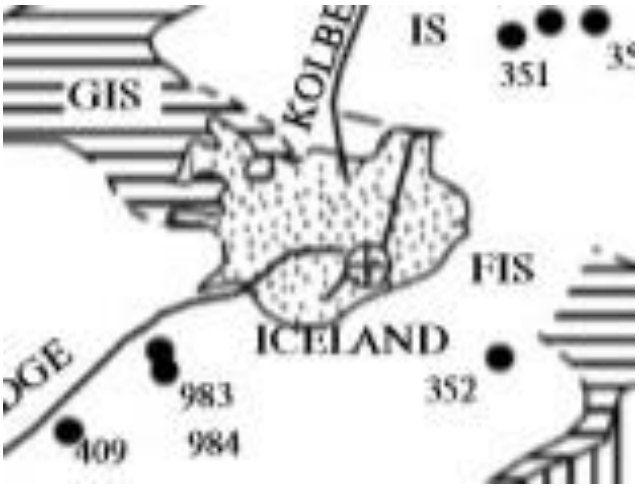

Figure 4. Location of the Iceland Mantle Plume, denoted on map by cross inside circle (modified from Kharin and Eroshenko, 2010).

VOLCANISM

There are 30 active volcanic systems in Iceland (Figure 5) (Gudmundsson and Högnadóttir, 2007; Gudmundsson et al., 2008). Currently, the most volcanically active region lies beneath Vatnajökull at the overlap of the hotspot and rifting zone, where the Eastern Volcanic Zone transitions to the Northern Volcanic Zone (NVZ) (Sigurdsson et al., 1995; Árnadóttir et al., 2009). Vatnajökull's most currently active volcanoes are Bárðarbunga and Grímsvötn, which last erupted in 2014 and 2011, respectively (Gudmundsson and Högnadóttir, 2007; Árnadóttir et al., 2009; Global Volcanism Program, 2013). Each of these volcanoes—like most in Iceland—consists of a central vent surrounded by a network of fissures (Sigmundsson,

2006; Gudmundsson and Högnadóttir, 2007; Thordarson and Larsen, 2007; Gudmundsson et al., 2008; Thordarson and Höskuldsson, 2008).

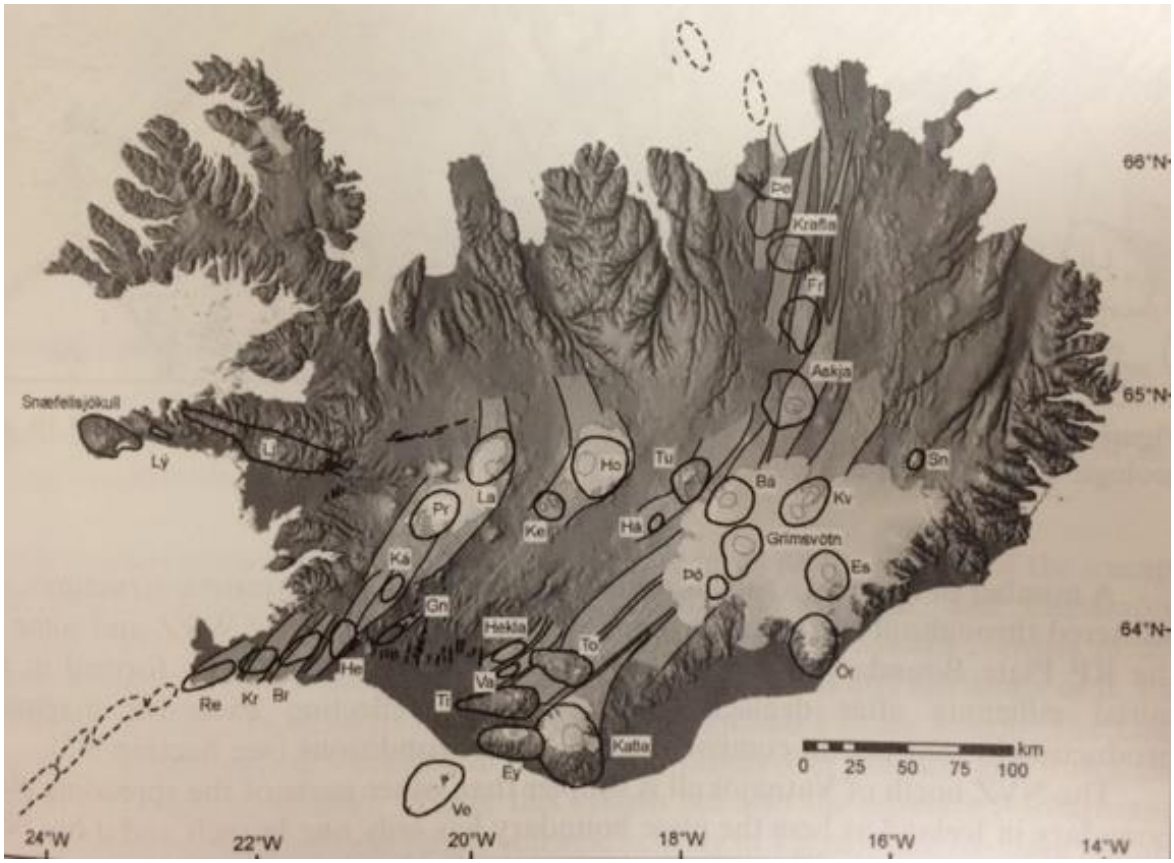

Figure 5. Volcanic systems of Iceland. White areas denote ice caps; light gray areas between black lines are fissure swarms; black circles mark central volcanoes; and gray circles show calderas. Beneath Vatnajökull: Grímsvötn; Ba=Bárðarbunga; Kv=Kverkfjöll; Þó= Þórðarhyrna; Es=Esjufjöll; Or= Öræfajökull (Sigmundsson, 2006).

GEOLOGIC UNITS

Iceland is an island of igneous rocks—overwhelmingly basalts—formed by the dual processes of tectonic spreading and the mantle plume (Sigmundsson, 2006). The oldest rocks are 14—16 million years old (Thordarson and Larsen, 2007) and are found at the western and eastern edges of the island, with progressively younger rocks occurring closer to the active

rifting zone (Figure 3) (Jóhannesson and Saemundsson, 1998a,b; Sigmundsson, 2006; Geirsdóttir et al., 2007; Gudmundsson et al., 2008; Thordarson and Höskuldsson, 2008). Icelandic rocks are divided into four major units based on age, as described by Sigmundsson (2006): 1) Tertiary; 2) Plio-Pleistocene; 3) Upper Pleistocene; and 4) Postglacial.

Tertiary rocks are the oldest, forming over 3.3 mya. They are principally tholeiitic basalt lavas—fine-grained basalts that are rich in silica, iron, and magnesium and low in sodium— that are thinly layered with a mix of soils, aeolian sediments, and ash with a clay-tuff texture. These rocks formed before the onset of extensive glaciation in Iceland (Sigmundsson, 2006), which began 3—5 mya (Geirsdóttir et al., 2007).

The second major rock type is Plio-Pleistocene rocks, which formed across the Pliocene-Pleistocene boundary between approximately 3.3 and 0.8 mya. This geologic unit reflects the frequent glaciations that characterized the beginning of the Quaternary, which occurred after 1 mya in cycles lasting 100 ka—120 ka (Sigmundsson, 2006; Geirsdóttir et al., 2007). During these early glacials, subglacial eruptions generated enormous quantities of hyaloclastite, pillow lava, and pillow breccia—all formed by the interaction of lava and water (Guðmundsson, 2005; Sigmundsson, 2006). During the interglacials, more moraine and fluvioglacial deposition occurred (Sigmundsson, 2006).

Upper Pleistocene rocks are the third major type in Iceland. Glaciation continued in the late Pleistocene beginning about 0.8 mya. Subglacial eruptions continued to generate hyaloclastite and pillow lava, which are collectively known as the Palagonite (or Móberg) Formation. These palagonite subglacial volcanoes resemble table mountains and are called tuyas (Guðmundsson, 2005; Sigmundsson, 2006) or—in Icelandic—stapis (Preusser, 1976;

Thordarson and Larsen, 2007). Lava flows from subglacial fissures produced hyaloclastite ridges with a similar composition (Guðmundsson, 2005). During interglacial periods in the late Pleistocene, eruptions spewed lava flows across deglaciated areas (Sigmundsson, 2006; Geirsdóttir et al., 2007).

Iceland's youngest rocks are classified as Postglacial and formed after the start of deglaciation roughly 11.5 ka BP. These Holocene materials include lava flows, pyroclastics, and fluvially deposited sediments (which are principally found at sandar—glacial outwash plains—and the mouth of the Jökulsá á Fjöllum). Postglacial lava flows are delineated into two types: prehistoric (formed before human settlement about 1100 years ago) and historic (after settlement) (Sigmundsson, 2006). Generally, lava flows mark interglacial periods, while hyaloclastites reflect glacial conditions, but of course hyaloclastites are still forming under glacial remnants during interglacials (Geirsdóttir et al., 2007).

TECTONIC UPLIFT, SUBSIDENCE, AND GLACIAL ISOSTATIC ADJUSTMENT

Iceland's intense tectonic activity and melting glaciers result in vertical crustal adjustments throughout the country. Isostatic rebound from Iceland's last glaciation—which ended roughly 10 ka BP—finished after only 1000 years (Sigmundsson, 1991; Thoma et al., 2001; Sigmundsson, 2006; Auriac et al., 2013). This is considerably faster than many other glaciated landscapes: isostatic rebound in the regions covered by the Laurentide and Fennoscandian Ice Sheets during the Pleistocene spanned a few thousand years, for example (Benn and Evans, 2010).

Current uplift in Iceland is predominantly in response to glacial thinning and magma intrusions (Árnadóttir et al., 2009). However, Árnadóttir et al. (2009) proposed several other

mechanisms to explain this uplift. One contributing factor may be erosion: as rock erodes, overlying pressure decreases, triggering an upward movement of the Earth's surface (Árnadóttir et al., 2009). Árnadóttir et al. (2009) also investigated the mantle plume's role in uplift, but measurements showed the effect to be almost undetectable. Finally, Árnadóttir et al. (2009) noted that it is crucial to account for nearby glaciers' mass balance changes, as these can affect rebound and uplift rates on a regional scale; many areas of rapid isostatic rebound are on shields that were once covered by much larger ice sheets than that in Iceland (Benn and Evans, 2010).

Isostatic adjustment rates depend on crustal thickness, mantle viscosity, and ice thickness and mass, among other factors. Studies report a wide spread of values for Iceland's crustal thickness, ranging between 10 and 40 km, with the thickest crust found above the mantle plume (Sigmundsson, 2006; Sturkell et al., 2006; Fleming et al., 2007; Gudmundsson and Högnadóttir, 2007; Árnadóttir et al., 2009; Auriac et al., 2013). Most studies have focused on uplift at Vatnajökull, where models estimate a relatively low asthenosphere viscosity in the range of 1018 Pa s, which allows for rapid uplift rates (Sigmundsson, 1991; Thoma et al., 2001; Sjöberg et al., 2004; Sigmundsson, 2006; Fleming et al., 2001; Pagli et al., 2007; Árnadóttir et al., 2009; Auriac et al., 2013). Pa s (Pascal-seconds) measure the viscosity of a fluid; the lower the viscosity, the higher the isostatic rebound rate (assuming all other factors are equal) (Turcotte and Schubert, 2002; Sigmundsson, 2006).

Current uplift rates—measured by a network of GPS stations and satellite radar interferometry—are greatest in southeastern and central Iceland, specifically around Vatnajökull, the Northern Volcanic Zone, and the Krafla volcanic system (Figure 6) (Sturkell et al., 2006; Árnadóttir et al., 2009). Pagli et al. (2007) measured uplift rates ranging from 9—25 mm per

year around Vatnajökull's perimeter, with rates decreasing with distance from the ice cap. Pagli et al. (2007) attributed this uplift to ice cap melting. Sjöberg et al. (2004) reported a similar reaction to ice cap thinning, measuring uplift rates of 5—19 mm per year at the edges of Vatnajökull. Auriac et al. (2013) recorded a slightly greater uplift rate at Vatnajökull's edges: about 24 mm per year from 1995—2002 and 31 mm per year from 2004—2009.

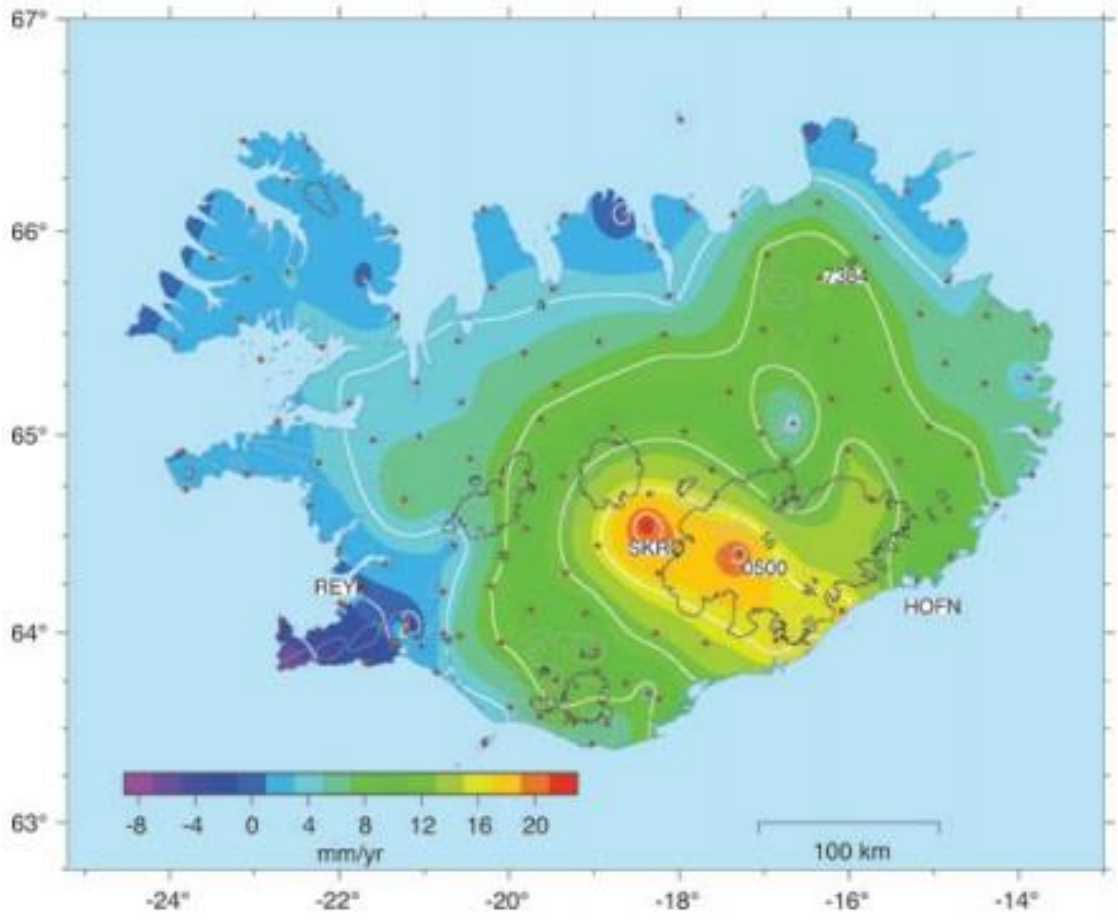

Figure 6. Surface elevation changes in Iceland, measured by GPS stations from 1993—2004 (Árnadóttir et al., 2009).

Pagli et al. (2007) also modeled future uplift in response to climate change. They calculated a total uplift of 2.4 m between 2000 and 2100 at the edges of Vatnajökull—an annual rate of 24 mm—if the ice cap continues to thin at its current rate. However, if atmospheric

temperature increases enough to double thinning rates, the models predicted a net uplift of 3.7 m by 2100—an average rate of 37 mm per year (Pagli et al., 2007).

Sturkell et al. (2006) observed uplift at Grímsvötn volcano (beneath the western part of Vatnajökull) before its eruptions in 1998 and 2004, likely due to a combination of ice thinning and an inflow of magma (Árnadóttir et al., 2009). The glacier surface above Grímsvötn subsided after each eruption due to the volcano's deflated magma chambers (Sturkell et al., 2006; Árnadóttir et al., 2009). Furthermore, the 2004 eruption was partially triggered by the draining of Grímsvötn's subglacial caldera lake in a jökulhlaup; without this overlying pressure, uplift intensified and the volcano erupted a few days later (Sturkell et al., 2006).

Uplift—likely due to an inflow of magma—is also occurring at the Krafla volcanic system and was measured at 8 cm between 1993 and 1999, or roughly 13 mm per year (Sturkell et al., 2006; Árnadóttir et al., 2009). Auriac et al. (2013) also recorded uplift at Upptyppingar due to a dike intrusion.

Not all of Iceland is uplifting, however. The Western Volcanic Zone (WVZ) and Reykjanes Peninsula (in the island's southwestern corner) are subsiding, as is the Askja volcanic system, the area beneath the Mýrdalsjökull ice cap, and the region between Askja caldera and Kverkfjöll (at Vatnajökull's northern edge) (Sturkell et al., 2006; Árnadóttir et al., 2009; Auriac et al., 2013), all at rates ranging from approximately 4—10 mm per year (Árnadóttir et al., 2009). Subsidence is likely due to extension in the tectonic spreading zone; cooling and contraction of solidifying magma; magma outflow; or a combination of these processes (Sigmundsson, 2006; Sturkell et al., 2006; Árnadóttir et al., 2009).

The numerous factors contributing to Iceland's vertical displacements demonstrate the strong link between Earth's spheres. Atmospheric temperatures control ice cap thinning, which affects uplift rates; the movement of magma in the asthenosphere causes uplift or subsidence of the lithosphere; and the drainage of subglacial lakes removes overlying ice pressure, contributing to uplift and volcanic eruptions. As with so many geologic processes, Iceland's vertical adjustment reflects the inextricable links between Earth's systems.

CHAPTER 3: GLACIATION, CLIMATE, AND SOILS IN ICELAND

GLACIATION HISTORY

Iceland was first glaciated approximately 3—5 mya. By 2.5 mya, the ice sheet had spread across most of the country. Periodic retreats and advances left behind glacial deposits, while subglacial volcanism produced hyaloclastite and pillow lava. Interglacials and interstadials were marked by lava flows. Approximately 1 mya, glaciations began to occur regularly on a 100,000 year (kyr) cycle (Geirsdóttir and Eiríksson, 1994; Geirsdóttir et al., 2007).

Iceland's last glaciation—the Weichselian—began about 100,000 calibrated years before present (100 kyr cal BP) (Hubbard et al., 2006). At the Last Glacial Maximum during the late Pleistocene—roughly 21 kyr BP—Iceland was covered by an ice sheet that extended almost to the edge of the basalt shelf (Figure 7) (Norðdahl and Pétursson, 2005; Hubbard et al., 2006; Geirsdóttir et al., 2007; Geirsdóttir et al., 2009; Ingólfsson et al., 2010). This sheet had an estimated surface area of 330,000 km^2 and was 1000—2000 m thick (Norðdahl and Pétursson, 2005; Hubbard et al., 2006; Ingólfsson et al., 2010).

The ice sheet began to break up and recede around 15 kyr cal BP during the Bølling and Allerød interstadials (Norðdahl and Pétursson, 2005; Ingólfsson et al., 2010). The process progressed in steps with periods of ice advance and retreat (Sigmundsson, 2006; Geirsdóttir et al., 2007; Geirsdóttir et al., 2009; Ingólfsson et al., 2010). By 13.9 kyr cal BP, the ice sheet had diminished in size by 25 percent (Ingólfsson et al., 2010).

Cooler temperatures during the Younger Dryas triggered significant ice sheet advances between 13 and 11.5 kyr cal BP (Figure 7) (Geirsdóttir et al., 2000; Norðdahl and Pétursson, 2005; Sigmundsson, 2006; Ingólfsson et al., 2010). After a brief recession, a second major advance occurred during the Preboreal, roughly 11.2 kyr cal BP, after which point the ice began

to retreat again (Figure 7) (Geirsdóttir et al., 2000; Norðdahl and Pétursson, 2005; Geirsdóttir et al., 2007; Geirsdóttir et al., 2009; Ingólfsson et al., 2010).

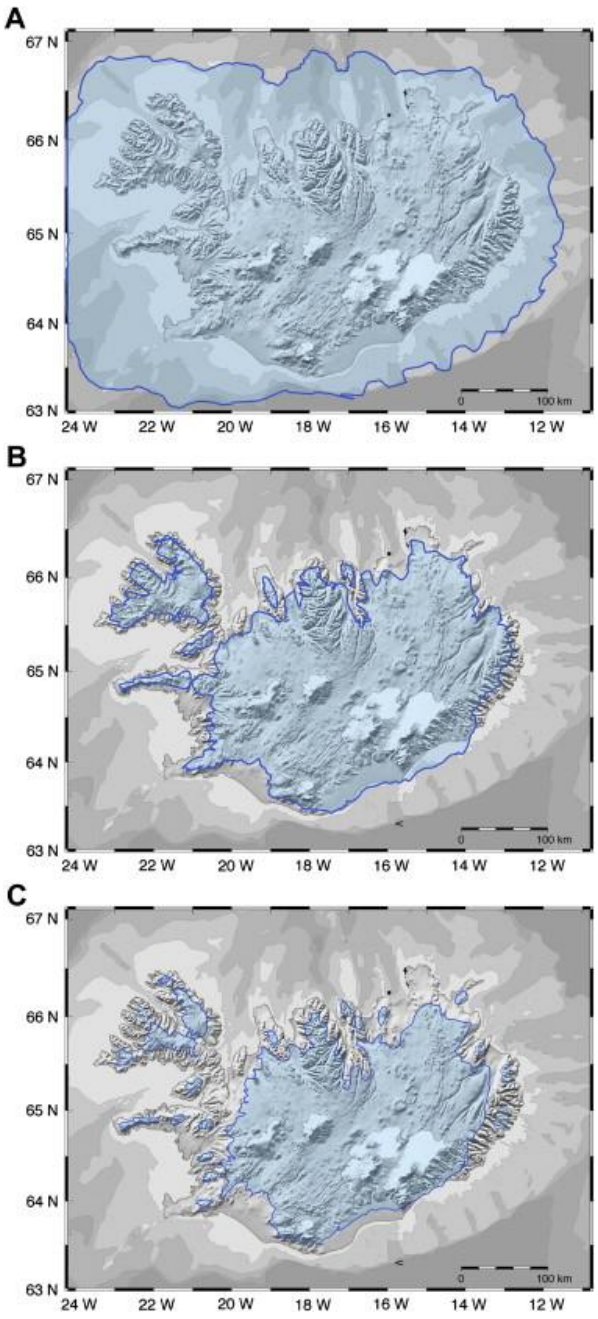

Figure 7. Estimated extent of ice sheet in Iceland. A: Last Glacial Maximum (roughly 21 ka BP); B: Younger Dryas (13 ka—11.5 ka BP); C: Preboreal (11.2 ka BP) (Geirsdóttir et al., 2009).

By the start of the Holocene, the ice sheet was in rapid retreat in response to warmer temperatures (Geirsdóttir et al., 2009). Moraine reconstruction and dating suggest that at 10.5 ka BP, the ice sheet still extended beyond Iceland's current northern coastline (Waitt, 2002). By roughly 10.3 ka BP, the ice sheet was retreating from the central highlands, withdrawing towards the south (Geirsdóttir et al., 2009); and by 9600 BP, it had receded to a point 70 km downstream of the Jökulsá á Fjöllum's current mouth (Waitt, 2002; Carrivick et al., 2013). The ice sheet had broken up by 8700 cal BP, leaving a handful of isolated ice caps in its wake, including Vatnajökull (Thoma et al., 2001; Ingólfsson et al., 2010). Ice extent reached a minimum at the end of the Holocene Thermal Maximum around 5000 cal BP when temperatures were about 2—4˚C warmer than those during the 20th century.

During the next period—Neoglaciation— ice extent fluctuated, advancing and retreating in response to temperature variations (Geirsdóttir et al., 2007; Geirsdóttir et al., 2009; Ingólfsson et al., 2010). A significant glacial advance occurred roughly 2600—2000 BP (Ingólfsson et al., 2010). The next—and last—major advance reflected a plunge in temperatures at the onset of the Little Ice Age (LIA), which stretched from about 1250—1900 AD (Geirsdóttir et al., 2009; Ingólfsson et al., 2010). Glaciation reached its greatest extent of the Holocene between 1700 and 1890 AD (Geirsdóttir et al., 2009; Ingólfsson et al., 2010). After 1890 AD, a temperature rise of 1—2˚C triggered rapid ice retreat, which continues today (Pagli et al., 2007; Geirsdóttir et al., 2009).

CLIMATE

Although Iceland lies less than one degree south of the Arctic Circle, it has a cool temperate climate due to the warm water of the Irminger Current, which is part of the Gulf Stream (Arnalds, 2004; Björnsson and Pálsson, 2008). Winter temperatures usually stay below freezing, and summers are cool—hovering around 10°C on average in the lowlands, but remaining closer to 7°C in the highlands (Arnalds, 2004; Björnsson and Pálsson, 2008). The lowlands generally receive between 450 and 2500 mm of precipitation a year, while the central highlands are drier, ranging from 400—700 mm annually (Arnalds, 2004; Björnsson and Pálsson, 2008). The southern ice caps—Vatnajökull and Mýrdalsjökull—receive the country's highest amount of precipitation, with 4000—7000 mm falling annually, most of it as snow (Björnsson and Pálsson, 2008).

SOIL TYPES AND EROSION

Soil Types

The parent material for Icelandic soils is volcanic material, particularly basalt and tephra (Arnalds, 2008). All soils are younger than roughly 10 ka BP, when Iceland's last ice sheet retreated (Arnalds, 2008). Iceland is underlain by five types of soils: Andisols; Vitrisols; Histosols; Cryosols; and Leptosols (Figure 8).

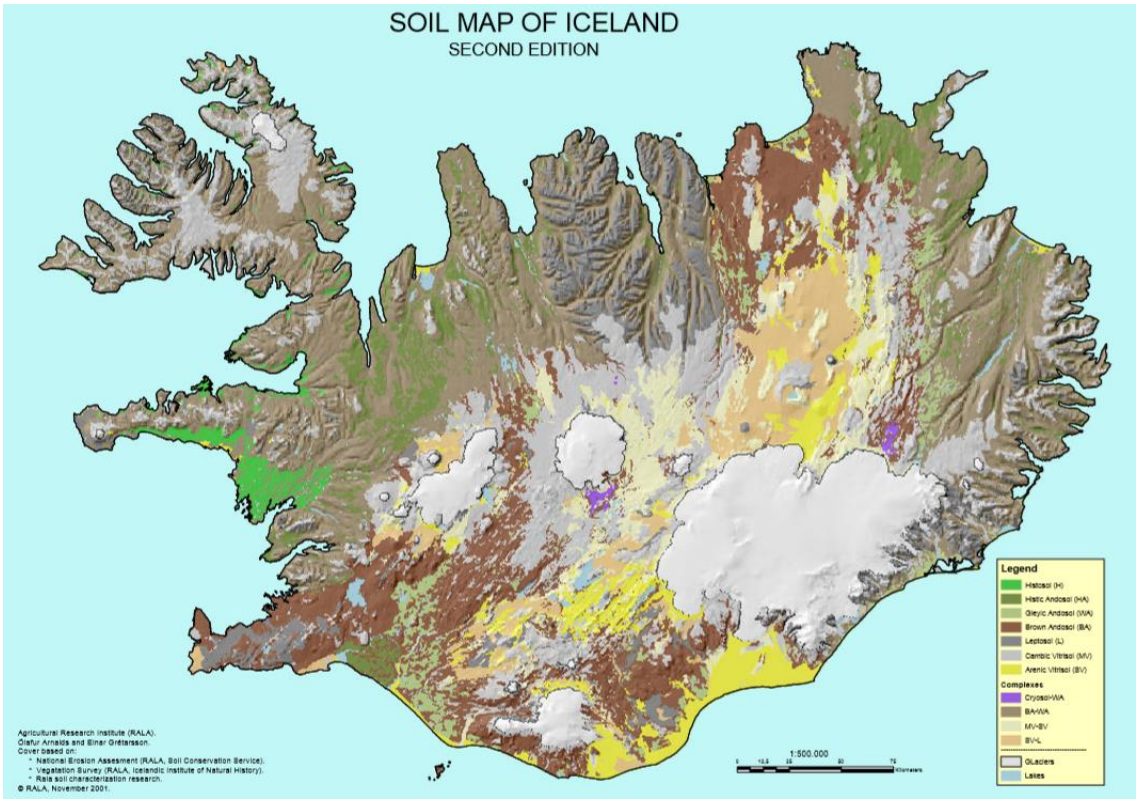

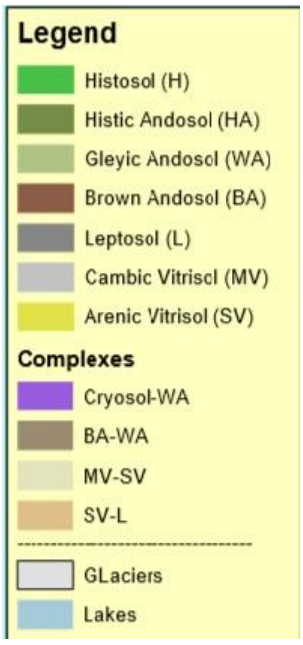

Figure 8. Soil map of Iceland (top) and enlarged legend (bottom) (Arnalds and Gretarsson, 2004).

Andisols and Vitrisols are the two most common soil types in Iceland, covering 48 and 17 percent of the island, respectively. Andisols principally ring the coastal lowlands. These soils form from the weathering of volcanic materials—mainly basaltic (and some rhyolitic) tephra—and support vegetation growth (Arnalds et al., 2001; Arnalds, 2004; Arnalds, 2005b; Arnalds, 2008). Vitrisols underlie most of the central highlands (Arnalds, 2008). These "desert soils" consist mainly of volcanic tephra, most of which forms from basalt, giving these sandy soils a black color (Arnalds et al., 2001; Arnalds, 2008). They are poorly developed and support little to no vegetation, which makes them easily erodible and thus the main source of aeolian sediment (Arnalds et al., 2001; Arnalds, 2004; Arnalds, 2005b; Arnalds, 2008).

Leptosols, Histosols, and Cryosols are far less prevalent on the island. Leptosols cover roughly 7 percent of Iceland, mostly in the mountainous area in the north central region. Additionally, 5 percent of the country—mostly in the central highlands—is covered by a Vitrisol-Leptosol complex (Arnalds, 2008). These soils are rocky, poorly developed, and shallow, forming less than 25 cm above bedrock (International Soil Reference and Information Centre (ISRIC), 2015). Histosols cover a mere 1 percent of Iceland's surface. These soils have a high concentration of organic matter, are very poorly drained—or even saturated—and form in bogs or wetlands, mainly in the western coastal lowlands (Arnalds, 2004; Arnalds, 2005b; Arnalds, 2008). Finally, small patches of Cryosols—soils with permafrost—have been found near the Vatnajökull and Hofsjökull ice caps. Their presence is often marked by palsas, ice-cored mounds up to 2 meters high (Arnalds, 2004; Arnalds, 2005b; Arnalds, 2008).

Soil Erosion

Because most Icelandic soils are fine-grained, unconsolidated, and low in organic material, they are extremely susceptible to erosion. Iceland's harsh climate inhibits vegetation growth, and this lack of root structures makes soils even more easily erodible. The paucity of vegetation also prevents the trapping of aeolian sediments and thus a means of sediment replacement (Runólfsson, 1987; Greipsson, 2012). Furthermore, Iceland has a constant supply of easily erodible material, including glaciofluvially-transported sediment and ash from eruptions (Arnalds et al., 2001; Alho, 2003). Aeolian processes easily remove particles and deposit them across the landscape, sometimes piling them up to form large sand fronts that can advance over 300 m per year, burying and killing vegetation and thus triggering more erosion (Arnalds et al., 2001; Arnalds, 2005b; Arnalds, 2008).

Rofabards are another common feature of soil erosion in Iceland. These "erosion escarpments" resemble pillars or pedestals of soil capped by vegetation mats (Figures 9-10). They form when Andisols erode beneath vegetation, often due to abrasion from aeolian particles. Erosion accelerates as a larger surface area becomes exposed, causing the rofabards to "retreat" across the landscape, leaving an unvegetated desert in their wake (Arnalds, 2000; Alho, 2003; Arnalds, 2005b; Arnalds, 2008). Rofabards move at a rate of a half-inch to a foot and a half every year and have eroded an estimated 5 mi^2 of soil annually since Norse settlement (Montgomery, 2012).

Figure 9. Rofabards near Mt. Herðubreið, Iceland (photo by author).

Figure 10. Rofabards and soil erosion escarpments near Mt. Herðubreið (photo by author).

Another driver of soil erosion in Iceland is cryoturbation. Soils repeatedly freeze and thaw, which loosens particles, thus accelerating erosion and producing hummocks across the landscape. Cryoturbation beneath Vitrisols pushes rocks to the surface and can create a type of desert pavement or polygonal patterned ground (Arnalds, 2004; Arnalds, 2005b; Arnalds, 2008).

Anthropogenic drivers have rapidly accelerated erosion since human settlement in 874 AD, mainly through deforestation and livestock grazing (Arnalds, 2000; Arnalds, 2005a). Roughly 95 percent of Iceland's forests have been cut down since Viking settlement for use as fuel and building materials, as well as to clear pastures for grazing livestock, principally sheep (Arnalds, 2005a; Greipsson, 2012). These sheep also trigger rapid erosion by removing vegetation through grazing and trampling, destroying root structures and exposing the underlying volcanic soils (Arnalds and Barkarson, 2003; Greipsson, 2012; Montgomery, 2012). Furthermore, the central highlands—mostly covered by Vitrisols—are communal grazing areas for sheep in summer, exacerbating erosion (Arnalds and Barkarson, 2003; Arnalds, 2005a). The most severe soil erosion in Iceland occurs in areas underlain by Vitrisols—principally in the central highlands and sandar (Arnalds, 2008).

CHAPTER 4: JÖKULHLAUP TRIGGERS AND DRAINAGE DYNAMICS

In most glaciated regions worldwide—particularly the Himalayas (Agrawala, 2008), Alps (Wiegandt and Lugon, 2008), and Andes (Carey, 2008)—glacial outburst floods result from glacial lakes that form as ice melts and pools in response to warming atmospheric temperatures, increasingly due to climate change (Figure 11) (Huggel et al., 2008). In Iceland, however, subglacial geothermal activity is the main generator of glacial lakes and outburst floods, though they can also occur during volcanically dormant periods due to subglacial lake drainage (Björnsson, 2002; Björnsson, 2009). These floods are called jökulhlaups, from the Icelandic words jökull (glacier) and hlaup (leap) (Agrawala, 2008; Carey, 2008; Benn and Evans, 2010). Jökulhlaups occur through two main processes: 1) glacial lake drainage; and 2) direct drainage (without storage) due to subglacial volcanic eruptions (Tweed and Russell, 1999; Björnsson, 2002; Guðmundsson, 2005; Gudmundsson et al., 2008; Björnsson, 2009).

Figure 11. Proglacial Imja Lake, Himalayas. With a volume of over 60 million m^3, Imja is one of Nepal's most dangerous glacial lakes (Byers et al., 2015).

SUBGLACIAL LAKE FORMATION

Glacial lakes can be supraglacial (on the glacier surface), marginal (at the glacier margins), proglacial (in front of the glacier snout), or subglacial (beneath the glacier); most of

Iceland's are subglacial (Tweed and Russell, 1999). The Vatnajökull ice cap occupies a unique position in Iceland, overlying both the Mid-Atlantic Ridge spreading center and the Iceland Mantle Plume (Sigmundsson, 2006). This intense volcanic and geothermal activity generates enormous quantities of meltwater, which often pools in subglacial lakes, either filling depressions—such as calderas—or forming a bubble of water extending up into the glacier (Figure 12) (Tweed and Russell, 1999; Björnsson, 2002; Björnsson, 2009). This water accumulation causes the overlying ice to subside because water provides a warmer and less rigid medium, creating a depression on the glacier surface over the lake (Björnsson, 2002; Björnsson, 2009). Vatnajökull is also an area with high precipitation and relatively warm conditions for a glacier, further contributing to meltwater lake formation (Björnsson and Pálsson, 2008).

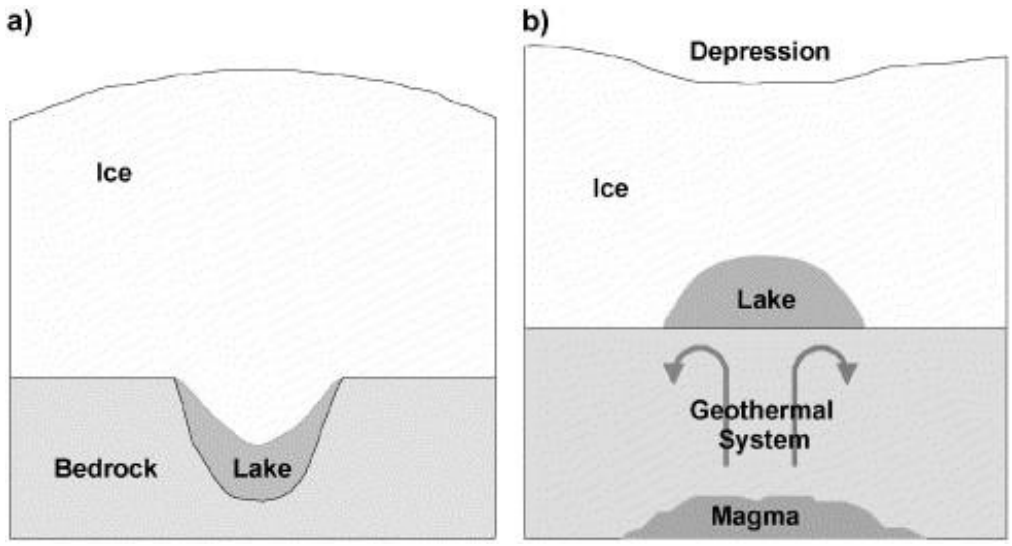

Figure 12. Subglacial lake formation. a): Meltwater lake forms in a depression such as a caldera. b): Meltwater lake forms as a bubble and pushes up into the overlying ice cap, creating a depression in the ice surface (Björnsson, 2002).

While proglacial and marginal lakes may be dammed by a moraine or an ice-cored moraine (Benn and Evans, 2010), subglacial lakes are generally dammed by an ice plug; their edges are hydraulically sealed by the overlying ice pressure (Tweed and Russell, 1999; Björnsson, 2002; Björnsson, 2009). Six known lakes lie beneath Vatnajökull, the largest of which lies in the Grímsvötn caldera. The lake has created a glacier surface depression 300 m deep and 10 km wide (Björnsson, 2002; Björnsson, 2009).

SUBGLACIAL LAKE DRAINAGE TRIGGERS

Subglacial lake drainage is triggered by two main mechanisms. In the first scenario, the lake reaches a depth—roughly 90 percent of the ice dam height—at which water pressure on the ice dam exceeds the pressure of the overlying ice, allowing water to flow under the dam and float it. In the second mechanism, basal meltwater exerts pressure on the overlying ice. When water pressure exceeds overlying ice pressure, the ice is lifted, breaking the ice dam's hydraulic seal and allowing water to leak out beneath the ice plug (Costa, 1988; Tweed and Russell, 1999; Björnsson, 2002; Björnsson, 2009). Ice dams can also be broken by earthquakes, volcanic eruptions, or hydrothermal melting (Tweed and Russell, 1999; Björnsson, 2002).

SUBGLACIAL VOLCANIC ERUPTIONS: DIRECT DRAINAGE

Volcanic eruptions generate enormous quantities of heat and pressure with ejected material. Often, the resulting meltwater volume is so great that it overflows existing subglacial lakes and immediately drains out the glacier margins without prior storage (Björnsson, 2002; Björnsson, 2009). When volcanic material is ejected directly into subglacial lakes, it can heat the water to boiling point, which accelerates melting of surrounding ice. Subglacially erupted material also displaces meltwater and forces it towards glacier margins (Björnsson, 2009).

Eruptions can also disarticulate the overlying glacier, allowing bergs to drop into the water and create turbulence and surface waves, which can cause the ice dam to fail (Tweed and Russell, 1999). Eruptions have triggered the largest jökulhlaups from Vatnajökull during historic times (Björnsson, 2009). Subglacial lake drainage generates more frequent and longer-lasting floods since draining meltwater slowly expands ice tunnels. Eruption-generated jökulhlaups, on the other hand, generally feature larger peak discharges and shorter durations due to their greater volume of meltwater, as well as the water's higher temperature and pressure and thus ability to melt larger conduits in the ice (Tweed and Russell, 1999; Björnsson, 2002; Gudmundsson et al., 2008; Björnsson, 2009).

SUBGLACIAL DRAINAGE DYNAMICS

Glacial meltwater can drain subglacially, supraglacially, marginally, or englacially (within the glacier) (Tweed and Russell, 1999). Water drains through ice tunnels, generally following weaknesses or existing conduits in the ice. These tunnels expand into larger passages over time due to frictional heating from the flowing water, as well as hydraulic fracturing (Tweed and Russell, 1999; Björnsson, 2002; Russell et al., 2006; Björnsson, 2009). However, if the overlying ice pressure exceeds the water pressure, the tunnels will reseal, which can occur before the lake is completely drained (Tweed and Russell, 1999; Björnsson, 2002; Björnsson, 2009). If the water volume is larger than the ice tunnels' capacities, meltwater may drain along the base of the glacier. This hydraulic pressure can lift the glacier, creating a basal channel through which the water can flow (Björnsson, 2002; Björnsson, 2009).

Ice conduits vary greatly in size and distribution pattern; for example, a jökulhlaup that drained the Grímsvötn caldera lake in 1996 flowed through one principal tunnel until it reached

the ice cap margins, where it stretched out to exit Vatnajökull over a 23 km-wide area across Skeiðarársandur (Tweed and Russell, 1999; Russell et al., 2006; Björnsson, 2009). This jökulhlaup reached a peak discharge of 4.5—5.3 x 10^4 m^3 s^{-1} and released a total volume of 3.2 km^3 of water in a mere 40 hours (Russell et al., 2006; Benn and Evans, 2010). The floodwaters also flowed supraglacially, carving a 700 m long, 100—300 m wide, 50 m deep ice canyon on the surface of the ice cap in under 17 hours (Russell et al., 2006).

During drainage, meltwater currents may break off blocks of ice from the sides of tunnels (Björnsson, 2002). Jökulhlaups also sweep out any sediment in their paths: some material is scooped off the glacier's base, while other sediment is frozen in transported ice blocks and later melts out (Tweed and Russell, 1999; Russell et al., 2006). The 1996 jökulhlaup from Grímsvötn transported roughly 1.8 x 10^8 tons of sediment (Russell et al., 2006). In rare cases—at the Sólheimajökull and Skeiðarárjökull glaciers on Mýrdalsjökull's and Vatnajökull's southern edges, respectively—this sediment load chokes ice tunnels, forming eskers (Russell et al., 2006).

CHAPTER 5: MEGAFLOODS

MEGAFLOODS ON EARTH

Megafloods—loosely defined as floods whose peak discharges exceed one million cubic meters per second (equal to one Sverdrup (Sv))—have occurred on Earth throughout the Quaternary and probably earlier (O'Connor et al., 2002; Baker, 2009b). The largest floods on Earth resulted from ice dam failures during the Pleistocene. As ice sheets receded during the last major deglaciation, vast glacial lakes formed behind ice dams, which were often glacier lobes (O'Connor et al., 2002; Baker, 2009b). When the dams failed or were overtopped, catastrophic floods ripped across the landscape. After drainage, the lakes often refilled, and the cycle repeated (O'Connor et al., 2002; Baker, 2009b).

The largest known flood on Earth is widely considered to have drained from the Chuja—Kuray glacial lake system in the Altai Mountains in Siberia. These lakes formed when meltwater from valley glaciers pooled behind glacier lobes. An ice dam failure in the late Pleistocene—between roughly 46 ka and 13 ka (Carling et al., 2009c)—produced a flood with an estimated peak discharge of 1.8×10^7 m^3 s^{-1} (Baker et al., 1993; O'Connor et al., 2002; Rudoy, 2002; Herget, 2005; Howard et al., 2012). Some studies, however, cite a peak discharge of only 1×10^7 m^3 s^{-1} (Herget, 2005; Carling et al., 2009c).

A series of approximately 25—40 megafloods repeatedly drained glacial Lake Missoula throughout the late Pleistocene between about 20 ka and 12 ka BP. As the Cordilleran Ice Sheet retreated, meltwater pooled in the lake behind one of the glacier's lobes. When this ice dam failed, the water cascaded out in cataclysmic floods, the largest of which had an estimated peak discharge of 1.7×10^7 m^3 s^{-1}. These megafloods surged across northern Idaho and sculpted the Channeled Scabland of eastern Washington before draining along the Columbia River to the

Pacific Ocean (Baker and Bunker, 1985; Baker et al., 1993; O'Connor et al., 2002; Baker, 2009a,b).

Another megaflood occurred when Lake Bonneville—a closed basin lake in northern Utah—overflowed its basin in the late Pleistocene around 14.5 ka. The lake drained northwest along the Snake River, flowing through the Channeled Scabland and the Columbia River before emptying into the Pacific Ocean (O'Connor, 1993). This flood attained a peak discharge of 1 x 10^6 m^3 s^{-1} (O'Connor, 1993; O'Connor et al., 2002).

Another series of megafloods drained from Lake Agassiz—North America's largest proglacial lake, which covered 1.5 million km^2 over the course of its 5000-year existence—across south-central Canada and the north-central United States between roughly 13 ka and 8 ka (Teller and Clayton, 1983; Kehew et al., 2009; Katz et al., 2011; Cronin et al., 2012). As the Laurentide Ice Sheet retreated, meltwater drained through a network of interconnected spillways and lakes, often pooling in isostatic depressions formed by the glacier's weight. These lakes were dammed by ice lobes or moraines (Teller and Clayton, 1983; Kehew et al., 2009; Katz et al., 2011). Eventually, the lake level crossed a threshold and either overflowed the basin or broke through the dam, usually at the lowest topographic point or the weakest part of the moraine. The resulting catastrophic release of water created heavily eroded saddles called spillways (Kehew et al., 2009).

Lake Agassiz drained multiple times during the late Pleistocene and early Holocene; Katz et al. (2011) cited at least 19 flood events. Estimates of the maximum peak discharge of the largest flood vary from 0.1—5 x 10^6 m^3 s^{-1}, although drainage likely spanned months or even a year (Kehew et al., 2009; Katz et al., 2011). Floodwaters followed five principal routes,

depending on which outlets opened due to ice margin shifts and isostatic adjustment: south through the Mississippi River Valley to the Gulf of Mexico; east through the St. Lawrence Estuary to the North Atlantic Ocean; east through the Hudson River Valley to the North Atlantic; north through Hudson Bay to the North Atlantic; and north through the Mackenzie River Valley to the Arctic Ocean (Kehew et al., 2009; Katz et al., 2011; Cronin et al., 2012).

The largest recorded jökulhlaup in historic times was triggered by the 1918 AD eruption of Katla, a volcano beneath Iceland's Mýrdalsjökull ice cap. Floodwaters reached a peak discharge of 3×10^5 m^3 s^{-1} and transported enough sediment to extend Iceland's southeastern coastline by 3 km (Baker, 2002; O'Connor et al., 2002; Guðmundsson, 2005; Björnsson, 2009; Larsen, 2010). Although this is not a comprehensive list of Earth's largest floods, these floods rank among the most studied and are useful analogues for Icelandic jökulhlaups along the Jökulsá á Fjöllum (Baker, 2002).

MEGAFLOODS ON MARS

Megaflood evidence is not limited to Earth. Many megaflood geomorphologic features on our planet closely resemble Martian landforms and are increasingly studied as analogues for processes on Mars. Features on Mars, however, have a much larger scale than those on Earth, suggesting floods with far greater magnitudes (Baker, 2002; Burr and McEwen, 2002; Howard, 2008; Baker, 2009b; Howard et al., 2012). Scientists hypothesize that most of these floods occurred roughly 1.8—3.7 billion years ago (Burr and McEwan, 2002; Baker, 2009b) and had peak discharges between 10^6 and 10^9 m^3 s^{-1}, after adjusting for Martian gravity (an equation explained in Carr, 1979) (Burr and McEwan, 2002).

CHAPTER 6: JÖKULHLAUP GEOMORPHOLOGIC FEATURES

Jökulhlaups leave behind distinctive geomorphologic features that provide clues to flood magnitude, path, and flow dynamics. These features fall into two categories: erosional and depositional. These landforms are well-documented for the Kuray, Lake Missoula, and Lake Bonneville floods and for jökulhlaups in Iceland, particularly those originating from Vatnajökull. Despite this widespread geographic distribution, these megafloods left behind similar features that enable direct geomorphologic comparison between sites.

Nonetheless, it is crucial to note that differences in megaflood landscapes exist. The Kuray floods, for example, flowed through the Altai Mountains' deep glaciofluvial valleys rather than slicing new pathways across a bedrock plateau, leaving behind predominantly depositional features and little erosional evidence (Rudoy, 2002; Herget, 2005; Carling et al., 2009b). This is a strikingly different landscape than the basalt canyons carved by the Lake Missoula floods in the Channeled Scabland, even though the two floods had almost the same peak discharge. As another example, the Lake Agassiz floods left behind few geomorphologic features apart from a series of spillways, largely because floodwaters eroded easily through the glacial till and sedimentary rocks along their routes (Kehew et al., 2009; Katz et al., 2011; Rayburn et al., 2011).

Despite these disparate landscapes, numerous studies have developed criteria for distinguishing jökulhlaup geomorphologic features. While some landforms are uniquely formed by megafloods, others mirror those formed by smaller floods or fluvial processes, except they occur on a much larger scale (Marren, 2002; Marren and Schuh, 2009). Teasing apart these processes presents an enormous challenge to landscape interpretation, particularly in an

environment like Iceland, where—to requote Sigurdsson et al. (1995, p. 2)— "…virtually all of the major geologic processes are at work."

JÖKULHLAUP EROSIONAL FEATURES

In describing the Channeled Scabland of eastern Washington, J Harlen Bretz wrote: "The scablands are wounds only partially healed—great wounds in the epidermis of soil with which Nature protects the underlying rock" (Bretz, 1928, p. 88). Bretz's description paints an accurate picture: the tremendous power of these cataclysmic floods stripped off soil and ripped through bedrock, slicing gorges and carving cataracts. Bretz continued: "Like great scars marring the otherwise fair face of the plateau are these elongated tracts of bare, or nearly bare, black rock carved into mazes of buttes and canyons" (Bretz, 1928, p. 88). Similar topography characterizes jökulhlaup-impacted landscapes worldwide, including the paleoflood zone along the Jökulsá á Fjöllum.

Erosional Processes

Jökulhlaups erode bedrock through several mechanisms, inflicting Bretz's described "wounds" on the Earth's surface. One erosional mechanism is cavitation, a process in which the pressure in water vapor bubbles exceeds the pressure of the surrounding water due to differences in flow velocity. When these bubbles burst, they exert enormous amounts of pressure—a "shock wave"—which can carve potholes or spillways in bedrock (Baker, 1978b; O'Connor, 1993; Wohl, 1998; Tómasson, 2002; Richardson and Carling, 2005; Baker, 2009c; Carling et al., 2009b). Cavitation mostly occurs in deep and fast-flowing water (Baker, 1978b; O'Connor, 1993; Alho et al., 2005).

A second erosional process is plucking, where vertical vortices of water—called kolks—pick up ("pluck") pieces of rock that have loosened along existing planes of weakness or fracture (Figure 13) (Baker, 1978b; Benito, 1997; Richardson and Carling, 2005; Baker, 2009c; Carling et al., 2009b). Although plucking—also termed hydraulic quarrying—can carve out potholes and other scoured bedrock features, it is an especially effective mechanism for fragmenting columnar basalt along its fracture planes. This "column toppling" leads to the upstream retreat of knickpoints (notches where erosion is more pronounced) to form cataracts and gorges (Baker, 1978a,b; O'Connor, 1993; Benito, 1997; Wohl, 1998; Carling et al. al, 2009b; Baynes et al., 2015b).

Baynes et al. (2015b) concluded that plucking is the predominant bedrock erosional process during jökulhlaups. They postulated that knickpoints in the Jökulsárgljúfur canyon—near the mouth of the Jökulsá á Fjöllum—retreated hundreds of meters in a matter of days during these enormous (but short-lived) Holocene jökulhlaups (Baynes et al., 2015b). Plunge pools—depressions carved from the force of water cascading over knickpoints—can also trigger knickpoint retreat through plucking (Richardson and Carling, 2005; Baynes et al., 2015b). The turbulent water in the plunge pool exerts pressure on the headwall behind it, weakening basalt columns to the point of collapse and shifting the knickpoint upstream (Baynes et al., 2015b).

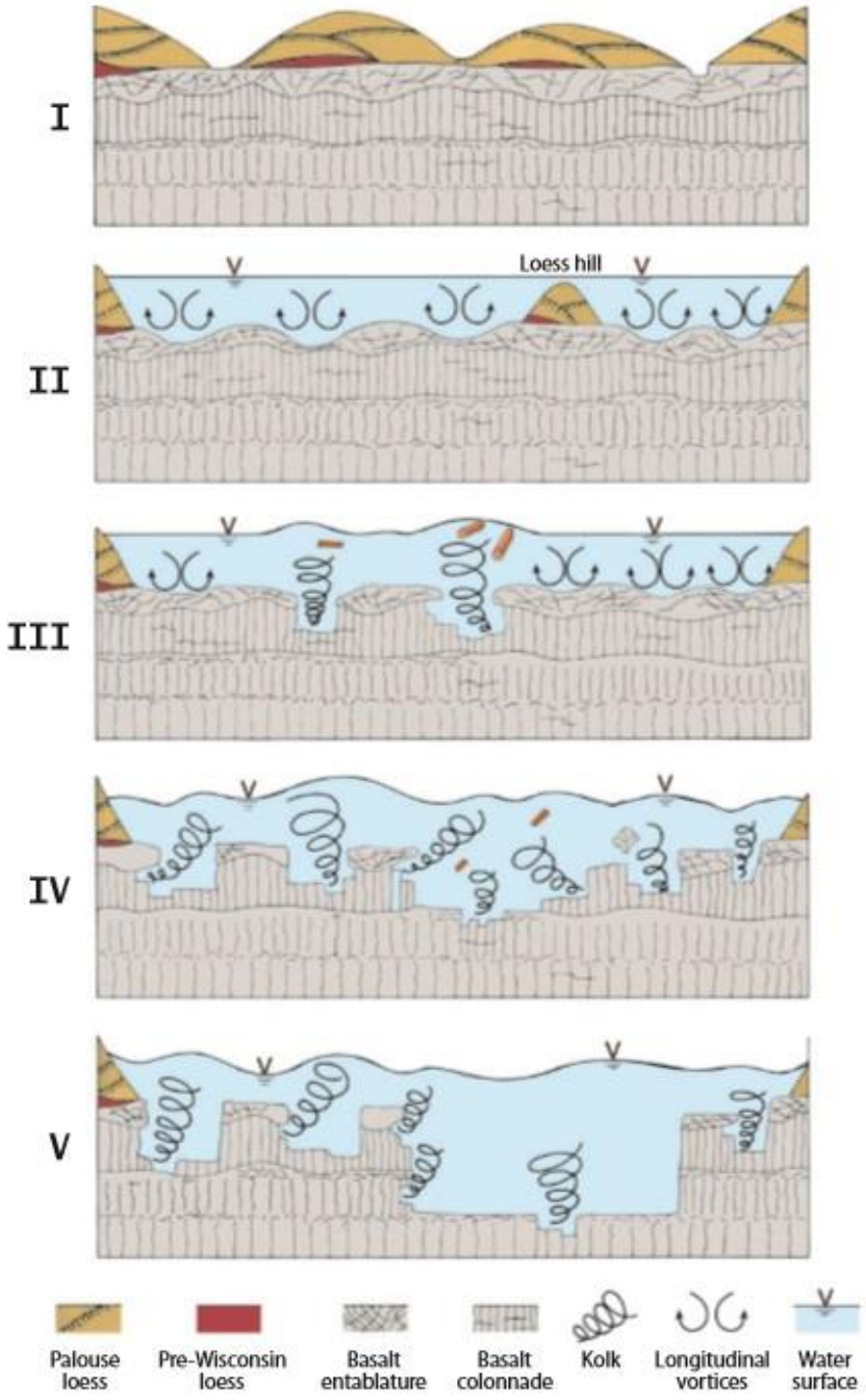

Figure 13. Jökulhlaup erosional processes in the Channeled Scabland: plucking of columnar basalt (Baker, 2009c).

Abrasion (also called corrasion) is another key jökulhlaup erosional process. Material carried in floodwaters—whether suspended or bedload—rips particles off surrounding rock, carving potholes, grooves, scours, flutes, and knickpoints (Wohl, 1998; Richardson and Carling, 2005; Carling et al., 2009b). Abrasion is the dominant erosional process acting on rocks with a "homogenous" composition—ones that lack fracture or weakness planes (Carling et al., 2009b). During Icelandic jökulhlaups, abrasion sculpts hyaloclastite and pillow lava to create streamlined hills, trimlines, and gorges—in contrast to plucking, which principally acts on columnar basalt (Carrivick et al., 2004a; Baynes et al. 2015a). Abrasion is likely the predominant erosive process during normal river flow, obscuring the distinction between fluvial and megaflood features except where this evidence exists well above current flood levels (Baynes et al., 2015b).

Gorges

Gorges are a primary feature found in jökulhlaup-impacted landscapes worldwide and have been well-documented along the Kuray, Lake Missoula, and Lake Bonneville flood routes (Baker, 1973; Baker et al., 1993; O'Connor, 2002; Rudoy, 2002; Herget, 2005; Carling et al., 2009b). Gorges are predominantly formed through plucking: floodwaters erode bedrock and cause knickpoints to retreat upstream, leaving scooped-out bedrock gorges in their wake (Baker, 1978a; O'Connor, 1993; Carling et al., 2009b; Baynes et al., 2015a,b). Lake Missoula floodwaters sliced an anastomosing maze of gorges, canyons, and spillways into the basalt surface of eastern Washington, creating "butte-and-basin" topography (Figure 14) (Baker, 1978a; Baker, 2009a; Baker, 2009c).

Figure 14. Butte-and-basin topography in the Channeled Scabland, eastern Washington (Baker, 2009c).

In Iceland, repeated Holocene jökulhlaups carved the Jökulsárgljúfur canyon, the basalt bedrock gorge through which the Jökulsá á Fjöllum flows for 28 km near its exit into the Arctic Ocean (Figure 15) (Baynes et al., 2015a,b). Waitt (2002) postulated that the river had incised most of the canyon before the Holocene jökulhlaups occurred, but that the floods enlarged it. Smaller gorges also appear further upstream.

Figure 15. Looking north downstream the Jökulsá á Fjöllum where it flows through the Jökulsárgljúfur canyon, a jökulhlaup-carved gorge (photo by author).

At Kverkfjallarani—the area in front of the Kverkjökull glacier—jökulhlaups sliced gorges up to 20 m wide and 30 m deep in hyaloclastite and pillow lava ridges (Carrivick et al., 2004a). Gorges are also found throughout the Herðubreið channel reach, notably at Vaðalda and Upptyppingar (Alho et al., 2005).

Cataracts

Cataracts—dry, abandoned waterfalls—are a key step in the process of gorge formation. As floodwaters plunge over a steep vertical drop at a knickpoint, the water erodes back the rock edge by abrasion and plucking, principally through fracturing and removal of basalt columns. This causes the knickpoints to migrate upstream (Baker, 1978a; O'Connor, 1993; Benito, 1997; Carling et al., 2009b; Baynes et al., 2015a,b). A series of knickpoints makes up a cataract; once floodwaters recede, this may resemble a set of dry bedrock steps (Richardson and Carling, 2005; Carling et al., 2009b).

Cataracts are found along the entire length of the Jökulsá á Fjöllum, notably in the study area near Herðubreið and Upptyppingar (Malin and Eppler, 1981; Waitt, 2002; Carrivick et al., 2004a; Howard et al., 2012; Carrivick et al. 2013). Jökulhlaups sculpted a series of cataracts in the Jökulsárgljúfur canyon when knickpoints such as Dettifoss, Selfoss, and Hafragilsfoss—which are present-day waterfalls along the Jökulsá á Fjöllum—retreated upstream (Baynes et al., 2015a,b). Another prominent cataract occurs at Ásbyrgi, a horseshoe-shaped dry canyon at the end of the Jökulsárgljúfur canyon that measures 1 km wide, 3 km long, and up to 90 m deep (Baynes et al., 2015a). Local legend attributes its formation to the hoof print of a horse ridden by the Norse god Odin (Bain and Averbuck, 2015); scientific research, however, reveals that it was sculpted by Holocene jökulhlaups roughly 10 ka BP (Baynes et al., 2015a).

The Lake Missoula floods sculpted a comparably-sized cataract in eastern Washington's Channeled Scabland. The basalt walls of Dry Falls extend 120 m above the canyon floor, and the canyon is 5.5 km wide. Dry Falls has two knickpoints (also known as head cuts) with plunge pools at their bases, suggesting that—like Ásbyrgi—the canyon formed by knickpoint retreat (Baker, 1978a; Baker, 2009a).

Grooves, Flutes, and Potholes

Another series of jökulhlaup erosional features are grooves, flutes, and potholes (Benito, 1997; Carrivick and Rushmer, 2006; Carling et al., 2009b). These features form when the water's sediment load—principally its bedload—scours out material from the bedrock; however, cavitation and plucking can play a role, as well. Feature orientations can provide clues to the direction of the current: longitudinal grooves extend parallel to flow direction (Baker, 1978a; Alho et al., 2005); and flutes are scalloped forms that are generally open in the downcurrent direction and are parabolic on the upstream side. Potholes are roughly circular (Richardson and Carling, 2005; Carling et al., 2009b).

These features occur on a wide range of scales: for example, the Lake Missoula floods left behind potholes up to 40 m wide (Richardson and Carling, 2005; Carling et al., 2009b). Many bedrock surfaces along the Jökulsá á Fjöllum display extensive evidence of scouring—including grooves, flutes, and potholes—at a variety of scales (Figure 16), as described by Malin and Eppler (1981); Waitt (2002); Carrivick et al. (2004a); Alho et al. (2007); Howard (2008); Howard et al. (2012); and Carrivick et al. (2013).

Figure 16. Fluting on bedrock surface near Jökulsá á Fjöllum channel. Field notebook for scale (photo by author).

Streamlined Hills

As jökulhlaups surge across a landscape, they often erode hills into a streamlined shape. Streamlined hills exist in megaflood-impacted landscapes worldwide (Baker, 2009a), and they are abundant along the Jökulsá á Fjöllum. Floodwaters have sculpted these hills to the most hydrodynamically-efficient shape possible in order to minimize drag. The result is a teardrop-shaped form—sometimes described as lemniscate—with the downstream end of the hill trailing off into a "tail" (Figure 17) (Baker, 1978a; Baker, 2002; Carrivick et al., 2004a; Baker, 2009a; Carling et al., 2009b; Howard et al., 2012). The shape also resembles an airfoil, which is logical given that airfoils are aerodynamically designed to reduce drag (for example, as with a propeller blade) (Malin and Eppler, 1981; Benito, 1997; Carrivick et al., 2004a; Baker, 2009a; Carling et

al., 2009b). Essentially, the floodwater stretches the hill by trimming material from its sides and depositing it downstream in the lee of the hill, thus creating a lengthening effect. As a result, streamlined hills often have steep sides, and the tail is composed of loose materials ranging up to boulder size (Carrivick et al., 2004a).

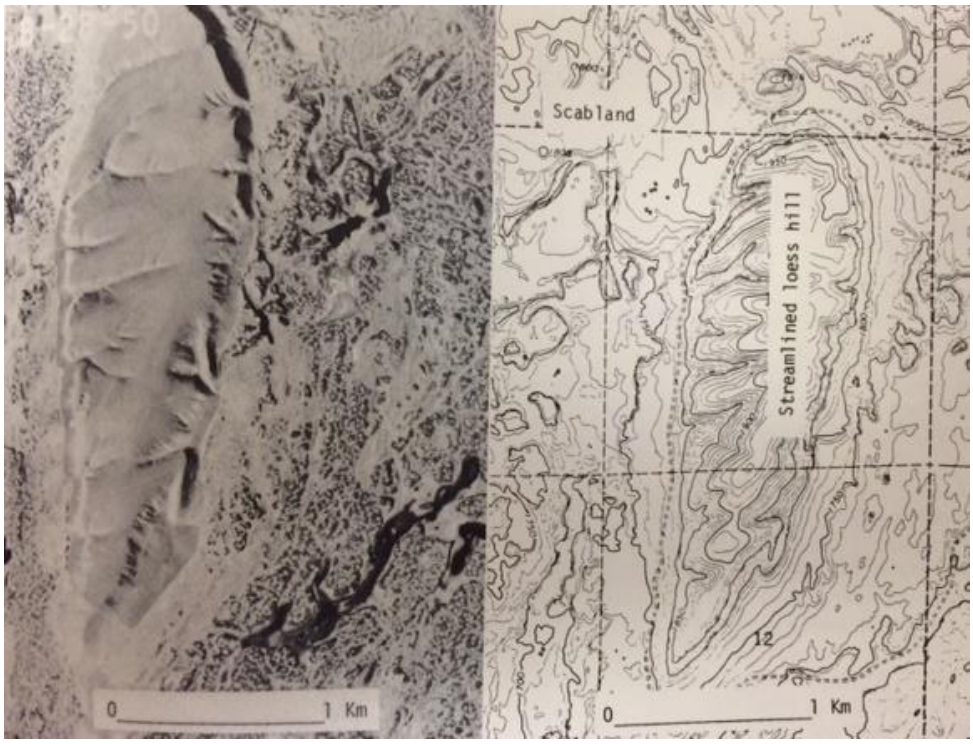

Figure 17. Streamlined loess hill in the Channeled Scabland, eastern Washington. Flow direction was from the top to the bottom of the photo; note the teardrop shape with the downstream "tail" (Baker, 1978a).

Streamlined hills sculpted by the Lake Missoula floods typically have lengths three times larger than their widths; however, it should be noted that most of these hills are composed of loess, as opposed to the hyaloclastite-pillow lava cores of Iceland's streamlined hills and ridges (Figure 18) (Baker, 1978a; Benito, 1997; Baker, 2002; Carrivick et al., 2004a; Baker, 2009a). No studies to date have reported dimension ratios of Icelandic streamlined hills.

Figure 18. Streamlined hills at Upptyppingar, Iceland (photo by author).

Spillways

Spillways are another jökulhlaup erosional landform that occurs in megaflood-sculpted landscapes across the planet. Spillways are passes—also described as "cols" or "saddles"—that form where floodwaters overtop a channel and flow into a neighboring one (Waitt, 2002; Carrivick et al., 2004a; Carrivick, 2007). The new channel is generally at a lower elevation than the spillway, causing the water to cascade over the edge and sometimes create a cataract (Waitt, 2002; Carrivick et al., 2004a). The tremendous force of water scars the bedrock with erosional features such as potholes, flutes, and grooves through plucking and abrasion (Carrivick and Rushmer, 2006; Kehew et al., 2009). Floodwaters also spread out as they move from their confining channels into these less-restrictive spillways, and flows in spillways are relatively

shallow. Floodwaters thus lose competence and can deposit their largest transported material, such as boulders (Carrivick et al., 2004a; Carrivick, 2007).

Spillways have been studied in landscapes inundated by the Kuray floods (Herget, 2005); Lake Bonneville flood (O'Connor, 1993); Lake Missoula floods (Baker et al., 1993; Baker, 2009a); and Lake Agassiz floods (Kehew et al., 2009). The Channeled Scabland is marked by an extensive network of valleys and spillways that makes up an "anastomosing" pattern (Baker, 1978a; Baker, 2009a). Spillways have also been observed in the jökulhlaup-inundated areas along the Jökulsá á Fjöllum, notably at Kverkfjallarani by Carrivick et al. (2004a). Another prominent spillway occurs at Upptyppingar and will be further discussed in Chapter 9.

Trimlines

Trimlines are another line of jökulhlaup erosional evidence. These marks are visible on the side of a mountain or ridge and show the maximum elevation of flood erosional action. Along with depositional features such as wash limits and slackwater deposits, trimlines are paleostage indicators (PSIs), which mark the upper reaches of floodwater geomorphologic impact (Carrivick, 2007; Howard et al., 2012; Carrivick et al., 2013). Trimline elevation is a crucial parameter that is plugged into hydraulic modeling programs to calculate jökulhlaup magnitude, volume, and peak discharge, as demonstrated along the Jökulsá á Fjöllum by Howard (2008); Howard et al. (2012); and Carrivick et al. (2013).

Obstacle Marks

As floodwaters rush around obstructions, they create obstacle marks. This term refers to both an erosional feature on the upstream front (described here) and a depositional feature on the downstream side (discussed later in this chapter). Erosional obstacle marks are crescent-shaped

scour marks that wrap around the upstream sides of obstacles of all sizes: from boulders to ice blocks to hills (Figure 19) (Baker, 1978a; Carling et al., 2009b; Marren and Schuh, 2009). The Kuray floods, for example, scoured out a 400 m wide, 90 m long, and 8 m deep depression in front of a hill (Herget, 2005; Carling et al., 2009b). The Lake Missoula floods also carved many obstacle marks in the Channeled Scabland (Baker, 2002).

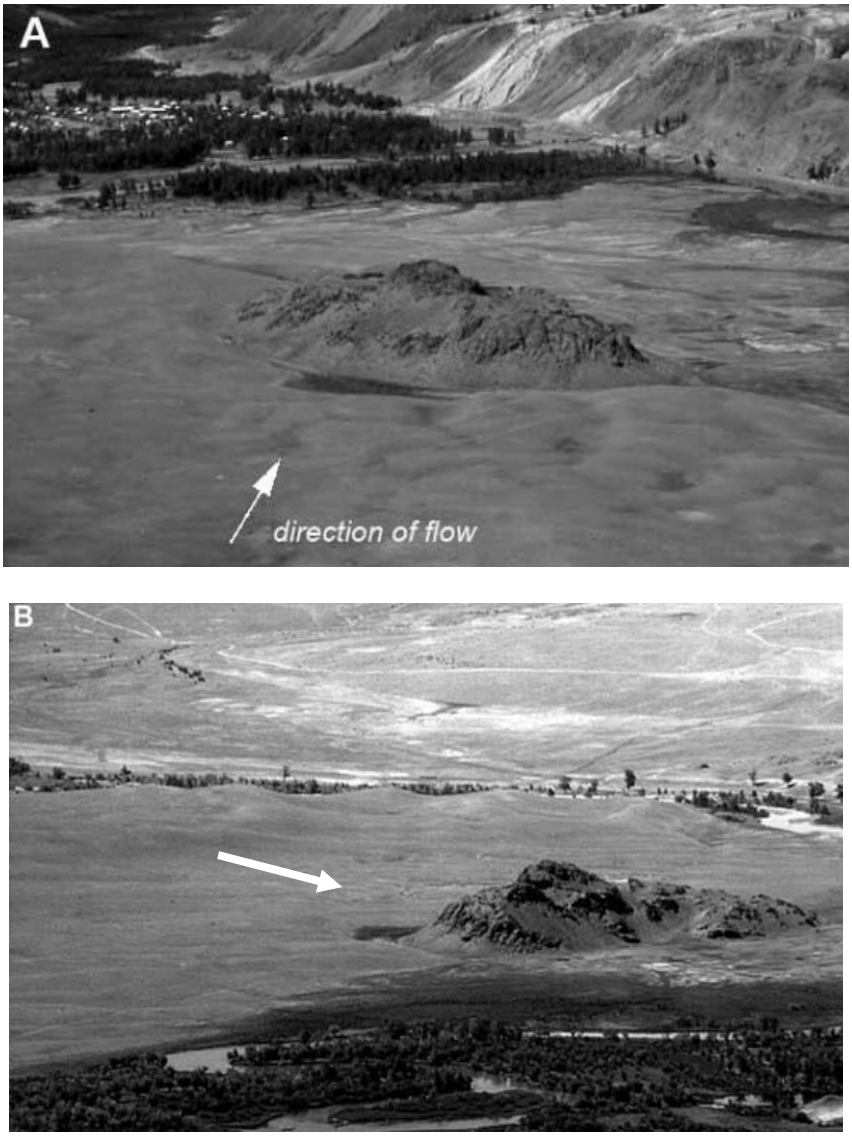

Figure 19. Obstacle marks in front of a hill in the Altai Mountains, Siberia. Floodwater direction marked by arrows (arrow added in photo B) (Herget, 2005).

Despite their prevalence in other megaflood-sculpted landscapes, obstacle marks have not been widely reported in studies on jökulhlaups along the Jökulsá á Fjöllum. However, Russell et al. (2006) observed obstacle scour marks in front of ice blocks deposited during the 1996 jökulhlaup that drained south across Skeiðarársandur. Russell et al. (2005) reported similar ice block obstacle marks from a jökulhlaup in Greenland, a finding also described by Maizels (1997).

JÖKULHLAUP DEPOSITIONAL FEATURES

Jökulhlaups have extremely high levels of energy, enabling them to fracture columnar basalt towers, excavate gorges, and streamline hyaloclastite hills. This energy gives megafloods a very high competence—they are able to transport extremely large particles. However, when water velocity decreases, competence decreases, and any particles that exceed this competence threshold will drop out of the flow and be deposited (Benito, 1997; Cenderelli and Cluer, 1998). Like their erosional counterparts, jökulhlaup depositional features often mirror those formed by fluvial and smaller flood processes, although megaflood deposits occur on a much larger scale. Nonetheless, some features are unique to jökulhlaup deposition (Marren, 2002; Marren and Schuh, 2009). The size, orientation, composition, and texture of these deposits provide insight into jökulhlaup magnitude and dynamics (O'Connor, 1993; Baker, 2002; Carrivick and Rushmer, 2006; Carling et al., 2009a; Marren and Schuh, 2009).

Boulder Clusters, Bars, and Erratics

Megafloods can transport an enormous range of particle sizes, from silt to boulders. When water competence decreases, particles with the largest mass—such as boulders—are deposited first. Some boulders are arranged in bars or clusters; others stand in isolation or in

unusual or unexpected settings (such as hill summits), earning them the title "boulder erratics." Megafloods and glaciers are among the few forces powerful enough to transport boulders; however, distinguishing between these provenances presents a significant challenge. Additionally, boulders may have been ice-rafted—trapped in ice blocks that were deposited by floodwaters, leaving behind the boulders when the ice melted (Baker, 1973; Herget, 2005).

Boulder characteristics provide clues that help to reconstruct a jökulhlaup's path and dynamics. Boulder dimensions and mass are used to calculate the flow competence, power, velocity, and depth capable of transporting them (O'Connor, 1993; Baker, 2002; Carrivick and Rushmer, 2006; Carrivick, 2007; Carling et al., 2009a; Howard et al., 2012). Boulder orientation can also indicate flow direction. Jökulhlaups generally deposit boulders with their longest axis perpendicular to flow direction (a less hydrologically efficient orientation, thus prompting deposition). Boulders are often tilted at an angle, sloping up in the downstream direction (O'Connor, 1993; Carrivick et al., 2004a). Some boulders are imbricated: they overlap in a pattern as if a row of dominos had been knocked down in the direction of flow (Figure 20) (O'Connor, 1993; Carrivick et al., 2004a).

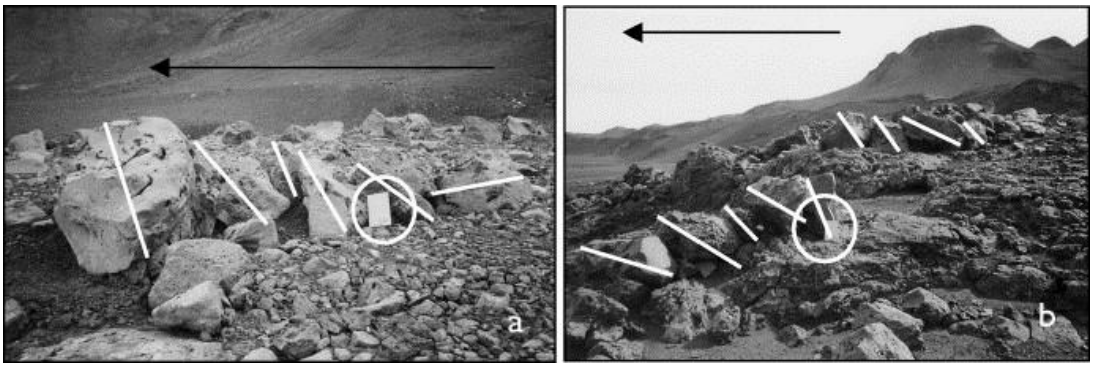

Figure 20. Imbricated boulder clusters in Kverkfjallarani, Iceland. Floodwater direction marked by arrows. White lines mark imbrication orientation. Field notebook is circled for scale (Carrivick et al., 2004a).

A boulder's composition also provides clues to its place of origin. Similarly, its degree of roundness may provide insight into how far it traveled in a flood: more rounded clasts were generally carried farther (O'Connor, 1993). Malin and Eppler (1981) also noted that rounder particles had more likely been transported by megafloods, while more angular particles had generally been moved by glaciers; however, they acknowledged that there are many exceptions to this rule and stressed that deposits must be interpreted in context.

Boulder deposits are widespread in areas inundated by the Lake Bonneville flood (O'Connor, 1993); Kuray floods (Herget, 2005); and Lake Missoula floods (Figure 21) (Baker, 1973).

Figure 21. Boulder erratic deposited by Lake Missoula floods in eastern Washington's Channeled Scabland. Note car for scale (Baker, 2009c).

Massive boulders are also littered across jökulhlaup pathways along the Jökulsá á Fjöllum. Some boulders lie in small clusters on the river banks; others are closely packed together, forming a boulder field; and erratics up to several meters in diameter perch like sentinels atop otherwise barren hills (Figures 22-23).

Figure 22. Boulder erratics perched on hills at Upptyppingar (photo by author).

Figure 23. Boulder erratic in front of Mt. Herðubreið (photo by author).

Several previous studies have examined boulder deposits along the Jökulsá á Fjöllum to calculate paleoflood competence and map flood extent, notably Maizels (1997); Waitt (2002); Carrivick et al. (2004a); Alho et al. (2005); Russell et al. (2005); and Carrivick and Rushmer (2006). Howard (2008), Howard et al. (2012), and Howard (unpublished, 2013) performed cosmogenic nuclide exposure dating on boulder erratics situated above or near the highest elevations of modeled floodwaters to determine if the erratics pre- or post-date deglaciation, and thus if they were transported by glaciers or jökulhlaups. A third possible explanation for boulder erratic placement is exhumation: boulders may have been glacially deposited and were exposed at the surface after the surrounding less-resistant sediment eroded. Boulder erratic elevation is used to hydraulically model jökulhlaup magnitude, volume, peak discharge, and inundation path (Howard et al., 2012).

Megaripples

Megaripples—also known as giant current ripples or dunes—are another jökulhlaup depositional feature. As their name suggests, megaripples have the same shape as ripples formed by fluvial or marine currents, but occur on a much larger scale (Maizels, 1997; Baker, 2002; Marren and Schuh, 2009). These features form where floodwaters spread out over a larger, unconfined area (Maizels, 1997). They are composed of coarse-grained material, mostly gravel- and pebble-sized particles; however, cobble- and boulder-sized rocks are often found on the upstream side of the dune (Baker, 1973; Maizels, 1997; Baker, 2009a; Carling et al., 2009a). The upstream face generally slopes more gently than the steeper downstream side of the ripple (Baker, 1973; Carling et al., 2009a). Flood currents push the gravel into 5—10 m thick foreset

beds where it is cross-bedded at an angle up to 30˚ (Baker, 1973; Maizels, 1997; Marren, 2002; Marren and Schuh, 2009).

Only extremely large floods are capable of creating these megaripples, making them a unique line of evidence for jökulhlaup deposition (Baker, 1973; Marren, 2002; Marren and Schuh, 2009). Megaripples can have such large wavelengths that they are indistinguishable from the ground; the pattern is only clear looking down from the air (Baker, 1973). The Lake Missoula floods produced giant current ripples spaced up to 200 m apart with 15-m-high crests (Figure 24) (Baker, 1973; Maizels, 1997; Baker, 2009a). Megaripples also appear throughout the Kuray flood-sculpted Altai Mountains in Siberia (Carling et al., 2002; Rudoy, 2002; Herget, 2005; Baker, 2009a).

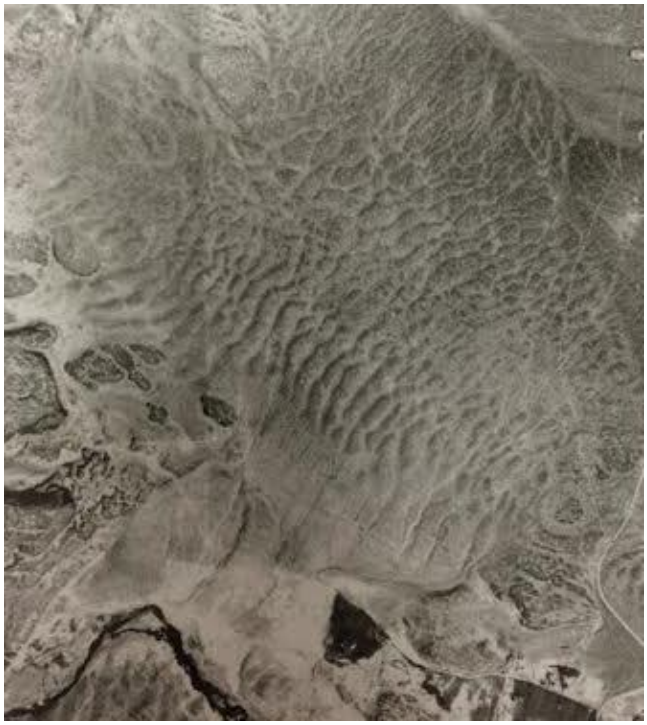

Figure 24. Giant current ripples in eastern Washington sculpted by Lake Missoula jökulhlaups. Ripples are up to 2—3 m high and spaced up to 60 m apart. Photo covers an area of roughly 9 km^2. Aerial photograph taken in 1957 (Baker, 2009a).

Along the Jökulsá á Fjöllum, giant current dunes have been reported by Malin and Eppler (1981), Waitt (2002), Alho et al. (2005), and Howard et al. (2012), although these studies do not specify dune sizes. Maizels (1997) also observed megaripples on Sólheimasandur—a sandur coming off the Mýrdalsjökull ice cap—that were 0.5 m high with 10.5 m wavelengths, likely formed by jökulhlaups with peak discharges on the magnitude of 10^4 m^3 s^{-1}.

Bars

Like megaripples, bars are another jökulhlaup depositional feature that resemble their fluvial counterparts, but occur on a much larger scale (Marren, 2002; Baker, 2009a; Marren and Schuh, 2009). Bars are categorized in terms of shape, composition, and particle orientation and size. Each of these components provides clues to flood magnitude, path, and the flood stage at which the material was deposited (Maizels, 1997; Marren, 2002; Baker, 2009a). Many bar deposits have been reworked by subsequent floods, complicating interpretation; furthermore, a bar's ultimate shape results from a combination of depositional and erosional processes (Benito, 1997; Maizels, 1997; Baker, 2009a).

Bar terminology is similarly complex. Studies of Icelandic jökulhlaups and the Lake Missoula and Lake Bonneville floods classify bars according to shape and material; however, these features are collectively described as "giant bars" in literature on the Kuray floods (Carling et al., 2002; Herget, 2005). Some publications simply categorize bars according to their predominant clast size, such as "gravel" or "boulder" bars. A variety of bar forms occur throughout the jökulhlaup-impacted areas along the Jökulsá á Fjöllum, as reported by Waitt (2002); Alho et al. (2005); Howard et al. (2012); and Carrivick et al. (2013).

Longitudinal Bars

Jökulhlaup-deposited longitudinal bars are tall, streamlined, and principally composed of gravel. Their longest axis is oriented parallel to flow direction (Baker, 1978a; Baker, 2009a). They form on wide, flat surfaces where floodwaters flow uniformly—not in places where the water's path is suddenly restricted or expands (Baker, 1978a).

Expansion Bars

Expansion bars—the largest bar type—form when floodwaters spill out (or "expand") from a confined channel to a wide, unconstrained area (Baker, 1973; O'Connor, 1993; Maizels, 1997; Carling et al., 2009a; Marren and Schuh, 2009). Although their particle size varies, they are largely made up of boulders, possibly due to winnowing—a process in which high-energy currents strip off finer particles, leaving behind an "armored" top coating of boulders (Baker, 1973; O'Connor, 1993; Maizels, 1997). In studying Lake Bonneville flood deposits, O'Connor (1993) found that many expansion bars increased in height with increasing distance downstream. In both the Lake Bonneville and Lake Missoula flood pathways, expansion bars were deeply incised where floodwaters and subsequent jökulhlaups continued to slice channels after bar deposition (Baker, 1973; Baker, 1978a; O'Connor, 1993; Carling et al., 2009a).

Pendant Bars

Pendant bars form when floodwaters lose velocity and deposit material downstream of a large obstacle, such as a protruding bedrock formation or a bend in the flood channel (Baker, 1973; Baker, 1978a; O'Connor, 1993; Maizels, 1997; Baker, 2009a; Carling et al., 2009a). These bars are composed of gravel and larger particles (up to boulder size) and have the same shape as streamlined hills in order to minimize drag and increase hydraulic efficiency (Baker, 1973; Baker, 1978a). The Lake Bonneville flood generated pendant bars up to 2 km long

(O'Connor, 1993; Maizels, 1997). Baker (1978a) measured pendant bars from the Lake Missoula floods that stretched over 3.2 km and reached heights of 30 m (Maizels, 1997). Although not described specifically as pendant bars, the Kuray floods deposited gravel bars of even greater size, with the largest standing 120 m high and extending over 5 km (Carling et al., 2002; Herget, 2005).

Eddy Bars and Slackwater Deposits

As jökulhlaups surge across a landscape, tongues of water are pushed up into tributary valleys. Separated from the flood's main pathway, this swirling water loses velocity and deposits material near the tributary mouth, forming an obstacle across the tributary valley (Baker, 1973; Baker, 1978a; O'Connor, 1993; Maizels, 1997; Carrivick and Rushmer, 2006; Baker, 2009a; Carling et al., 2009a). These deposits—known as eddy bars—are made up of a wide variety of particles, from silt to boulders. Although some layers are well-sorted, eddy bars typically contain a mélange of particle sizes and orientations, reflecting the turbulent swirl of the backwater eddies; and compared to other bar types, they are poorly sorted (Baker, 1973; Baker, 1978a; Maizels, 1997).

Materials deposited up-valley of eddy bars are referred to as slackwater deposits. High-energy floodwaters push larger clasts farther up a tributary valley, after which the lower-velocity receding flow deposits smaller particles (such as fine gravel) closer to the tributary mouth as the water drains back to the main flood channel (Baker, 1973; Baker, 1978a). Overall particle size, however, generally decreases with increasing distance up a tributary valley: as flow velocity slows, larger particles are deposited first, with sand, silt, and clay sediments settling out farther up the valley. Furthermore, deposit thickness tends to decrease upstream since less sediment is

transported as the water flows farther and loses competence. Many sediment bed orientations reflect this up-valley flow direction, as well (Baker, 1973; Baker, 1978a; Baker and Bunker, 1985; Maizels, 1997).

In areas of particularly low-energy flows (where water "ponds"), the finest particles fall out of suspension and form rhythmites—repeating layered beds of sand, silt, and/or clay (Figure 25) (Baker 1973; Baker and Bunker, 1985; O'Connor, 1993; Maizels, 1997). Each sequence is upward-fining, usually consisting of coarse sand on the bottom and silt or clay at the top (Baker, 1973; Baker and Bunker, 1985; Maizels, 1997). While it is tempting to assign each sequence to one flood event, a single flood can deposit multiple rhythmites. Surges can occur when water levels rise—for instance, if water breaks through a cataract upstream in the main flood channel. This pulse of water carries an extra influx of sediment into tributary valleys, depositing rhythmites on top of previously-formed sequences. Floodwaters can also rework these fine-grained sediments, thus complicating the match between rhythmite sequences and flood events (Baker, 1973; Baker and Bunker, 1985; Maizels, 1997).

Figure 25. Rhythmite sequence in a slackwater area in Skeiðarársandur, formed by the 1996 jökulhlaup from Grímsvötn (Russell et al., 2005).

O'Connor (1993) reported on eddy bars and slackwater deposits from the Lake Bonneville flood; and Baker (1973), Baker, (1978a), and Baker and Bunker (1985) thoroughly documented those from the Lake Missoula floods. Along the Jökulsá á Fjöllum, Carrivick et al. (2004a,b) observed extensive slackwater deposits at Kverkfjallarani and concluded that these could only have been deposited by high-magnitude, sediment-laden floods. Slackwater deposits serve as paleostage indicators, and their elevations are input into hydraulic models to calculate flood parameters (Baker, 1978b; Carrivick et al., 2004a,b; Carrivick, 2007).

Point Bars

Point bars—like many jökulhlaup depositional features—mirror their fluvial counterparts but occur on a much larger scale. Point bars form on the inside of channel curves where flow velocity decreases and deposits material (O'Connor, 1993). Those deposited by jökulhlaups are often composed of gravel and sand covered by a layer of cobbles and boulders, the latter sequence forming when high-energy flows strip off finer particles from the top layer of the bar (Maizels, 1997).

Wash limits

Wash limits mark the maximum extent of jökulhlaup deposits (Carrivick et al., 2004a; Carrivick, 2007; Howard et al., 2012; Carrivick et al., 2013), such as the highest point at which slackwater deposits occur in a tributary valley (Baker, 1978b). Like trimlines—their erosional counterpart—wash limits are paleostage indicators, and we use their dimensions (such as elevation) in hydraulic models to estimate paleoflood parameters (Carrivick, 2007; Howard et al., 2012).

Ice blocks and Kettle Holes

As jökulhlaups exit a glacier, raging floodwaters break off blocks of ice. These can be enormous: the massive 1996 Grímsvötn jökulhlaup deposited ice blocks with diameters as large as 55 m on Skeiðarársandur (Russell et al., 2005). As flow loses velocity and competence, the ice blocks drop out of suspension. This leads to the formation of several depositional features, namely kettle holes and obstacle marks (Maizels, 1997; Russell et al., 2005; Russell et al., 2006; Marren and Schuh, 2009). These features produce a hummocky, uneven terrain—a useful indicator of a jökulhlaup-impacted landscape (Figure 26) (Maizels, 1997; Russell et al., 2005; Russell et al., 2006).

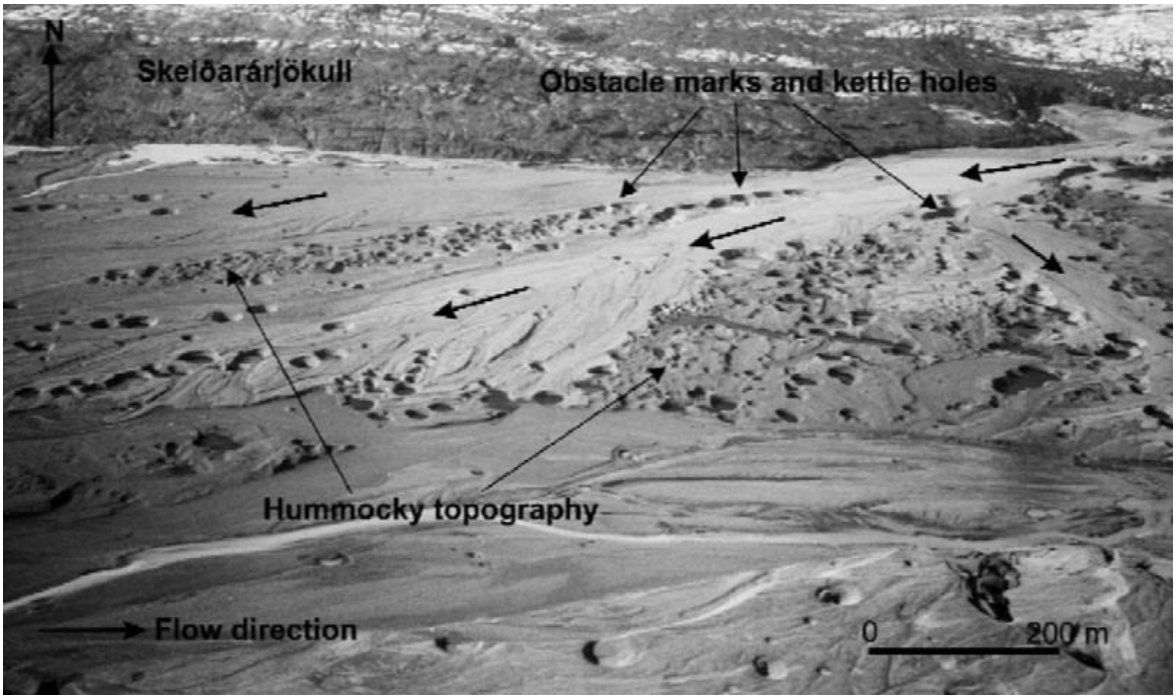

Figure 26. Hummocky topography on Skeiðarársandur resulting from ice block deposition, kettle holes, and obstacle marks from the 1996 Grímsvötn jökulhlaup. Skeiðarárjökull glacier in background. Floodwater direction marked by arrows (Russell et al., 2006).

Floodwaters continue to flow and deposit sediment around the dropped ice blocks. The ice eventually melts, leaving a depression called a kettle hole. These holes can exceed 20 m in diameter and are often partially filled in with sediment (Figure 27). This sediment can be windblown or can collapse in from the sides of the hole (Russell et al., 2005; Russell et al., 2006; Marren and Schuh, 2009). Melting ice blocks also deposit the material that was frozen inside them, leaving behind a sediment rim around the kettle hole, or—if the block had a large sediment load and was only partially buried—a raised mound in the hole (Figure 28) (Maizels, 1997; Russell et al., 2005; Russell et al., 2006; Marren and Schuh, 2009).

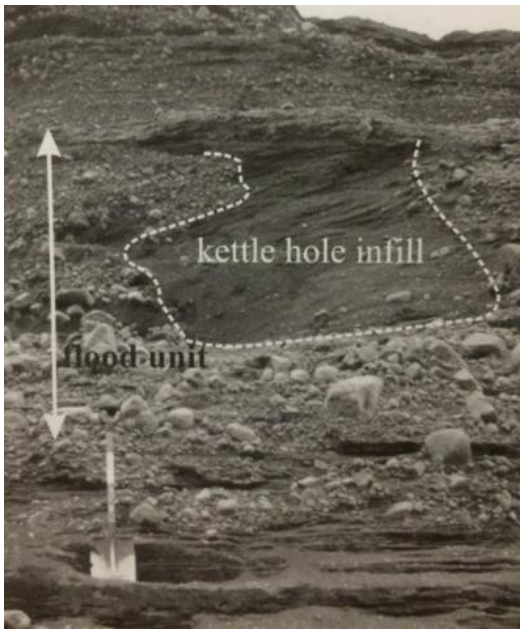

Figure 27. Kettle hole amidst jökulhlaup deposits, infilled with aeolian sand. Shovel for scale (Marren and Schuh, 2009).

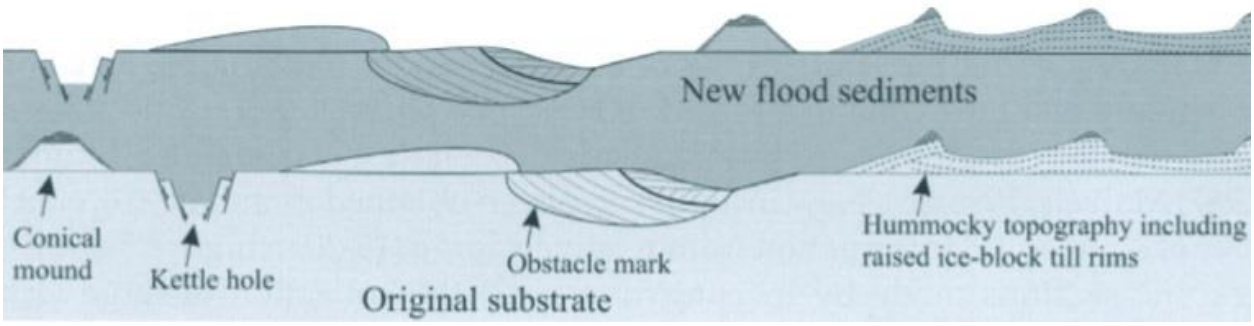

Figure 28. Diagram of depositional features from two jökulhlaups. Note hummocky topography; obstacle marks; kettle holes; and conical mound and till rims from sediment infilling (Russell et al., 2005).

Larger ice blocks are deposited closer to the glacier, with block size decreasing downstream. These blocks often form chains as increasingly smaller blocks are deposited in the lees of their larger doppelgängers (Russell et al., 2005; Russell et al., 2006; Marren and Schuh, 2009). However, Russell et al. (2006) noted some exceptions to this rule. First, while smaller blocks may drop out of the water column in the shadow of larger blocks, large blocks that are still floating may have too much momentum to be deposited and will continue downstream, eventually settling out past the smaller blocks. Second, as water volume and velocity wane towards the end of the flood, smaller blocks that recently broke off the glacier are deposited closer to the ice margin among the previously-stranded larger blocks (Russell et al., 2006).

Jökulhlaups often drop ice blocks at higher elevations where flow velocity decreases, such as channel margins or the top of a bar or hill. Here, the blocks stand above the main flood pathway and avoid complete inundation. As water rushes past a stranded block, it scours out a crescent-shaped hollow around its front and sides, forming an erosional obstacle mark (discussed in a previous section). Floodwaters deposit this material in the lee side of the ice block where they lose momentum (Maizels, 1997; Russell et al., 2005; Russell et al., 2006; Marren and

Schuh, 2009). Finer-grained sediments settle out first, trailing to larger clasts farther downstream in the ice block shadow (Maizels, 1997). These deposits are also referred to as obstacle marks, and it is important to distinguish them from the erosional feature with the same name (Maizels, 1997; Carrivick et al., 2004a; Russell et al., 2005; Russell et al., 2006; Marren and Schuh, 2009).

Rip-up Clasts

Rip-up clasts are another jökulhlaup depositional feature. As a jökulhlaup drains, it rips frozen chunks of sediment off of the glacier bed or channel sides. Since these blocks of sediment are frozen, they remain intact in the flow and are deposited when floodwaters lose the competence required to transport them. The blocks eventually thaw, leaving behind a cohesive mass of sediment—also called an intraclast—that is usually distinguishable in sedimentary profiles. Rip-up clasts consist of coarse-grained particles; in Iceland, diamicton (poorly sorted sediment (Benn and Evans, 2010)) is a common constituent (Figures 29-30) (Russell and Knudsen, 2002; Russell et al., 2005; Marren and Schuh, 2009). Intraclasts are deposited by fluvial processes, as well; however, these are usually composed of clay and are smaller than jökulhlaup rip-up clasts, whose diameters have measured up to 3 m in Iceland (Marren and Schuh, 2009). Rip-up clasts were extensively reported in deposits from the massive 1996 jökulhlaup that drained across Skeiðarársandur (Russell and Knudsen, 2002; Russell et al., 2005; Russell et al., 2006; Marren and Schuh, 2009). Rip-up clasts from Icelandic jökulhlaups provide strong evidence that the flood eroded subglacial bed material as it exited the glacier (Russell and Knudsen, 2002; Russell et al., 2005; Russell et al., 2006).

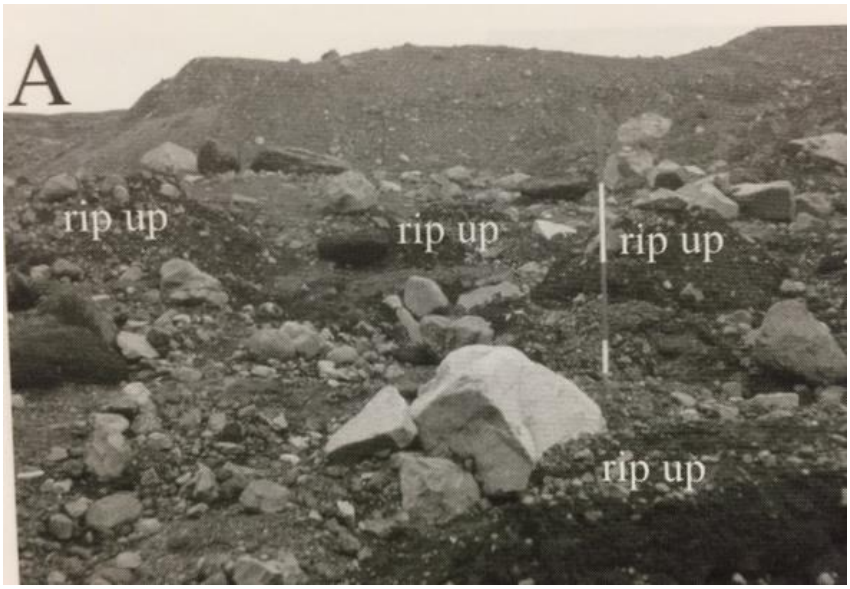

Figure 29. Rip-up clasts deposited by the 1996 Grímsvötn jökulhlaup on Skeiðarársandur. Survey pole is 2 m long for scale (Marren and Schuh, 2009).

Figure 30. Rip-up clast on Skeiðarársandur, Iceland (Russell et al., 2005).

Jökulhlaup Sedimentology

As with geomorphologic features, the orientation, size, composition, sorting, and texture of deposited sediments provide vital clues that help reconstruct flood magnitude and path (Marren, 2002). Furthermore, sedimentological structures can point to the flood stage at which material was deposited (rising or waning), as well as whether sediments were reworked after deposition (Marren, 2002; Russell and Knudsen, 2002; Russell et al., 2005; Marren and Schuh, 2009). As with geomorphologic features, sedimentological structures often resemble those created by rivers or normal-sized floods, and distinguishing landforms unique to megafloods presents a considerable challenge (Marren, 2002; Marren and Schuh, 2009).

Marren (2002) and Marren and Schuh (2009) described the principal flags marking jökulhlaup deposits in the sedimentary record, although they cautioned that some of these are not unique to jökulhlaup deposition and must be interpreted in context: 1) hyperconcentrated deposits, which reflect an extremely large volume of sediment: larger than what could be transported by fluvial or normal flood processes, yet less concentrated than a debris flow; 2) clast orientation indicating flow in one direction: clasts are uniformly oriented at both a local scale and at points throughout the channel; 3) upwards-coarsening (inversely graded) sediment layers; and 4) large foreset beds (5—10 m thick) composed of coarse gravel (Marren, 2002; Marren and Schuh, 2009). Malin and Eppler (1981) also reported that jökulhlaup deposits were generally better-sorted than glacial deposits. In addition to flood dynamics, sedimentology helps to reconstruct flood timing; for example, if a sediment layer shows evidence of erosion, it may have been the top layer of a jökulhlaup depositional sequence, which was then eroded during its surface exposure and later buried by deposits from a subsequent flood (Marren, 2002).

Although this paper focuses on the geomorphologic features of jökulhlaups, several studies provide an extensive review of jökulhlaup sedimentological evidence in Iceland, notably: Maizels (1997); Marren (2002); Russell and Knudsen (2002); Carrivick et al. (2004b); Russell et al. (2005); Russell et al. (2006); Marren and Schuh (2009); and Marren et al. (2009).

CHAPTER 7: JÖKULHLAUP HISTORY ALONG THE JÖKULSÁ Á FJÖLLUM

By the early Holocene—roughly 10.3 ka BP—Iceland's ice sheet had retreated from the central highlands (Geirsdóttir et al., 2009); and by around 8700 BP, all that remained was a handful of ice caps, including Vatnajökull (Ingólfsson et al., 2010). Jökulhlaups have drained from Vatnajökull along the Jökulsá á Fjöllum channel throughout the Holocene; however, intense debate exists over flood timing and magnitude (Waitt, 2002; Alho et al., 2005; Marren et al., 2009; Howard et al., 2012; Carrivick et al., 2013). Researchers have used a variety of tools to reconstruct a Holocene jökulhlaup timeline, including: geomorphologic evidence; sedimentology; hydraulic modeling; tephrochronology; and cosmogenic nuclide exposure dating. These methods will be discussed in detail in Chapters 9 and 10. These Holocene jökulhlaups likely drained over the course of mere days, demonstrating the importance of catastrophic events in the geologic record as opposed to gradual processes (Björnsson, 2002; Baynes et al., 2015b).

Most studies identify two exceptionally large Holocene jökulhlaups along the Jökulsá á Fjöllum. Tephrochronological records suggest that one of these floods occurred in the early Holocene between 9000 and 8000 BP (Waitt, 2002; Alho et al., 2005; Alho et al., 2007). Baynes et al. (2015a,b) dated this flood to 10 ka—9000 BP using cosmogenic nuclide exposure dating of bedrock in the Jökulsárgljúfur canyon. Alho et al. (2005) reported that Sæmundsson (1973) and Waitt (1998) extended the flood's lower time constraint to 7100 BP. Similarly, Howard et al. (2012) concluded that this catastrophic jökulhlaup occurred between 9000 and 7100 BP. A second cataclysmic flood occurred between 2500 and 2000 BP (Tómasson, 2002; Waitt, 2002; Alho et al., 2005; Kirkbride et al., 2006). Baynes et al. (2015a,b) cited evidence for a slightly

younger flood (2000—1500 BP), whereas Alho et al. (2005) cited studies by Sæmundsson (1973) and Waitt (1998) which expanded the time window to 2900—2000 BP.

Using geomorphologic field observations and hydraulic modeling, Alho et al. (2005) determined that the largest jökulhlaup in the Jökulsá á Fjöllum had an estimated peak discharge of 0.9×10^6 m^3 s^{-1}, a figure also cited by Marren et al. (2009); Baynes (2012); and Baynes et al. (2015a,b). However, Alho et al. (2005) did not specify whether this discharge occurred during the early Holocene flood (about 9000—8000 BP), the late Holocene event (about 2500—2000 BP), or both.

Howard et al. (2012) found geomorphologic evidence near Mt. Herðubreið, which estimated a peak discharge of $2.2—4.5 \times 10^7$ m^3 s^{-1} when plugged into hydraulic models. This magnitude would make this the largest known flood in Earth history, surpassing both the Kuray floods (1.8×10^7 m^3 s^{-1}) and the Lake Missoula floods (1.7×10^7 m^3 s^{-1}) (Baker et al., 1993). Howard et al. (2012) hypothesized that this catastrophic jökulhlaup swept through the Jökulsá á Fjöllum channel between 9000 and 7100 BP.

The millennia between 8000 and 4000 BP saw a series of smaller jökulhlaups; deposits from at least 16 floods have been found along the Jökulsá á Fjöllum (Waitt, 2002; Kirkbride et al., 2006; Alho et al. 2007; Baynes et al. 2015a,b). Carrivick et al. (2013) reported that this pattern continued up to 3000 BP. These floods had estimated peak discharges ranging from $0.2—0.7 \times 10^6$ m^3 s^{-1} (Tómasson, 2002; Waitt, 2002; Alho et al., 2005; Kirkbride et al., 2006; Alho et al., 2007). A few studies have discerned specific flood events during this period, notably a jökulhlaup roughly 5000 BP (Baynes et al., 2015a,b) and another flood between 4400 and 4000 BP (Kirkbride et al., 2006; Carrivick et al., 2013).

Jökulhlaups occurring after the last major Holocene event (2500—2000 BP) have had considerably smaller magnitudes. At least nine jökulhlaups flowed through the Jökulsá á Fjöllum between 1477 and 1730 with peak discharges on the order of 10^4 m^3 s^{-1} (Waitt, 2002; Knudsen and Russell, 2002; Alho et al., 2005; Alho et al., 2007; Marren et al., 2009). A jökulhlaup in the channel in 2002 peaked at a mere 2.6 x 10^3 m^3 s^{-1} (Alho et al., 2007; Marren et al., 2009). Timing and magnitude of the largest Holocene jökulhlaups along the Jökulsá á Fjöllum are summarized in Figure 31.

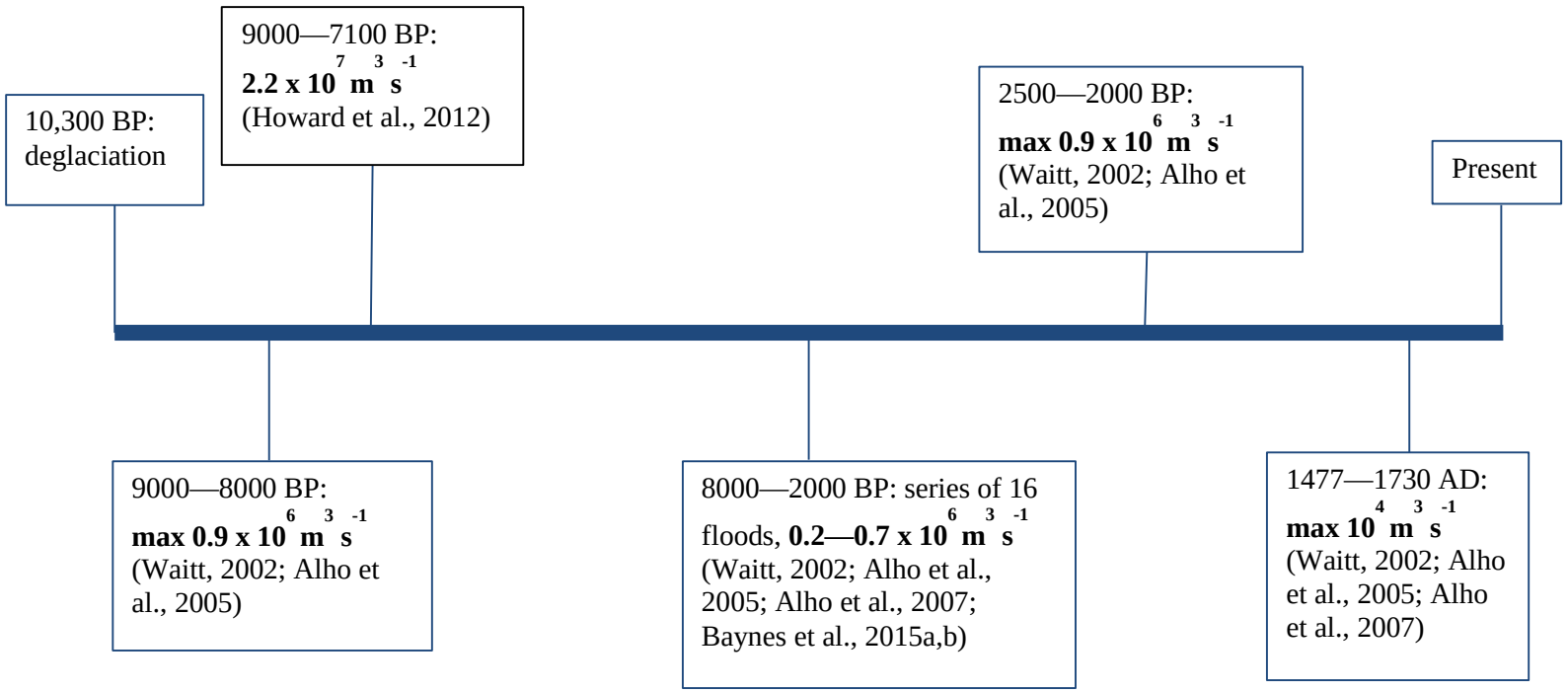

Figure 31. Timeline of the largest jökulhlaups along the Jökulsá á Fjöllum during the Holocene from deglaciation to present.

PART II: REVIEW AND CRITIQUE OF CURRENT EVIDENCE

CHAPTER 8: STUDY AREA

FIELD SITE

General Topography

This project focuses on the area around Mt. Herðubreið, a tuya whose name translates to "broad-shouldered" in Icelandic and whose local pseudonyms include "the Queen of the Mountains" and "the wedding cake" (Figure 32) (Howard et al., 2012; Bain and Averbuck, 2015). Field work was primarily conducted along an approximately 40 km stretch of the Jökulsá á Fjöllum between Vaðalda (941 masl) and Arnardalsalda (648 masl)—roughly 30 km and 70 km from the river's exit at Vatnajökull, respectively. The study area extended about 25 km on each side of the river (Figure 33). The region is situated on a plateau roughly 500—700 masl. Several tuyas and ridges rise up to around 1000 masl; Mt. Herðubreið is the highest with an elevation of 1682 masl.

Figure 32. Mt. Herðubreið (1682 masl), pictured at Herðubreiðarlindir, the campsite which our team used as a base from which to conduct our field work (photo by author).

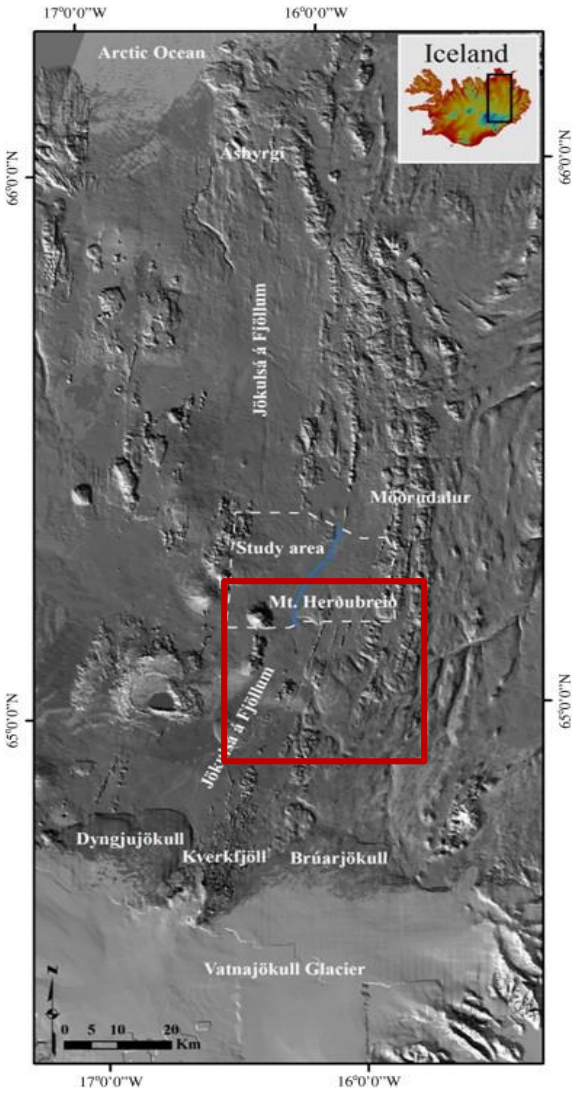

Figure 33. Jökulsá á Fjöllum's course from Vatnajökull to the Arctic Ocean. Study area marked by red box. Howard et al.'s (2012) study area marked by white dashed box (modified from Howard et al., 2012).

Like much of Iceland's central highlands, the area is underlain by basalt lava flows composed of a'a, pahoehoe, and columnar basalt. These beds are exposed on the surface in some places, while other areas are covered by igneous material including tephra, pumice, basalt sand, and rocks ranging in size from pebbles to boulders up to several meters in diameter (Figures 34-37) (Howard et al., 2012). Many of these rocks—particularly boulders on hill summits—display

ventifaction, resulting from abrasion by aeolian particles (Howard, unpublished, 2013). In some places, aeolian processes have raked the surface material into regular patterns, such as alternating bands of dark basalt pebbles and white tephra and pumice (Figure 38).

Figure 34. Lava flows partly covered by mix of pumice, tephra, and aeolian sediments (light-colored deposits); Mt. Herðubreið in background (photo by author).

Figure 35. Pahoehoe lava flows at Herðubreiðarlindir, with Mt. Herðubreið in the background (photo by author).

Figure 36. Jökulsá á Fjöllum channel lined with columnar basalt at Upptyppingar bridge during the day (photo by author).

Figure 37. Jökulsá á Fjöllum channel lined with columnar basalt at Upptyppingar bridge at dusk (photo by author).

Figure 38. Pumice, tephra, and aeolian sediments (light-colored deposits) and pebble-cobble deposits, swept into striped pattern by wind at Upptyppingar (photo by author).

Most of the study area is underlain by tephra-rich Vitrisols, and erosion is rampant throughout the region. The area is largely unvegetated, although clusters of grasses and bushes grow atop small patches of Andisols in wetlands adjacent to rivers and lakes (Figure 39). The landscape is also marked by a scattering of rofabards linked to erosion that has predominantly occurred since Norse settlement roughly 1100 years ago (Figure 40) (Arnalds, 2000; Arnalds, 2005b; Arnalds, 2008).

Figure 39. Vegetation in study area. Clockwise from top left: Patch of vegetation covering the shores of Þríhyrmngsvatn lake near Mt. Herðubreið; Vegetation surrounding tributary stream running through Herðubreiðarlindir; Tufts of grass clinging to Vitrisols on the banks of the Jökulsá á Fjöllum near Mt. Herðubreið; Isolated patches of vegetation growing on Vitrisols on the summit of Arnardalsalda (photos by author).

Figure 40. Rofabards near Mt. Herðubreið (photo by author).

Geology

The study site's plateau consists of two interspersed lava units with a basic—intermediate composition: 1) lava formed during the Holocene between 11 ka and 1100 years ago; and 2) Upper Pleistocene lava erupted supraglacially or during interglacial periods between 0.8 mya and 11 ka (Jóhannesson and Saemundsson, 1998a,b). Most tuyas and ridges—namely Upptyppingar (1084 masl) (Figure 41), Herðubreiðartögl (1070 masl), and Herðubreið—formed from subglacial eruptions during the late Pleistocene and consist of basic and intermediate hyaloclastite, pillow lava, and sediments (Jóhannesson and Saemundsson, 1998a,b; Guðmundsson, 2005; Howard et al., 2012).

Figure 41. Upptyppingar. Note columnar basalt and lava flows in foreground (photo by author).

Vaðalda is an anomaly among these mountains, formed from lava flows during supraglacial or interglacial eruptions during the late Pleistocene (Jóhannesson and Saemundsson, 1998a,b). The summits of Arnardalsalda and Herðubreið are also composed of this supraglacial—interglacial unit, although their bases are made up of hyaloclastite (Figures 42-43) (Jóhannesson and Saemundsson, 1998a,b). Preusser (1976) attributed Herðubreið's structure to a

subglacial volcano whose peak reached above the glacier surface, extruding a summit cap of subaerial lava (Guðmundsson, 2005).

Figure 42. Hyaloclastite outcrops on the side of Upptyppingar; Mt. Herðubreið in the background (photo by author).

Figure 43. Hyaloclastite ridge near Mt. Herðubreið (photo by author).

VATNAJÖKULL

Vatnajökull is Europe's largest ice cap, covering 8100 km^2 in the island's southeastern corner (Björnsson, 2002; Sjöberg et al., 2004; Pagli et al., 2007). It is a remnant of the ice sheet that retreated across Iceland roughly 10 ka BP (Thoma et al., 2001; Geirsdóttir et al., 2009). Ice is up to 900 m thick (Pagli et al., 2007), with an average thickness of 400 m (Fleming et al., 2007; Auriac et al., 2013). Glacier tongues radiate from the central ice cap in all directions, and a network of rivers drains glacial meltwater (Figures 44-45) (Hannesdóttir et al., 2015). Vatnajökull is the source of the Jökulsá á Fjöllum, as well as the jökulhlaups that have surged down the river's channel throughout the Holocene.

Figure 44. Vatnajökull ice cap, looking south from Holuhraun lava field (photo by author).

Figure 45. Vatnajökull ice cap. Photo taken from Kverkfjallarani looking south at Kverkjökull glacier, one of the Jökulsá á Fjöllum's exit points (photo by author).

Tectonic Setting and Volcanism

Vatnajökull straddles two major geothermal features. It sits atop the Mid-Atlantic Ridge and the eastern edge of the Eastern Volcanic Zone; and the mantle plume is situated beneath the ice cap's northwestern corner (Gudmundsson and Högnadóttir, 2007; Pagli et al., 2007). At least five volcanic systems lie beneath Vatnajökull, and several central volcanoes protrude above the ice surface (Figure 46) (Björnsson, 2002; Sigmundsson, 2006; Gudmundsson and Högnadóttir, 2007; Pagli et al., 2007). Grímsvötn (1719 masl) has been the most active since Norse settlement (Sigmundsson, 2006), tallying over 75 eruptions (Gudmundsson and Högnadóttir, 2007), the most recent of which was in 2011 (Global Volcanism Program, 2013; Icelandic Meteorological Office (IMO), 2015). Besides Grímsvötn central volcano, the volcanic system includes Þórðarhyrna volcano and the Laki and Gjálp fissures, which dramatically erupted in

1783 and 1996, respectively (Sigmundsson, 2006; Sturkell et al., 2006; Gudmundsson and Högnadóttir, 2007; Gudmundsson et al., 2008; Thordarson and Höskuldsson, 2008).

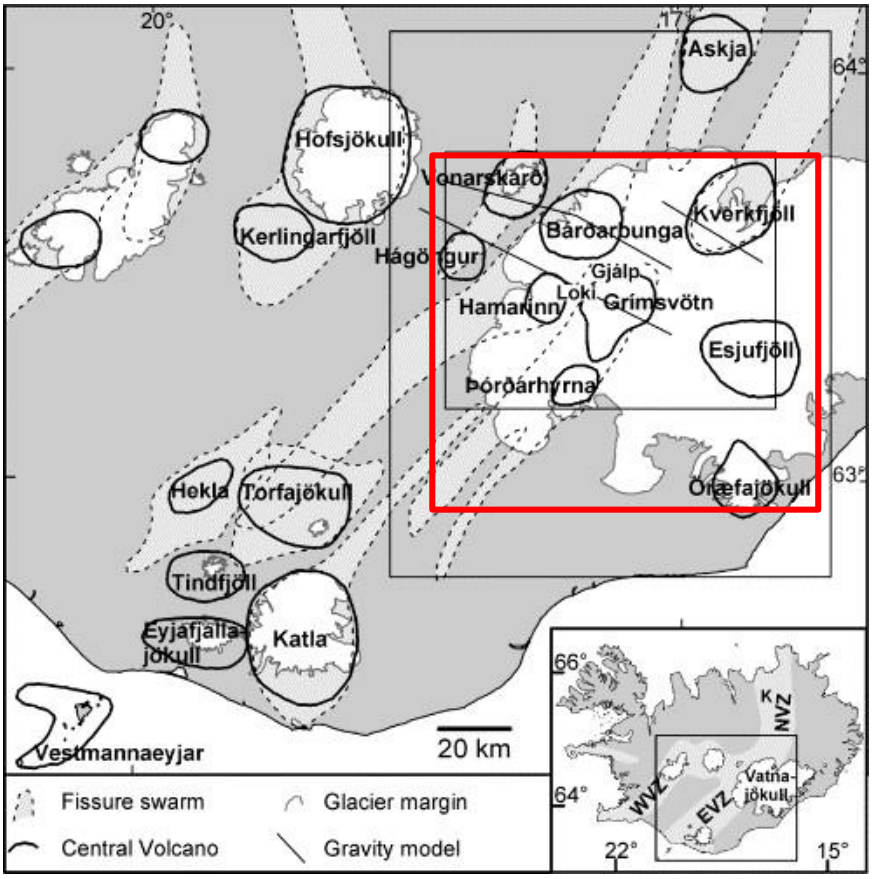

Figure 46. Volcanic systems in southern Iceland. Systems beneath Vatnajökull are marked by the red box (modified from Gudmundsson and Högnadóttir, 2007).

From 1783 to 1784, the Laki fissure eruption poured out 15.1 km^3 of lava across an area southwest of Vatnajökull (Thordarson and Höskuldsson, 2008; Mikhail, 2015). Although the lava swallowed 565 km^2 of land—much of it farmland—the most harmful effect of the Laki eruption was the enormous quantity of sulphur dioxide (SO_2) that it pumped into the atmosphere (Þórðarson, 2005; Thordarson and Höskuldsson, 2008; Mikhail, 2015). As the sulphur-rich magma spewed out of surface vents, it degassed, releasing roughly 120 megatons of SO_2

(Gudmundsson et al., 2008; Mikhail, 2015). The SO_2 reached an altitude of 10—15 km, combined with moisture in the atmosphere to produce around 200 megatons of sulfuric acid aerosol (H_2SO_4-), and was carried east by the polar jet stream. This toxic plume spread across the Northern Hemisphere, covering Europe with a sulfuric "haze" within a mere few weeks (Þórðarson, 2005; Mikhail, 2015). Sulfuric acid and fluorine (released in tephra) mixed with precipitation, wiping out a sizable amount of Iceland's flora and proving lethal to over half of the island's livestock, who died after grazing on the toxic grass (Þórðarson, 2005; Gudmundsson et al., 2008). This environmental catastrophe triggered a famine which killed 13,000 people—a fifth of Iceland's population (Þórðarson, 2005; Mikhail, 2015). Similar effects occurred throughout Europe, particularly in the north.

The Laki haze also triggered a plunge in global temperatures. The sulfuric acid aerosol particles reflected incoming solar radiation, cooling the planet and bringing severe winter conditions—and in some cases, winter weather during summer—to regions as far flung as Denmark, Japan, and New Orleans. In North America and Europe, average surface temperatures dropped by 1.5˚C for three years after the eruption (Þórðarson, 2005; Mikhail, 2015).

The Laki haze has even been credited with contributing to the downfall of Ottoman control in Egypt. The enormous pulse of SO2 weakened monsoons over the Indian Ocean, leading to a downwards spiral of reduced precipitation, lower flow (by some estimates, a reduction of 18 percent), and less flooding in the Nile from 1783—1784 (Mikhail, 2015). This in turn crippled food production, leading to famine and greater susceptibility to disease. Laki was only one thread in a complex web of factors undermining Ottoman control in Egypt in the 1780s; yet Mikhail (2015, p. 273) argued that the eruption's environmental effects may have

been “the straw that broke the camel’s back,” allowing local elites to concentrate their power over rural areas and challenging the Ottomans’ centralized control over Egypt. Mikhail (2015, p. 276) proposed that this set the stage for political, social, and economic affairs in Egypt for the next 150 years and went so far as to state, “…the Ottomans lost to the volcano.”

The Gjálp fissure eruption in 1996 also serves as a dramatic example of the environmental and societal impacts of the intense activity in Iceland’s EVZ. Gjálp—situated beneath Vatnajökull between Grímsvötn and Bárðarbunga volcanoes—erupted for 13 days, mostly ejecting material subglacially with very little tephra and no surface lava (Sturkell et al., 2006; Gudmundsson et al., 2008). This geothermal activity, however, melted enormous quantities of ice, filling Grímsvötn caldera lake and resulting in a catastrophic jökulhlaup with a peak discharge of 4.5—5.3 x 10^4 m^3 s^{-1}. A total of 3.2 km^3 of water deluged Skeiðarársandur, destroying a bridge and several roads (Figure 47) (Björnsson, 2002; Russell et al., 2005; Benn and Evans, 2010).

Figure 47. Skeleton of a bridge on Skeiðarársandur destroyed by the 1996 Grímsvötn jökulhlaup (photo by author).

Few volcanic systems in Iceland have impacted the environment and society as severely as those in the Grímsvötn system. Yet other active systems lie beneath Vatnajökull, as well. Iceland's most recently active volcano, Bárðarbunga (2009 masl), last erupted in August 2014 (Sigmundsson, 2006; Gudmundsson and Högnadóttir, 2007; IMO, 2015; Riel et al., 2015; Global Volcanism Program, 2013). A tectonic rifting event triggered a dyke intrusion along a series of fissures, which drained the magma chamber beneath Bárðarbunga and caused the caldera to collapse and subside by up to 50 cm per day (Riel et al., 2015). By the end of January 2015, Bárðarbunga had poured out 1.4 km^3 of lava at Holuhraun (Figure 48) (Global Volcanism Program, 2013). The eruption was declared officially over in February 2015 (IMO, 2015); however, the fresh lava fields are still steaming as they cool (Figure 49). Bárðarbunga's volcanic system also encompasses the Dyngjuháls and Veiðivötn-Vatnaöldur fissure swarms (Sigmundsson, 2006).

Figure 48. Holuhraun lava field: contact between columnar basalt bedrock (left) and a'a lava erupted from August 2014—February 2015 (right) (photo by author).

Figure 49. Holuhraun lava fields: one year old and still steaming (photo by author).

The other three volcanic systems beneath Vatnajökull are less active. Kverkfjöll (1929 masl), a volcano on the northern edge of Vatnajökull, most recently erupted in 1968 (Sigmundsson, 2006; Gudmundsson and Högnadóttir, 2007; Global Volcanism Program, 2013). The Öræfajökull-Snæfell Volcanic Flank Zone includes the central volcanoes Öræfajökull (2119 masl), Snæfell (1383 masl), and Esjufjöll (1522 masl). Out of this trio, Öræfajökull is the only one that has been volcanically active in the Holocene, last erupting in 1727 (Sigmundsson, 2006; Pagli et al., 2007; Thordarson and Höskuldsson, 2008). Finally, the Loki-Fögrufjöll Volcanic System runs between Grímsvötn and Bárðarbunga and consists of the Loki ridge, Fögrufjöll fissure swarm, and Hamarinn volcano (Sigmundsson, 2006; Gudmundsson and Högnadóttir, 2007). Its last confirmed eruptive activity was in 1910 (Global Volcanism Program, 2013).

Jökulhlaup Generation

This intense geothermal activity beneath Vatnajökull generates enormous quantities of meltwater that frequently drains in jökulhlaups, often after storage in subglacial lakes (Tweed and Russell, 1999; Björnsson, 2002). In fact, Vatnajökull translates to “glacier of lakes” (*vatn*

means lake; *jökull* means glacier). Six known lakes exist beneath the ice cap, pooling in calderas at Grímsvötn (the largest), Kverkfjöll, Pálsfjall, and Skaftá (three lakes) (Figure 50) (Björnsson, 2002; Björnsson, 2009; Guðmundsson, 2005; Russell et al., 2005; Sigmundsson, 2006; Gudmundsson and Högnadóttir, 2007; Benn and Evans, 2010; Howard et al., 2012).

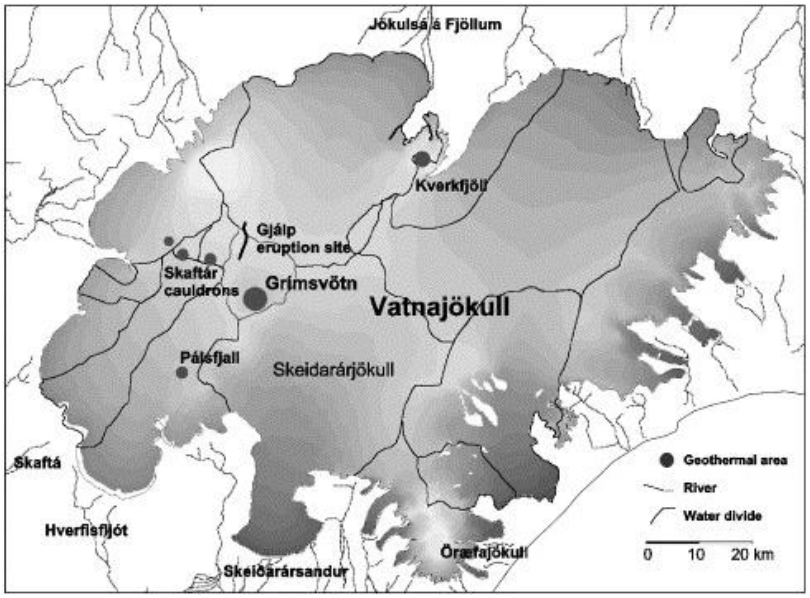

Figure 50. Geothermal areas and subglacial lakes beneath Vatnajökull (Björnsson, 2002).

Jökulhlaups originating from the calderas at Bárðarbunga and Kverkfjöll drain north from Vatnajökull through the Jökulsá á Fjöllum channel, whereas jökulhlaups originating from Grímsvötn generally flow south through the Skeiðará river (Björnsson, 2002; Carrivick et al., 2004a; Guðmundsson, 2005; Sigmundsson, 2006; Gudmundsson and Högnadóttir, 2007; Gudmundsson et al., 2008). Glacial meltwater draining south throughout the Holocene has created Skeiðarársandur, a vast plain of glacial outwash sediment (known as a sandur; plural sandar) (Magilligan et al., 2002; Guðmundsson, 2005; Russell et al., 2005; Sigmundsson, 2006).

With an area of over 1000 km^2 and a sediment depth ranging from 80—250 m, this is likely the largest active sandur in the world and, of course, the origin of the generic term (Magilligan et al., 2002; Robinson et al., 2008).

Glacial Fluctuations

Vatnajökull is a residual of the ice sheet that covered Iceland during the Pleistocene. Since the ice sheet's break-up in the early Holocene, Vatnajökull's mass balance has fluctuated significantly (Thoma et al., 2001; Ingólfsson et al., 2010). Around 900 AD, the ice cap reached its minimum extent—estimated at 6453 km2 (Fleming et al., 2001)—due to warmer temperatures between 0 and 1200 AD (Pagli et al., 2007). It expanded during the Little Ice Age, which began around 1200—1300 AD and lasted until about 1890 AD. After this time, it began a rapid recession in response to a temperature increase of 1—2˚C, a retreat that continues today (Pagli et al., 2007; Geirsdóttir et al., 2009). Based on marine and lacustrine sediment reconstructions, Geirsdóttir et al. (2009) concluded that Iceland's glaciers reached their maximum extent (post-deglaciation) between 1700 and 1850 AD. Vatnajökull's surface area was estimated to have reached its post-deglaciation maximum of 8600 km^2 in 1890 AD, before shrinking to 8300 km^2 by 1973 AD and even further to 8100 km^2 today (Fleming et al., 2007; Pagli et al., 2007). This amounts to an estimated total loss of 435 km^3 of ice between 1890 and 2003 AD (Pagli et al., 2007; Auriac et al., 2013).

Hannesdóttir et al. (2015) reported that between 1890 and 2010 AD, outlet glaciers on Vatnajökull's southeastern side retreated 1—4 km, lost roughly 16 percent of their area and 22 percent of their volume, and dropped 150—270 m in elevation near their termini. Although these rates have varied across decades, the fastest ice loss at most glaciers occurred between

2002 and 2010 AD (Hannesdóttir et al., 2015). Furthermore, temperatures in Iceland since the 1990s have increased three to four times more than the average temperature rise in the Northern Hemisphere, suggesting that Iceland's glaciers—notably Vatnajökull—are particularly vulnerable to global climate change (Hannesdóttir et al., 2015). Using current climate change models, Björnsson and Pálsson (2008) predicted that Iceland's glaciers will have retreated to only the highest mountains in 150—200 years. The vast majority of climate models—including those in the most recent IPCC report—predict a runaway increase in global temperatures in the foreseeable future, which will trigger rapid retreat and thinning of Iceland's glaciers: no small consequence in a country where ice covers ten percent of the land mass (Björnsson, 2002; Björnsson and Pálsson, 2008; Intergovernmental Panel on Climate Change (IPCC), 2014).

This ice cap thinning could result in significant environmental changes, including: decreased overlying ice pressure and thus higher uplift rates and more volcanic eruptions; increased meltwater flow in rivers; larger and more widespread glacial lakes and consequently jökulhlaups; and sea level rise (Hannesdóttir et al., 2015). Hannesdóttir et al. (2015) calculated that since 1890 AD, glacial melt from Vatnajökull alone has contributed 0.15 mm to global sea level rise, which has totaled 210 mm since 1880 AD (Church and White, 2011). Björnsson and Pálsson (2008) estimated this contribution to be 1 mm and further predicted that if all of Iceland's glaciers melted, global sea level would rise by 1 cm.

JÖKULSÁ Á FJÖLLUM

The Jökulsá á Fjöllum is Iceland's second longest river, flowing for 206 km from Vatnajökull to the Arctic Ocean (Howard et al., 2012). Its channel is the principal drainage route for jökulhlaups originating from Bárðarbunga and Kverkfjöll (Björnsson, 2002; Gudmundsson

and Högnadóttir, 2007). The Jökulsá á Fjöllum exits Vatnajökull through ice caves at Kverkjökull and Dyngjujökull—glaciers extending from the northern edge of the ice cap—and flows north (Figures 51-52).

Figure 51. One of the ice caves through which the Jökulsá á Fjöllum exits Vatnajökull at Kverkjökull (photo by author).

Figure 52. Inside the ice cave at Kverkjökull (pictured in Figure 51), one of the Jökulsá á Fjöllum's exit points from Vatnajökull. Two researchers for scale (photo by author).

The river's course runs through the corridor of the Northern Volcanic Zone, which displays extensive evidence of this tectonic activity: the year-old Holuhraun lava field; fumaroles and a geothermal lake at Askja caldera (Figures 53-54); and boiling mud pots at Námafjall Hverir in the Krafla volcanic system (Figure 55), to name a few (Sigmundsson, 2006; Howard et al., 2012).

Figure 53. Askja caldera lake (background) and Viti crater lake (foreground), both formed from an eruption in 1875. Geothermal evidence such as fumaroles is abundant throughout the area, and Viti is geothermally heated (measured at 22°C) (photo by author).

Figure 54. Extinct fumarole on the shore of Askja caldera lake, evidence of the extensive geothermal activity in the region. Feature is 0.5 m wide (photo by author).

Figure 55. Geothermal features at Námafjall Hverir in the Krafla volcanic system. Left: boiling mud pots. Right: geothermal field (photos by author).

Although the Jökulsá á Fjöllum is sourced from geothermal meltwater beneath Vatnajökull, many tributaries along its route contribute freshwater from runoff, snowmelt, and groundwater (Waitt, 2002). The river's catchment area is approximately 5178 km^2 (IMO, 2016). The Kreppa is another glacial river that exits the eastern side of Kverkjökull and flows into the Jökulsá á Fjöllum near Mt. Herðubreið (Kristmannsdóttir et al., 1999). The Jökulsá á Fjöllum's discharge at Grímsstaðir—roughly 110 km from the river's headwaters—ranges from roughly 20 $m^3\ s^{-1}$ in winter to around 700 $m^3\ s^{-1}$ during summer floods (Kristmannsdóttir et al., 1999). Waitt (2002) reported an average discharge of 150—200 $m^3\ s^{-1}$ in July and August, but did not specify which part of the river yielded this measurement. As a point of comparison, flow discharge from 12—23 August 2015 varied between 185—260 $m^3\ s^{-1}$ at Grímsstaðir; and 85—123 $m^3\ s^{-1}$ farther downstream at Upptyppingar. Flow between 27 April and 4 May 2016 ranged from 93—105 $m^3\ s^{-1}$ at Grímsstaðir; and 50—54 $m^3\ s^{-1}$ at Upptyppingar (IMO, 2016).

For the first approximately 160 km, the Jökulsá á Fjöllum flows across a relatively flat plain at an elevation of 400 to 800 masl. Several tuyas rise up from the plateau to elevations

over 1600 masl (Waitt, 2002; Guðmundsson, 2005; Howard et al., 2012). The river enters a confined basalt channel in the Jökulsárgljúfur canyon, where it cascades down to sea level over a series of waterfalls for the next 28 km: from south to north, Selfoss; Dettifoss (Europe's most powerful, where it plunges 54 m); Hafragilsfoss, Réttarfoss, and Vígabjargsfoss (Waitt, 2002; Baynes et al., 2015a,b). After exiting the basalt channel near Ásbyrgi canyon, the Jökulsá á Fjöllum splits into two main distributaries that flow the remaining 18 km into the Arctic Ocean (Baynes et al., 2015a,b).

The Jökulsá á Fjöllum flows through three main geologic units: Holocene lava flows (erupted between 11 ka and 1100 years ago); Upper Pleistocene supraglacial—interglacial lava beds dating from 0.8 mya to 11 ka; and Upper Pleistocene hyaloclastite and pillow lava formed between 0.8 mya and 11 ka. After exiting Ásbyrgi canyon, the river flows through Holocene sediments for its remaining 18 km to the ocean (Jóhannesson and Saemundsson, 1998a,b).

CHAPTER 9: EVIDENCE OF HOLOCENE JÖKULHLAUPS ALONG THE JÖKULSÁ Á FJÖLLUM: FLOOD MAGNITUDE AND EXTENT

Although there is extensive evidence that jökulhlaups surged down the Jökulsá á Fjöllum channel throughout the Holocene, there is heated debate over the timing, magnitude, and path of these floods. Our research goal is to reconstruct a timeline of Holocene jökulhlaups along the channel, and specifically to test Howard et al.'s (2012) hypothesis of the largest known flood on Earth. To unravel this puzzle and understand how this landscape formed, we must assemble all the pieces of evidence we can. In this section, I review and critique research methods and results from previous studies of Holocene jökulhlaups along the Jökulsá á Fjöllum, as well as present new evidence from field work in August 2015. This chapter examines methods and evidence used to reconstruct flood magnitude and extent—geomorphologic evidence and hydraulic modeling—while Chapter 10 reports on methods and evidence used to determine flood timing—tephrochronology and cosmogenic nuclide exposure dating.

GEOMORPHOLOGIC EVIDENCE

Most previous studies of Holocene jökulhlaups along the Jökulsá á Fjöllum channel have relied on geomorphologic evidence to estimate flood magnitude, path, and dynamics. The formation of jökulhlaup features is dictated by flow dynamics, which in turn are partly controlled by topography and geology. Erosion occurs where floodwater velocity is high, such as areas of flow constriction; and deposition prevails in zones of low flow velocity (Carrivick et al., 2004a; Carrivick, 2007). Features can be formed by both erosional and depositional processes, however, complicating interpretation. As an added challenge, a cocktail of geologic processes has acted on the zone along the Jökulsá á Fjöllum, including glacial, fluvial, volcanic, megaflood, and aeolian, making it extremely difficult to distinguish individual processes' roles in

landscape evolution. Alho et al. (2005) produced the most extensive flood inundation model to date, calculating a peak discharge of 0.9×10^6 m^3 s^{-1}. Alho et al. (2005) interpreted flow dynamics in three sections of the channel—Vaðalda, Upptyppingar, and Möðrudalur—and Baynes et al. (2015a,b) reconstructed jökulhlaup action in the Jökulsárgljúfur and Ásbyrgi canyons. Our field work focused on the Vaðalda, Upptyppingar, and Herðubreið channel reaches; however, megaflood erosional and depositional features extend along the entire length of the river, from Vatnajökull to Ásbyrgi.

Kverkfjallarani

Numerous studies have examined jökulhlaup impacts at Kverkfjallarani—the area in front of Kverkjökull, a glacier that is one of the Jökulsá á Fjöllum's exit points from Vatnajökull. Jökulhlaups draining from subglacial lakes in the Bárðarbunga and Kverkfjöll calderas exit Vatnajökull and drain north across Kverkfjallarani, leaving behind a suite of erosional and depositional features. Erosional landforms include: gorges; cataracts; spillways; streamlined hyaloclastite-pillow lava hills and ridges; obstacle scouring marks; and scoured bedrock, such as potholes and flutes (Waitt, 2002; Carrivick et al., 2004a; Carrivick, 2007; Carrivick, 2009).

Kverkfjallarani also displays extensive evidence of jökulhlaup deposition, notably: boulder and gravel bars; boulder erratics and clusters; slackwater deposits; and valley-fill deposits (sedimentological layers of flood deposits that occur in the main flood valley) (Waitt, 2002; Carrivick et al., 2004a,b; Carrivick, 2007; Carrivick, 2009). Marren et al. (2009) examined the sedimentology of the sandur immediately in front of Kverkjökull and concluded that it was formed by at least six jökulhlaups during the Little Ice Age (1200—1890 AD).

Vaðalda

Moving downstream from Kverkfjallarani, floodwaters first spread out across a valley, leaving behind few distinguishing geomorphologic landforms. Immediately before Vaðalda, however, there is evidence of bars, imbricated boulders, and cataracts (Waitt, 2002). Floodwaters wrapped around Vaðalda (941 masl), depositing bars and boulder erratics, as well as sculpting bedrock into scabland (Waitt, 2002). The Vaðalda reach represented the "first major constriction" of floodwaters (Alho et al., 2005) as the water was forced into a preexisting gorge between Vaðalda and a series of hyaloclastite ridges (Alho et al., 2005; Alho et al., 2007). This created predominantly erosional features such as streamlined hills, scoured lava surfaces, potholes, and grooves (Waitt, 2002; Alho et al., 2005; Alho et al., 2007). However, the area east of Vaðalda displays evidence of a backwater zone where flow velocity dropped, leaving bars and boulder erratics (Waitt, 2002; Alho et al., 2005).

Upptyppingar

Downstream from Vaðalda, floodwaters split around Upptyppingar (1084 masl), a hyaloclastite-pillow lava mountain (Alho et al., 2005). Floodwaters were confined at two points (Alho et al., 2005), resulting in an increase in flow power and thus extensive bedrock erosion—predominantly though plucking and cavitation—as evidenced by cataracts, scouring, potholes, and scabland topography (Waitt, 2002; Alho et al., 2005; Alho et al., 2007). Bars occur upstream of the first constriction where floodwaters ponded before rushing through (Waitt, 2002; Alho et al., 2005; Alho et al., 2007). We found extensive evidence of jökulhlaups on Upptyppingar, notably streamlined hills and boulder erratics near the summit (Figure 56).

Figure 56. Boulder erratics on Upptyppingar (photos by author).

New Evidence: Cataract and Spillway

During field work in August 2015, our team observed two geomorphologic features at Upptyppingar that have not been previously reported in the literature: a spillway and a cataract. Both features corroborate Alho et al.'s (2005) interpretation of flood dynamics at Upptyppingar, and Alho et al. (2005) described the location as the first flow constriction—although they did not label it as a spillway or cataract.

According to Alho et al. (2005), floodwaters wrapped around Upptyppingar in two branches (Figure 57). One branch flowed north, passing Upptyppingar's western side. The second branch flowed east, with one arm funneling through the spillway—which connects the valley on the western side of Upptyppingar with the present-day river channel on the eastern side of the mountain—while the other arm flowed south of the spillway through the present-day river channel (Alho et al., 2005).

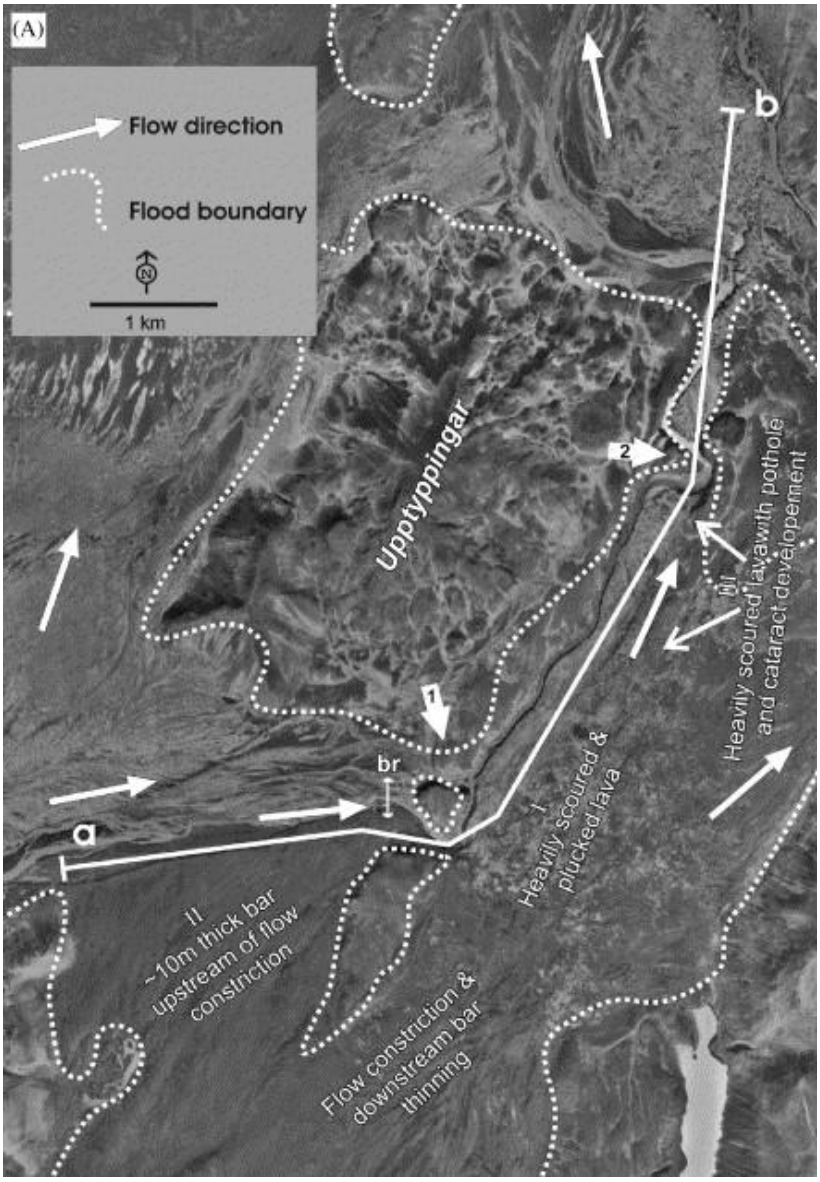

Figure 57. Paleohydraulic reconstruction of floodwater routes and geomorphologic impacts at Upptyppingar. Spillway observed by the author is in the same location as Arrow 1. Arrows 1 and 2 denote flow constrictions; br = Upptyppingar bridge (Alho et al., 2005).

Floodwaters likely flowed east out of the main valley through the spillway, heavily scouring its lava floor (Figure 58)—a megaflood characteristic described by Carrivick et al. (2004a) and Carrivick and Rushmer (2006). The high-energy floodwaters then plunged into the

neighboring valley, eroding a knickpoint in the cliff edge (Figure 59). This knickpoint retreated via plucking of columnar basalt, eroding back to its current position (Figure 60). The present-day Jökulsá á Fjöllum flows on the east side of Upptyppingar below the dry cataract. Our team sampled boulder erratics on the sides of the spillway to reconstruct flood timing, and the samples are currently undergoing cosmogenic nuclide exposure dating.

Figure 58. Looking west towards the main valley from the spillway saddle. Note the jökulhlaup-scoured lava surface and gentle slope back towards the valley, where the present-day Jökulsá á Fjöllum flows (photo by author).

Figure 59. Spillway (three overlapping photos). Cataract lip is marked by arrow. Present-day Jökulsá á Fjöllum flows on the far left and in the valley in the distance on the far right. Note jökulhlaup-scoured lava surface on spillway floor (photos by author).

Figure 60. Cataract at end of spillway. Note columnar basalt formations on sides, evidence which suggests knickpoint retreat via plucking. Present-day Jökulsá á Fjöllum flows in the foreground (photo by author).

This sequence of events corroborates our geomorphologic observations. Today, the Jökulsá á Fjöllum flows along the eastern flank of Upptyppingar through a deep, columnar basalt-lined gorge (Figure 61). On the western side of the current channel, Upptyppingar rises in a steep cliff. On the eastern side, a broad lava plain extends beyond the channel lip. The lava is heavily scoured and is littered with boulder erratics, which is indicative of megaflood erosion (Figure 62). This scoured topography is upstream of Alho et al.'s (2005) second flow constriction (which lies roughly 3 km downstream of the spillway) and was also described by Alho et al. (2005).

Figure 61. Jökulsá á Fjöllum slicing through columnar basalt channel, viewed from eastern slope of Upptyppingar. Eastern channel bank is marked by heavily scoured lava surfaces and boulder erratics. Cataract is marked by arrow (photo by author).

Figure 62. Close-up view of jökulhlaup-scoured lava surfaces and boulder erratics on eastern bank of Jökulsá á Fjöllum. Photo taken from eastern slope of Upptyppingar (photo by author).

New Evidence: Boulder Field, Cataract, and Moat

Roughly 2 km northwest of the spillway, our team found a second line of jökulhlaup geomorphologic evidence previously unreported in the literature: a boulder field leading to a cataract. This feature lies north of the road, right before it crosses the Jökulsá á Fjöllum at Upptyppingar bridge. A flat plain extends to the west and south of Upptyppingar, underlain by scoured lava beds interspersed with tephra-pumice deposits. A large boulder field abruptly cuts across this plain, measuring several hundred meters wide and several hundred meters long (Figure 63). Most boulders are less than 2 m in diameter, although scattered erratics reach up to several meters in diameter. Many rocks are fluted and/or scoured, indicating high-energy floodwaters (Figure 64). Boulders displayed both angular and rounded textures, and rocks did not appear to be imbricated or preferentially oriented. Our team sampled one erratic in the boulder field, and it is currently undergoing cosmogenic nuclide exposure dating to determine age of deposition (Figure 65).

Figure 63. Plain underlain by scattered boulders and a mix of pumice, tephra, and aeolian sediments. Boulder field leading up to cataract is in background. End of the cataract is marked by arrows. Upptyppingar rises up on the right of the photo (photo by author).

Figure 64. Fluting on boulders in the boulder field (photo by author).

Figure 65. Sampling an erratic in the boulder field for cosmogenic nuclide exposure dating. Upptyppingar rises in the background (photo by author).

The boulder field ends abruptly at a cataract—a horseshoe-shaped canyon several hundred meters wide that opens to the north (Figures 66-71). The canyon is rimmed by columnar basalt walls that rise approximately 1—3 m above the canyon floor. This wall almost completely encircles the canyon except for a small gap on the northern side, which opens out to the surrounding plain. Some of the rock walls have been undercut; other areas have been infilled by a mélange of pumice, tephra, and aeolian sediments, forming a gentle slope down to the canyon floor. Plunge pools are also visible in some places along the base of the rim. The canyon floor is infilled with pumice-tephra-aeolian deposits, which display extensive evidence of recent fluvial erosion, and a cluster of boulders lies in the center.

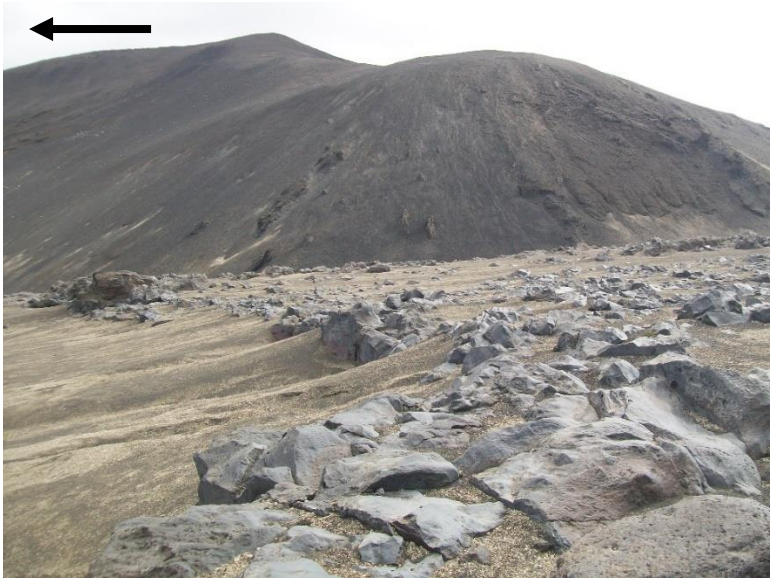

Figure 66. Rim of the cataract; infilled sediments slope down to cataract floor (to the left of the photo). Note fluted boulder surfaces. Upptyppingar is in the background. Arrow points north (photo by author).

Figure 67. Boulder field looking north towards cataract; end of cataract is marked by arrows (photo by author).

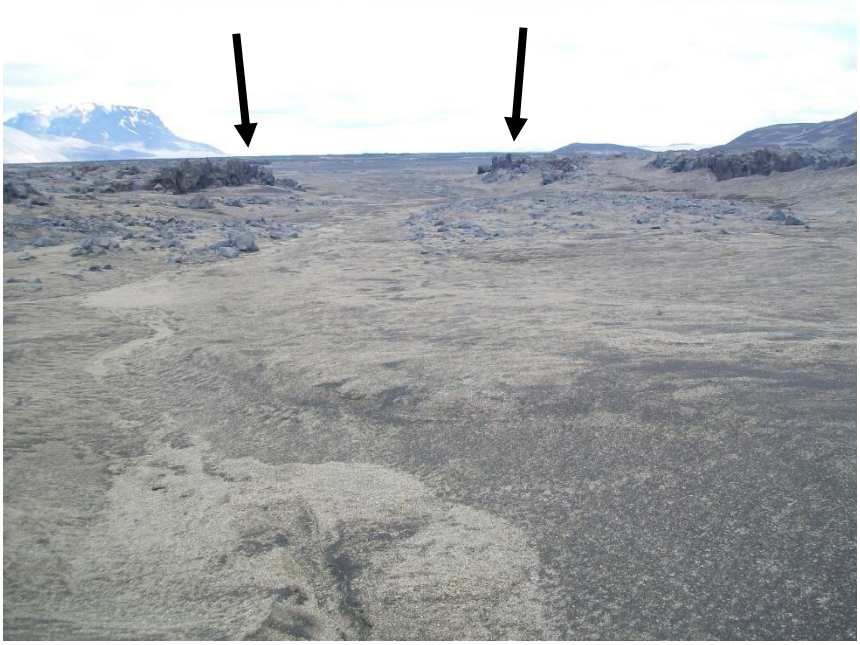

Figure 68. End of cataract (marked by arrows) looking north. Basalt bedrock rim extends on each side of the picture. Mt. Herðubreið towers in the background (photo by author).

Figure 69. Cataract (three overlapping photos). Middle photo (same as Figure 68) shows end of cataract where it opens up to the valley. Cataract is rimmed by basalt bedrock. Mt. Herðubreið is in the background (photos by author).

Figure 70. Boulder cluster on floor of cataract. Mt. Herðubreið looms in the background (photo by author).

Figure 71. Cataract lip composed of columnar basalt. Plunge pools are at the base of the wall. Photo is a close-up view of the far-left picture in Figure 69 (photo by author).

We hypothesize that the bedrock outcrop originally extended to the canyon edge. A jökulhlaup (or series of jökulhlaups) eroded back this bedrock via plucking, toppling columnar basalt towers and causing the knickpoint to retreat to its present-day position, scooping out the canyon in the process—a sequence of events similar to the one that formed the cataract at the Upptyppingar spillway. We postulate that the boulder field upstream of the cataract was formed when floodwaters lost velocity and competence as they ponded before plunging over the cataract (similar to a pool immediately upstream of the lip of a waterfall), causing the largest particles to drop out of suspension. Carrivick et al. (2004a) reported a similar feature at Kverkfjallarani, observing "boulder accumulations" at cataract heads. This fits with flow patterns reported by Waitt (2002), Alho et al. (2005), and Alho et al. (2007), who concluded that this area was inundated by the western branch of floodwaters that split around Upptyppingar, spreading out over the plain and likely losing velocity.

Another component of this jökulhlaup-sculpted system is a moat that runs between the eastern cataract rim and the western flank of Upptyppingar (Figures 72-73). We hypothesize that some floodwaters spilled to the east of the cataract, eroding a channel along the plane of weakness at the contact of two rock units: the columnar basalt of the cataract rim and the hyaloclastite-pillow lava complex of Upptyppingar. The moat is lined to the west by a wall of columnar basalt a few meters high, and to the east by the hyaloclastite slope of Upptyppingar—which has been eroded into a smooth surface, possibly by a jökulhlaup. The moat floor is partially infilled with pumice-tephra-aeolian deposits.

Figure 72. Moat, looking north. Columnar basalt wall (eastern side of cataract) on the left; western hyaloclastite slope of Upptyppingar on the right (photo by author).

Figure 73. Moat, looking south. Columnar basalt wall on the right (eastern side of cataract); western hyaloclastite slope of Upptyppingar on the left (photo by author).

Waitt (2002) also reported moats west of Upptyppingar, although the description is too vague to ascertain if they are the same as the one we observed. Carrivick et al. (2004a) reported a similar feature in Kverkfjallarani, where 15—20 m-deep gorges stretched between subaerial lava outcrops and hyaloclastite-pillow lava units at the edges of valleys (Figure 74). The Upptyppingar moat is yet another line of evidence of megafloods along the Jökulsá á Fjöllum.

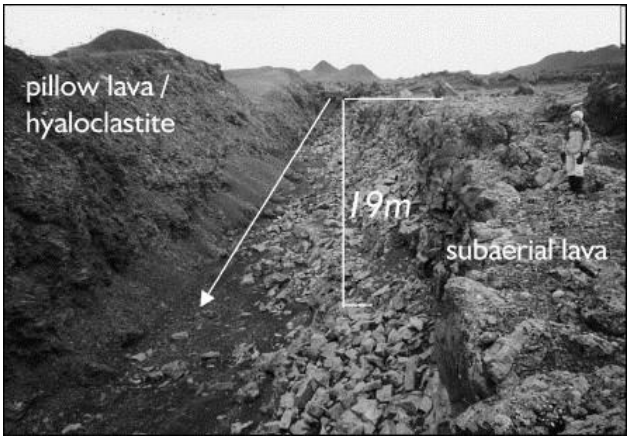

Figure 74. Jökulhlaup-sculpted gorge at the contact between hyaloclastite-pillow lava and subaerial lava at Kverkfjallarani. Feature resembles moat observed at Upptyppingar (Carrivick et al., 2004a).

Herðubreið

Like other reaches of the Jökulsá á Fjöllum, the Herðubreið channel stretch is replete with jökulhlaup evidence. Mt. Herðubreið—a 1682 masl tuya—towers over the surrounding plain to the west of the Jökulsá á Fjöllum (Figure 75).

Figure 75. Mt. Herðubreið (1682 masl) in all its glory. Car for scale (photo by author).

Arnardalsalda—a 648 masl hill—lies directly east of Mt. Herðubreið on the east bank of the river (Figure 76).

Figure 76. Arnardalsalda (648 masl) (photo by author).

Field work revealed numerous streamlined landforms such as hyaloclastite-pillow lava hills and gravel bars. Trimlines are visible on some ridges and hills, namely Mt. Herðubreið

(Howard et al., 2012). Many lava and bedrock surfaces are scoured, exhibiting grooves, flutes, and potholes (Figure 77).

Figure 77. Bedrock erosional features near Mt. Herðubreið. Clockwise from top left: fluting (Jökulsá á Fjöllum flows in the background); Scoured basalt lava surfaces on the banks of the Jökulsá á Fjöllum; Scoured lava and bedrock surfaces on the plain surrounding Mt. Herðubreið (Jökulsá á Fjöllum flows through middle); Scoured basalt lava surfaces near Mt. Herðubreið (photos by author).

Boulder erratics are found throughout the area, perched atop ridges and hills and also scattered across the plain (Figures 78-79). Howard (unpublished, 2013) sampled erratics in several locations for cosmogenic nuclide exposure dating to ascertain whether the boulders were deposited before or after deglaciation, and we continued this sampling during August 2015 field work. Several other studies have examined geomorphologic features in the Herðubreið reach, namely Howard (2008); Howard et al. (2012); Carrivick et al. (2013); and Howard (unpublished, 2013).

Figure 78. Boulder erratic (marked by arrow) perched on a ridge near Mt. Herðubreið (photo by author).

Figure 79. Boulder erratic cluster near the base of Mt. Herðubreið; erratic marked by arrow is the same rock pictured in Figure 23 (photo by author).

New Evidence: Boulder Field and Cataract

Approximately 10 km west of Þríhyrmngsvatn lake, we found a boulder field leading up to a cataract: a very similar feature to the one we observed at Upptyppingar, and one that has not been previously reported in the literature. The boulder field is roughly a few hundred meters wide and a few hundred meters long. Boulders are generally smaller than about 1—2 m in diameter and have a wide range of textures, from rounded to angular. Some display evidence of fluting (Figure 80). This boulder run-up cascades over a ledge that gently slopes down to a channel floor several meters below (Figures 81-84). The channel extends a few hundred meters and is covered with a mélange of pumice, tephra, and aeolian sediments. Its walls are covered in boulders, some of which have slid down to settle on the channel floor. Beyond the channel, the

landscape abruptly returns to a flat plain devoid of boulders and covered by interspersed aeolian sediments and lava beds.

Figure 80. Fluting on boulders at lip of cataract. Geologist's legs for scale on left (photo by author).

Figure 81. Boulder field leading up to cataract (which begins on the left of the photo where the boulders start to slope downhill). Two cars circled for scale (photo by author).

Figure 82. Boulder field leading up to cataract; cataract lip is marked by arrow. Two researchers for scale (photo by author).

Figure 83. Cataract. Photo taken at the end of the boulder field on the lip of the cataract (photo by author).

Figure 84. Cataract (photos are almost overlapping). Note cataract sides covered with boulders. Arrow marks location from which photo in Figure 83 was taken. Right photo shows end of cataract (where it opens up to plain) (photos by author).

We hypothesize that—similar to the boulder field-cataract system at Upptyppingar—a knickpoint began to form at the present-day end of the channel. Floodwaters eroded back the knickpoint to its present location—excavating the channel in the process—mainly by toppling and plucking basalt columns; however, unlike the cataract at Upptyppingar, columnar basalt bedrock is not exposed at the surface. We postulate that the boulder field formed as floodwaters pooled before plunging over the cataract, losing velocity and competence and thus depositing their largest transported particles. To test this interpretation, we would need to know the rock structure beneath the boulder covering and aeolian sediment: for example, whether the sides of the channel are composed of columnar basalt (which would strengthen the case for knickpoint retreat).

Möðrudalur

As floodwaters entered the Möðrudalur reach, they spread out onto a broad plain, bursting out from the more confined Herðubreið stretch and losing velocity (Alho et al., 2005). As a result, Möðrudalur predominantly displays jökulhlaup depositional features such as slackwater deposits (Alho et al., 2007), gravel dunes (Waitt, 2002), boulder fields, boulder bars, and expansion bars (Alho et al., 2005). Flow was confined downstream of Möðrudalur in a canyon near Lambafjöll (Waitt, 2002; Alho et al., 2005; Alho et al., 2007), causing floodwaters to pond on the plain, lose velocity, and deposit material (Alho et al., 2005). After funneling through the canyon at Lambafjöll, floodwaters spread out again south of Grímsstaðir (Alho et al., 2007), depositing a series of gravel bars (Waitt, 2002).

Jökulsárgljúfur

Approximately 160 km after exiting Vatnajökull, the Jökulsá á Fjöllum funnels into the Jökulsárgljúfur canyon, a basalt gorge 28 km long (Baynes et al., 2015a,b). Although Waitt (2002) postulated that the Jökulsá á Fjöllum had previously incised much of the canyon, Baynes et al. (2015a,b) concluded that the canyon was predominantly sculpted by a series of Holocene jökulhlaups via knickpoint retreat (Baynes et al., 2015a,b). Jökulhlaups toppled basalt columns, eroding back knickpoints to create cataracts. These cataracts are now waterfalls: from south to north, Selfoss; Dettifoss; Hafragilsfoss; Réttarfoss; and Vígabjargsfoss (Waitt, 2002; Baynes et al., 2015a,b). Dettifoss—Europe's most powerful waterfall—is the highest, plunging 54 m (Figure 85-86) (Baynes et al., 2015a,b).

Figure 85. The Jökulsá á Fjöllum plunges 54 m over Dettifoss—Europe's most powerful waterfall (photo by author).

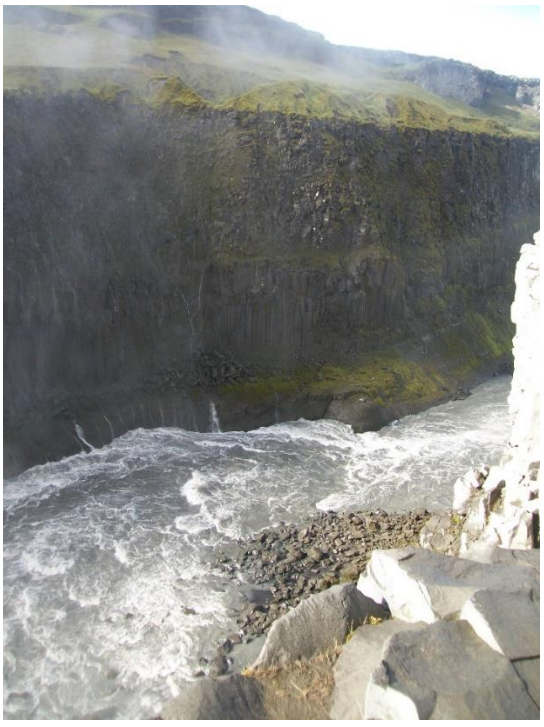

Figure 86. Columnar basalt lining the Jökulsárgljúfur canyon; jökulhlaups plucked these basalt columns, triggering knickpoint retreat to form gorges and cataracts. Dettifoss is to the left of the photo (photo by author).

The first 4 km of the Jökulsárgljúfur canyon contain extensive megaflood erosional evidence. In addition to three major cataracts —the waterfalls Selfoss, Dettifoss, and Hafragilsfoss—the bedrock canyon displays scouring, scabland buttes and channels, dry cataracts, and spillways out of the main gorge (Waitt, 2002; Baynes et al., 2015a,b). Baynes et al. (2015b) also found three strath terraces, which they interpreted as previous river beds; each terrace is the surface of a lava flow and displays extensive fluvial erosional evidence, such as fluting and polishing. Floodwaters eroded cataracts into these terraces, leading to their abandonment (Baynes et al., 2015b). Baynes et al. (2015a,b) postulated that floods incised this section after about 8500 BP, when a fissure eruption deposited the basalt into which the gorge is incised.

Approximately 9 km downstream of the start of the Jökulsárgljúfur canyon, the Jökulsá á Fjöllum cascades over Réttarfoss and is confined into a narrow gorge—characterized by Baynes et al. (2015a) as a slot canyon—which has heavily scoured surfaces that now lie abandoned above the channel (Figure 87). The river then enters the Forvöð valley, where floodwaters spread out and deposited bars and boulders, as well as boulder-rich mounds of sediment that form terraces up to 47 m thick (Waitt, 2002; Baynes et al., 2015a). Baynes et al. (2015a) postulated that these materials were deposited when floodwaters ponded and lost energy before funneling into the narrow Kjaffbjarg gorge downstream of Forvöð. After exiting the gorge, floodwaters scoured the Vesturdalur area, leaving scabland topography, a large cataract, and boulder erratics in their wake (Waitt, 2002; Baynes et al., 2015a).

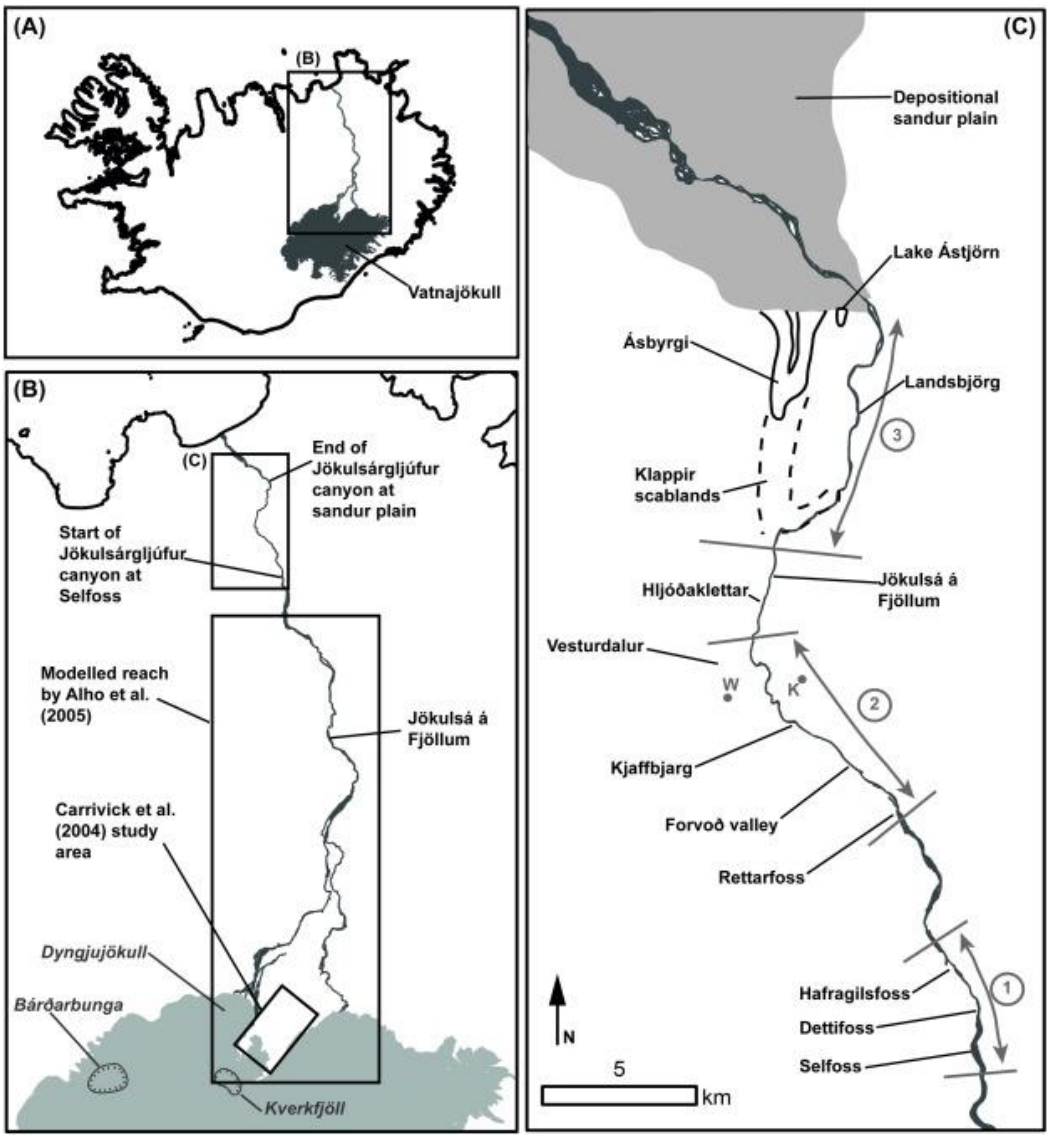

Figure 87. (a) and (b): maps of Jökulsá á Fjöllum. (c): map of Jökulsárgljúfur canyon. Numbers refer to study areas in Baynes et al. (2015a); W and K mark sedimentological sequences reported by Waitt (2002) and Kirkbride et al. (2006), respectively (Baynes et al., 2015a).

After leaving the Jökulsárgljúfur canyon, the Jökulsá á Fjöllum splits into two main distributaries and flows across a wide sandur for 18 km before emptying into the Arctic Ocean (Figure 88) (Baynes et al., 2015a).

Figure 88. Jökulsá á Fjöllum near Ásbyrgi, 15 km before it empties into the Arctic Ocean. Note black basalt sand (typical of Icelandic sandar) (photo by author).

Cosmogenic nuclide dates from rock surfaces in the Jökulsárgljúfur and Ásbyrgi canyons suggest that three major flood events stripped overlying basalt, likely through knickpoint retreat and columnar basalt toppling: one between 10 ka and 9000 BP, a second around 5000 BP, and a third at about 2000 BP (Baynes, 2012; Baynes et al., 2015a,b). However, the 16 smaller jökulhlaups in the mid-Holocene may have contributed to knickpoint retreat, as well (Baynes et al., 2015a).

Ásbyrgi

The final section of the Jökulsárgljúfur canyon parallels the Klappir scabland and the Ásbyrgi canyon, which both show extensive megaflood erosional evidence. The Jökulsá á Fjöllum currently flows through Jökulsárgljúfur immediately to the west of Klappir and Ásbyrgi. Baynes et al. (2015a) reported that an early Holocene jökulhlaup carved Ásbyrgi—a horseshoe-shaped dry canyon measuring 1 km wide, 3 km long, and up to 90 m deep— roughly 10 ka BP, a

date determined through cosmogenic nuclide exposure dating of bedrock erosional surfaces (Figure 89) (Baynes, 2012; Baynes et al., 2015a,b). Floodwaters likely followed the course of the Jökulsá á Fjöllum at that time before spilling out of the channel and tearing across Klappir, which is underlain by scabland topography such as potholes, scouring, and cataracts. After inundating Klappir, floodwaters split into two main branches. The western branch incised two channels, which deepened and lengthened via knickpoint retreat. These channels eventually connected, leaving behind an island in the middle of the canyon, which is known as Eyjan ("island" in Icelandic) (Figure 90) (Waitt, 2002; Baynes et al., 2015a).

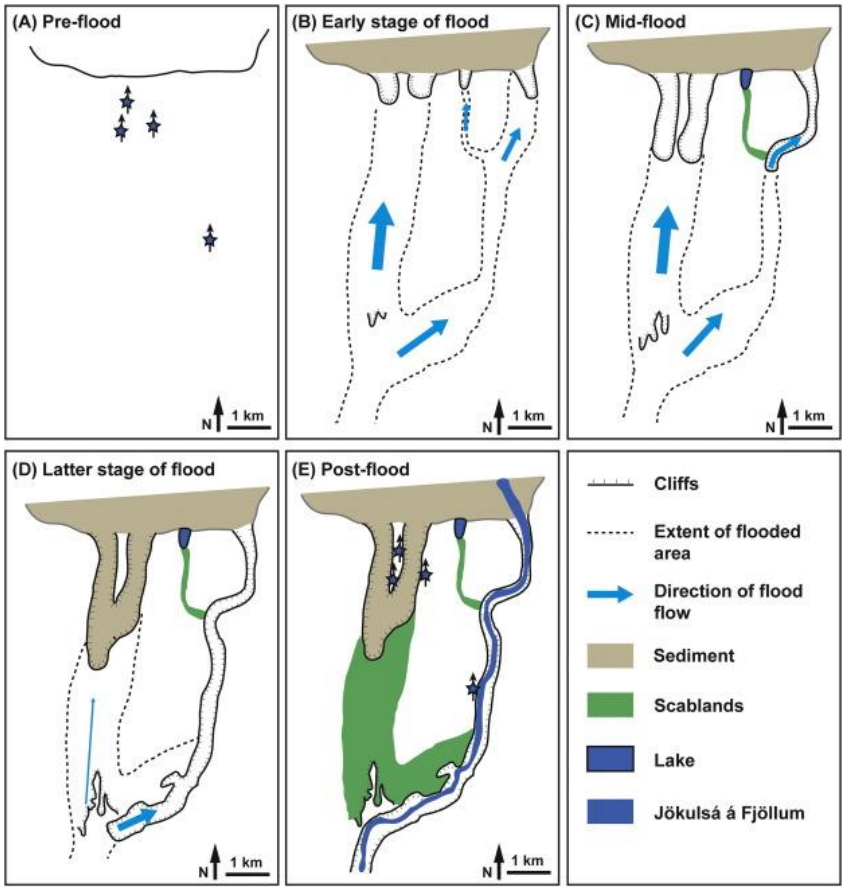

Figure 89. Schematic diagram of jökulhlaup sculpting of Klappir scabland and Ásbyrgi canyon (Baynes et al., 2015a).

Figure 90. Ásbyrgi canyon, looking south (photo by author).

Eyjan's surface—as well as areas on Ásbyrgi's eastern rim and Jökulsárgljúfur's western edge—exhibit small-scale fluvial bedrock erosional features, suggesting that the Jökulsá á Fjöllum flowed across Ásbyrgi before jökulhlaups excavated the canyon. Baynes et al. (2015a) offered two hypotheses to explain this: 1) the pre-flood Jökulsá á Fjöllum was significantly wider and had a larger discharge than at present owing to greater quantities of meltwater as the ice sheet receded; and 2) the channel migrated over time across Ásbyrgi. Most of Ásbyrgi's rim, in contrast, is heavily scoured and marked with megaflood-scale flutes, grooves, and potholes (Baynes et al., 2015a). The rim is also etched with cataracts and knickpoints that lie above plunge pools, providing strong evidence for knickpoint retreat during jökulhlaups (Waitt, 2002; Baynes et al., 2015a).

After the flood roughly 10 ka BP, the Jökulsá á Fjöllum switched its course, and it has flowed along the split's eastern branch ever since (Baynes et al., 2015a). Cosmogenic nuclide exposure dating of rock surfaces in Ásbyrgi suggests that subsequent floods did not have enough

power to erode bedrock, and/or that subsequent jökulhlaups drained only through the eastern branch. As a result, Ásbyrgi canyon has remained untouched by jökulhlaup erosion since its creation around 10 ka BP (Baynes et al., 2015a,b).

CRITIQUES OF GEOMORPHOLOGIC INTERPRETATION

With such a large suite of geologic processes acting concurrently along the Jökulsá á Fjöllum, one of the most formidable challenges in reconstructing jökulhlaup events is determining which processes formed which features. The landscape has been modified by fluvial, glacial, megaflood, volcanic, and aeolian forces throughout the Holocene, imprinting landforms with signatures from multiple processes. Interpreting landscape evolution is extremely complex.

While many megaflood features—such as bars and potholes—mirror their fluvial counterparts, they are generally distinguishable by their different scales (Marren, 2002; Marren and Schuh, 2009). Other processes are more difficult to tease apart. Glaciers and megafloods are a prime example since they sculpt similar erosional and depositional features (Malin and Eppler, 1981; Carrivick and Rushmer, 2006; Howard et al., 2012; Carrivick et al., 2013). Much of the glacial—megaflood debate centers around boulder erratics. Few geomorphologic processes are powerful enough to transport boulders up to several meters in diameter. Howard et al. (2012) and Howard (unpublished, 2013) hypothesized that if boulder erratics in the study area date to older than 10.3 ka BP—the time of deglaciation in the region—they were transported by glaciers; if they are younger than 10.3 ka BP, however, they were likely transported and deposited by megafloods (either as bedload or ice-rafted).

There are other hypotheses for boulder origin, however. Boulders could have been exhumed from glacial moraines: finer particles eroded, leaving behind the erratics (Carrivick et al., 2013). Freeze-thaw cycles or tectonic processes such as rifting could have broken boulders off from rock formations (Carrivick et al., 2013). In describing erratics deposited by the Kuray floods in Siberia, Herget (2005) postulated that boulders could have been transported by mass movement events. A boulder's composition can also provide clues to its origin. If its composition cannot be traced to the surrounding geology, it was likely transported from elsewhere—possibly by a glacier or megaflood (Herget, 2005).

Boulder texture may offer further clues to glacial versus jökulhlaup origin. Generally, glacial deposits tend to be angular, while particles transported by rivers or megafloods are more rounded (Malin and Eppler, 1981; Carrivick et al., 2013). However, there are many exceptions to this pattern; for example, angular boulders could have been ice-rafted in a jökulhlaup or might have only traveled a short distance (Malin and Eppler, 1981). Conversely, glaciers can carry rocks that have already been rounded by fluvial transport. Malin and Eppler (1981) and Carrivick et al. (2013) cautioned against overreliance on texture to interpret particle origins. While geomorphologic evidence may suggest that a jökulhlaup occurred, it is usually impossible to distinguish separate flood events from the geomorphologic record (Carrivick and Rushmer, 2006). Landscapes may preserve evidence from only the most recent megaflood, as jökulhlaups may have stripped off previous flood deposits or scoured out previously eroded bedrock surfaces.

Reworking of deposits is another confounding factor when interpreting jökulhlaup features. Floodwaters mix materials deposited by previous jökulhlaups, disrupting layers that preserved clues to flood dynamics (e.g. particle orientation or fining). Similarly, the waning

stages of a flood can rework sediments deposited during earlier flow (Maizels, 1997; Carrivick and Rushmer, 2006).

Other geomorphologic processes can also modify or erase jökulhlaup evidence. Although the last catastrophic jökulhlaup along the Jökulsá á Fjöllum occurred roughly 2500—2000 BP, the river and smaller floods have continued to incise its bedrock channel, albeit with considerably less erosive impact. Boulder erratics may have been similarly modified through ventifaction (Howard, unpublished, 2013) or freeze-thaw processes (Figure 91), erasing evidence of jökulhlaup transport and deposition. Lava flows can also cover jökulhlaup-eroded surfaces, complicating our interpretation of megaflood geomorphologic impacts on this dynamic landscape (Carrivick et al., 2004a).

Figure 91. Left: boulder on Upptyppingar displaying ventifaction. Right: boulder on summit of Arnardalsalda fractured by freeze-thaw cycles (photos by author).

Another point of contention arises around how to interpret a lack of geomorphologic evidence. For example, Howard et al. (2012) observed boulder erratics, "smooth undulating topography," and a lack of trimlines on Ferjufjall (a 558 masl hill), leading them to conclude that Ferjufjall was completely inundated by a jökulhlaup. However, does a lack of evidence indicate

that an event did not occur? Could a jökulhlaup have partially inundated the hill without leaving trimlines?

A final challenge to using geomorphologic features to estimate jökulhlaup magnitude and extent centers around paleocompetence. Competence is measured by the largest particle size that floodwaters have the power to transport. Boulder dimensions and mass are used to calculate flow power, which can be derived to estimate flood magnitude (O'Connor, 1993; Baker, 2002; Carrivick and Rushmer, 2006; Carrivick, 2007; Carling et al., 2009a; Howard et al., 2012). This approach dictates caution, however, since peak discharge is not constant along a jökulhlaup's path; flow power attenuates as floodwaters move farther downstream. Therefore, a flood with a peak discharge of 2.2×10^7 m^3 s^{-1} may deposit boulders whose sizes accurately reflect its maximum competence in areas where floodwaters reach this peak discharge; but the same flood can deposit smaller boulders in zones where this peak flow is not reached (e.g. farther downstream). In other words, a boulder can be deposited by a flood with a peak discharge and competence different from that estimated by its dimensions.

HYDRAULIC MODELING

Geomorphologic features offer clues to jökulhlaup magnitude, path, and dynamics, but they do not provide quantitative flood hydraulics. To calculate these, scientists must input geomorphologic field data into hydraulic modeling programs, which estimate hydraulic parameters such as flow velocity, peak flow discharge, flow depth, shear stress, and stream power. These programs also use topographic data to map flood inundation area (Alho et al., 2005; Alho et al., 2007; Carrivick, 2007; Howard et al., 2012).

Paleoflood reconstruction generally uses the hydraulic modeling program HEC-RAS (Hydrologic Engineering Center River Analysis System), developed by the U.S. Army Corps of Engineers (Dyhouse et al., 2003; Howard et al., 2012). Most paleoflood modeling uses one-dimensional step-backwater models, which make several assumptions about flow and channel dynamics (such as a channel slope gradient of less than 10 percent and a constant flow energy across a given cross-section) (Alho et al., 2005; Alho et al., 2007; Carrivick, 2007; Howard et al., 2012). For detailed explanations of one-dimensional step-backwater modeling parameters and methods, see Dyhouse et al. (2003); Alho et al. (2005); Alho et al. (2007); Carrivick (2007); and Alho and Aaltonen (2008).

One-dimensional step-backwater models have several parameters. Flow can be modeled as steady—where flow depth and velocity remain constant over time at a given point in the channel—or unsteady, where depth and velocity change over time (Dyhouse et al., 2003; Ward and Trimble, 2004; Howard et al., 2012). Modeled flow can also be subcritical or supercritical, a parameter which is quantified by the Froude number—the ratio of inertial to gravitational forces at a given point in the flow. In subcritical flows, gravitational forces dominate, resulting in slow-moving, deep water, and the Froude number is less than one. Supercritical flows are shallow and fast, dominated by inertial forces, and have a Froude number greater than one (Dyhouse et al., 2003; Ward and Trimble, 2004).

Recent studies have examined the efficacy of one-dimensional versus two-dimensional hydraulic models to model paleofloods. Two-dimensional models—created in programs such as TELEMAC-2D (Alho and Aaltonen, 2008) and SOBEK (Carrivick, 2007)—model more complex flow dynamics and channel morphology than their one-dimensional counterparts

(Carrivick, 2007; Alho and Aaltonen, 2008). Carrivick (2007) reported that two-dimensional modeling more accurately estimates paleoflood hydraulics and dynamics. Alho and Aaltonen (2008), on the other hand, concluded that 1D and 2D flood models are comparable and equally accurate, a study also cited by Howard et al. (2012).

HEC-RAS works in tandem with HEC-GeoRAS, a HEC-RAS adaptation using ArcGIS that was created by the Army Corps of Engineers in cooperation with ESRI (Environmental Systems Research Institute) (Dyhouse et al., 2003; Howard et al., 2012). Remote sensing satellite images are used to generate a DEM (digital elevation model) of the study area. HEC-GeoRAS is then used to construct a series of cross-sections that accurately represent the modeled channel's geometry (Dyhouse et al., 2003; Alho et al., 2005; Howard et al., 2012). Scientists use Manning's n coefficient to estimate channel roughness along the modeled cross-sections (Dyhouse et al., 2003; Ward and Trimble, 2004; Alho et al., 2005; Alho et al., 2007; Howard et al., 2012).

Once the channel is modeled, geomorphologic field data is input into HEC-RAS. Scientists use a GPS unit to record the locations and highest elevations of flood geomorphologic features. These pieces of evidence are termed "paleostage indicators" (PSIs) and include both erosional and depositional features such as trimlines, wash limits, and boulder erratics (Alho et al., 2005; Carrivick and Rushmer, 2006; Howard et al., 2012; Carrivick et al., 2013). Once these field data are entered, the HEC-RAS model is run. Peak flow discharge is gradually increased until the modeled flood dimensions line up with the PSIs (Alho et al., 2005; Howard et al., 2012).

Alho et al. (2005) used HEC-RAS and HEC-GeoRAS to generate the most comprehensive model of the largest Holocene jökulhlaup along the Jökulsá á Fjöllum to date, modeling flood extent from Vatnajökull to the Jökulsárgljúfur canyon. Alho et al. used aerial photographs and field observations to determine the elevations and locations of wash limits (scoured lava surfaces and boulder erratics). When they input the data into HEC-RAS, the resulting flood model had an estimated peak discharge of 0.9×10^6 m^3 s^{-1}. Alho et al. also examined three channel reaches—Vaðalda, Upptyppingar, and Möðrudalur—to compare observed jökulhlaup geomorphologic features with the model (Figure 92). Field evidence largely corroborated their model: elevations of geomorphologic features matched the modeled flood surface within 1.5 m throughout the study area—except in Möðrudalur, where modeled flood levels reached about 8 m above observed wash limits (Alho et al., 2005).

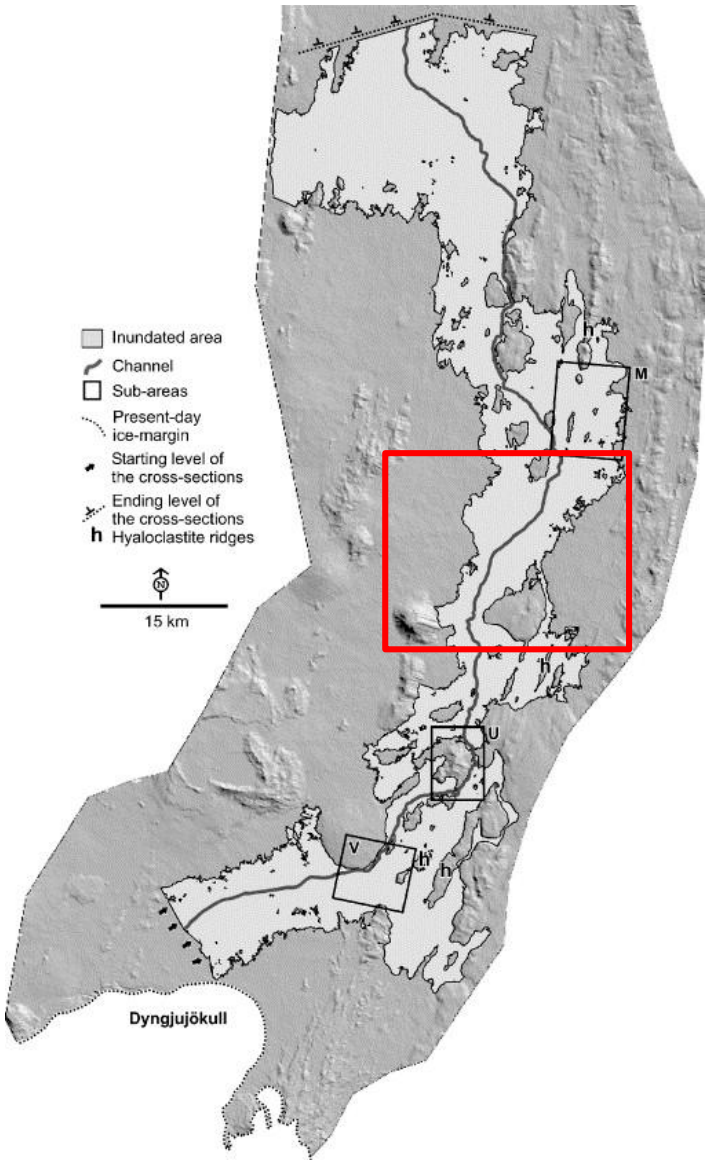

Figure 92. Alho et al.'s (2005) modeled inundation map of a jökulhlaup with a peak discharge of 0.9×10^6 m^3 s^{-1} along the first 140 km of the Jökulsá á Fjöllum after it exits Vatnajökull. V = Vaðalda; U = Upptyppingar; M = Möðrudalur. Red box denotes approximate area modeled by Howard et al. (2012) (Alho et al., 2005).

Howard et al. (2012) intended to fill Alho et al.'s (2005) geographical research gap by modeling the largest Holocene jökulhlaup in the Herðubreið reach (Figure 93). Howard et al. collected geomorphologic evidence throughout the channel, namely elevations and locations of trimlines, boulder erratics, and scoured surfaces. They also interpreted the lack of trimlines on Ferjufjall—a 558-m hill—as a sign that the hill was completely inundated. This geomorphologic data modeled a flood with a peak discharge of 2.2 x 10^7 m^3 s^{-1}: more than an order of magnitude greater than Alho et al.'s (2005) modeled flow (Figure 94). Furthermore, when Howard et al. input their highest observed trimline—670 m—the model output a peak discharge of 4.5 x 10^7 m^3 s^{-1} (Figure 95).

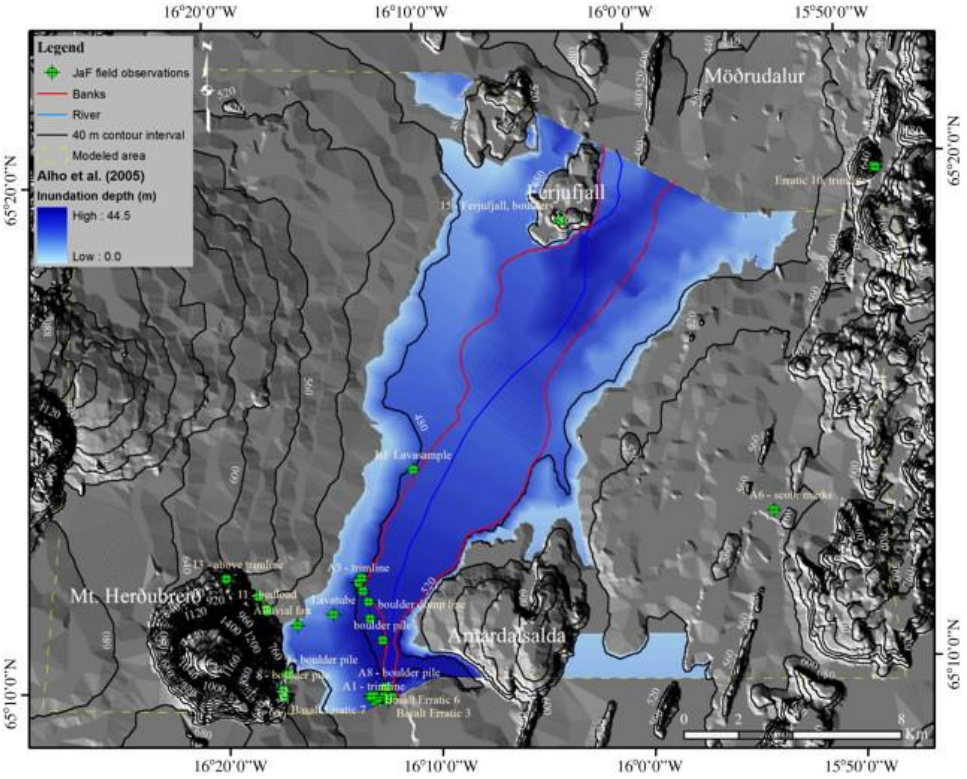

Figure 93. Howard et al.'s (2012) model of a jökulhlaup with a peak discharge of 0.9 x 10^6 m^3 s^{-1} in the Mt. Herðubreið channel reach. Flood inundation area closely matches that modeled by Alho et al. (2005) (Howard et al., 2012).

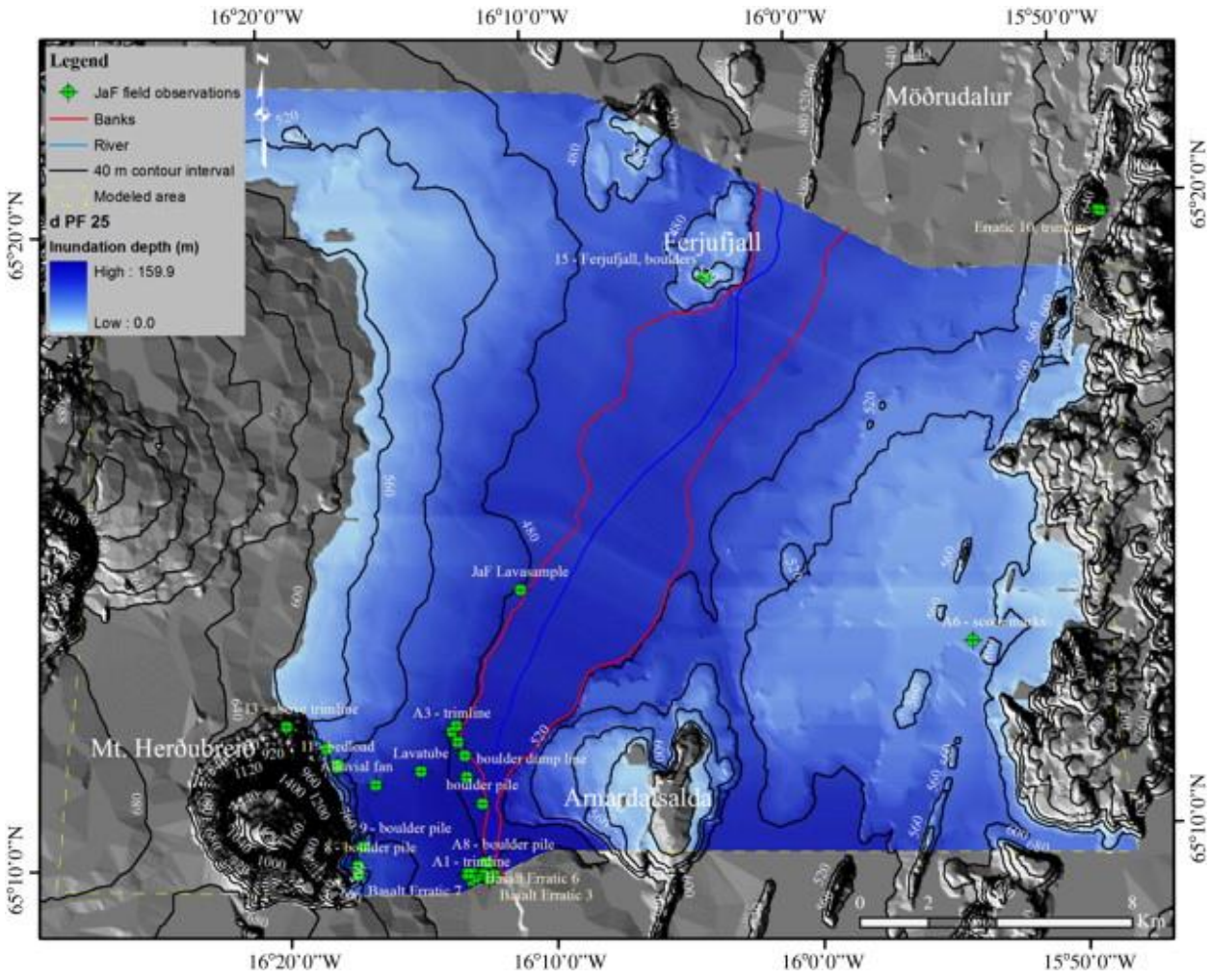

Figure 94. Howard et al.'s (2012) model of a jökulhlaup with a peak discharge of 2.2 x 10^7 m^3 s^{-1} in the Mt. Herðubreið channel reach (Howard et al., 2012).

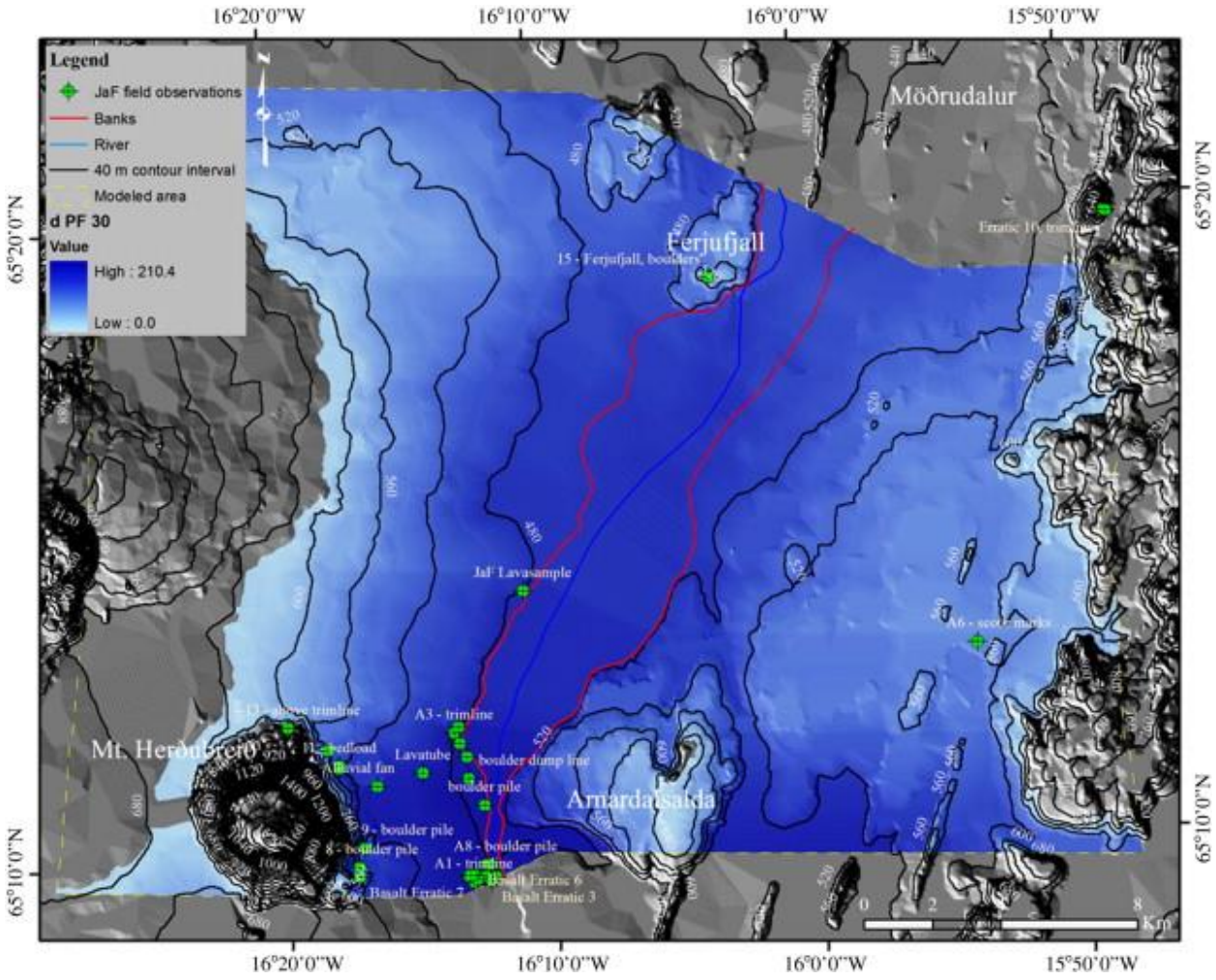

Figure 95. Howard et al.'s (2012) model of a jökulhlaup with a peak discharge of 4.5 x 10^7 m^3 s^{-1} in the Mt. Herðubreið channel reach (Howard et al., 2012).

The discrepancies between Alho et al.'s (2005) and Howard et al.'s (2012) flood models have sparked a heated debate. Which model (if either) is correct? What was the peak discharge of the largest Holocene jökulhlaup along the Jökulsá á Fjöllum? The two studies used many of the same model parameters, though some differences existed. Both ran one-dimensional step-backwater models with steady state flow (Alho et al., 2005; Howard et al., 2012). Howard et al. (2012) calculated subcritical flow for each of their channel cross-sections. Alho et al. (2005)

calculated subcritical flow along most of the river course, with two exceptions: the gorges at Upptyppingar and downstream of Möðrudalur had a supercritical Froude number of 1.4, the highest along the flood's path.

Alho et al. (2005) estimated Manning's n from satellite images interpreted by Alho (2003), calculating a range of surface roughness coefficients from 0.025—0.075. Howard et al. (2012) used a nearly identical range of Manning's n values—0.03—0.075—although they measured them in the field at the channel cross-sections. Alho et al. (2005) and Howard et al. (2012), however, acknowledge the potential for error in choosing Manning's n values. Howard et al. (2012) used Alho et al.'s (2005) estimated peak discharge to calibrate their model, which produced a similar flood inundation map to Alho et al.'s and also matched Howard et al.'s lowest elevation of observed jökulhlaup geomorphologic evidence. Since modeling parameters were very similar overall, the main cause of difference in modeled flood magnitude and extent appears to be Howard et al.'s higher observed geomorphologic features.

CRITIQUES OF HYDRAULIC MODELING

Although hydraulic modeling is an invaluable tool for modeling paleoflood hydraulics, it is not a panacea for the uncertainty of Holocene jökulhlaup reconstruction. Alho et al. (2005) recognized that a potential source of modeling error was uncertainty of the channel's pre-jökulhlaup topography. Channel morphology may have been extensively modified by subsequent floods or tectonic processes, yet paleoflood models are based off of current DEMs (Alho et al., 2005).

Another source of uncertainty in HEC-RAS modeling stems from the estimation of Manning's n value. Estimating surface roughness leaves considerable room for error; guidelines

exist, but assigning values is still subjective (Dyhouse et al., 2003; Ward and Trimble, 2004). Estimations are also subject to differences in methodology: for example, Alho et al. (2005) estimated values based off satellite images, whereas Howard et al. (2012) calculated Manning's n from field work along channel cross-sections. Furthermore, although the flood models used a similar overall range of Manning's n coefficients, the models examined different channel cross-sections (Alho et al., 2005; Howard et al., 2012).

A third major source of modeling uncertainty is Alho et al.'s (2005) and Howard et al.'s (2012) assumption of steady state flow—where flow depth and velocity do not change over time at a given point in the channel. This is an unrealistic scenario in a natural setting, especially during a flood with such an enormous quantity of water across such a topographically varied landscape. This assumption may result in modeling error (Dyhouse et al., 2003; Ward and Trimble, 2004).

Alho et al. (2005) and Howard et al. (2012) both recognized another source of uncertainty in their models: a dearth of field evidence. Peak flood discharge is calculated with a "best fit" of water surface profile with geomorphologic features (Alho et al., 2005; Howard et al., 2012); therefore, the more geomorphologic evidence, the more accurate the model. Collecting more field evidence will strengthen these models and improve our understanding of paleoflood dynamics.

CHAPTER 10: EVIDENCE OF HOLOCENE JÖKULHLAUPS ALONG THE JÖKULSÁ Á FJÖLLUM: FLOOD TIMING

Geomorphologic evidence and hydraulic modeling provide clues to flood magnitude, path, and dynamics. Yet to reconstruct a timeline of Holocene jökulhlaups along the Jökulsá á Fjöllum, one crucial piece remains missing from the puzzle: flood timing. Until recently, tephrochronology was the primary method to date flood events along the Jökulsá á Fjöllum; in the last few years, however, researchers have begun using cosmogenic nuclide exposure dating on bedrock surfaces and boulder erratics to investigate jökulhlaup timing.

TEPHROCHRONOLOGY

Most previous studies of Holocene jökulhlaups along the Jökulsá á Fjöllum have used tephrochronology to date sediment sequences. Interpretation draws heavily on tephra layers deposited by three eruptions from the Hekla volcano: H3 (3200—3100 BP); H4 (4300—4200 BP); and H5 (7000—6900 BP) (Waitt, 2002; Kirkbride et al., 2006). As an example, Waitt (2002) found that a stratigraphic sequence along the Jökulsá á Fjöllum was missing all tephra layers older than a sediment sequence dated between H3 and an eruption in 1477. This suggests that a large jökulhlaup occurred after H3's deposition (3200—3100 BP) but before the bottom layer was deposited, confining the flood to around 2500—2000 BP (Waitt, 2002). Waitt (2002) also reported a sedimentary sequence of silt, sand, and tephra layers above Vesturdalur near the Jökulsárgljúfur canyon that contains layers deposited by slackwaters from at least 16 floods between about 8000 and 4000 BP (Figure 96).

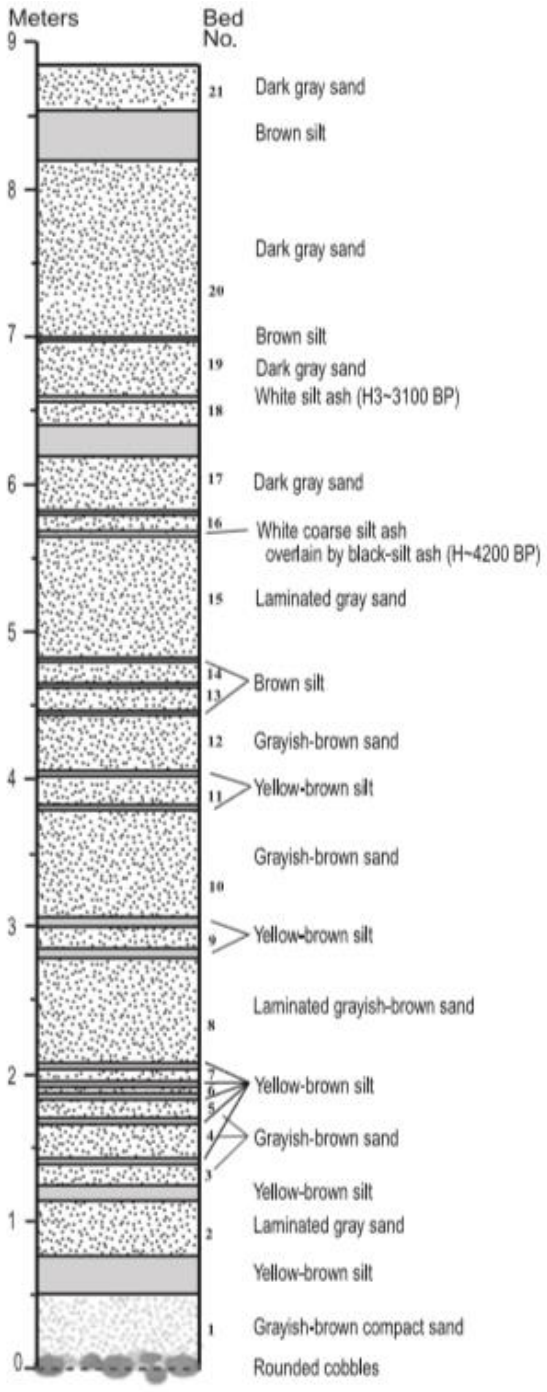

Figure 96. Sedimentological sequence from Vesturdalur of sand, silt, and tephra layers showing evidence of at least 16 jökulhlaups from about 8000—4000 BP (Waitt, 2002).

In another study, Tómasson (2002) reported that the oldest tephra layer within the estimated flood path dates to around 2000 BP; the next-oldest expected tephra layer is from an eruption around 2800 BP. Like Waitt (2002), this tephrochronological evidence suggests that a large jökulhlaup tore down the Jökulsá á Fjöllum around 2500 BP. However, as Tómasson (2002, p. 124) stated, "The question of whether or not there has been more than one catastrophic flood cannot be answered by tephrochronology."

COSMOGENIC NUCLIDE EXPOSURE DATING

Studies have recently begun to employ cosmogenic nuclide exposure dating to reconstruct a timeline of Holocene jökulhlaups along the Jökulsá á Fjöllum. This technique measures the amount of time a rock surface has been exposed to the atmosphere. Depending on the cosmogenic nuclide measured, it can report ages ranging from 1000 to 10 million years. Cosmogenic nuclides are often used to date moraines to reconstruct glacier or ice sheet position (Cockburn and Summerfield, 2004; Davies, 2014). For jökulhlaup timeline reconstruction, the method is employed in two ways: 1) to date bedrock surfaces to determine when the surface was scoured (Baynes, 2012; Baynes et al., 2015b); and 2) to date boulder erratics to determine when the rock was deposited (Howard et al., 2012; Howard, unpublished, 2013).

Cosmogenic nuclides are generated by supernovas. They enter Earth's atmosphere and bombard its surface as cosmic rays. This neutron bombardment alters some minerals, breaking apart their nuclei and creating new elements or isotopes through a reaction called spallation. Measuring the concentration of the reaction product allows scientists to calculate the amount of time the surface has been exposed to cosmic rays (Cockburn and Summerfield, 2004; Davies, 2014).

Different minerals generate different products under spallation. Helium-3 (^{3}He) is produced when ^{4}He decays during the spallation reaction between cosmic rays and olivine, and the ratio of $^{3}He/^{4}He$ reveals the exposure age (Cockburn and Summerfield, 2004; Baynes, 2012; Baynes et al., 2015b). Cosmic rays alter quartz to Beryllium-10 (^{10}Be), which is used to measure exposure ages of sandstone and granite (Cockburn and Summerfield, 2004; Davies, 2014). Calcite decays to Chlorine-36 (^{36}Cl), which is used to date basalt (Cockburn and Summerfield, 2004; Licciardi et al., 2008). Licciardi et al. (2008) noted that ^{36}Cl dating can be used on almost every surface in Iceland. We measure ^{36}Cl concentrations to date our boulder erratic samples.

Numerous factors govern the selection of boulders to sample in the field. The ideal boulder is free of lichen, vegetation, and snow cover; has minimal shielding (no topographic features that shadow the rock and block incoming cosmic rays); and has not rolled, moved, or been buried since deposition (Figure 97) (Cockburn and Summerfield, 2004; Davies, 2014; Howard, personal communication, 2015). Sampling follows several steps: 1) photograph the target boulder from all angles; 2) measure inclination and shielding; and 3) chisel 500 g of rock off the top 2—3 cm of the boulder's surface (cosmic rays only penetrate the top few centimeters of the rock (Figures 98-99) (Davies, 2014)).

Figure 97. Left: Sampled boulder erratic on Upptyppingar: a prime candidate due to large size, minimal shielding, and lack of vegetation cover. Right: Assessing a candidate for sampling in the Upptyppingar boulder field (photos by author).

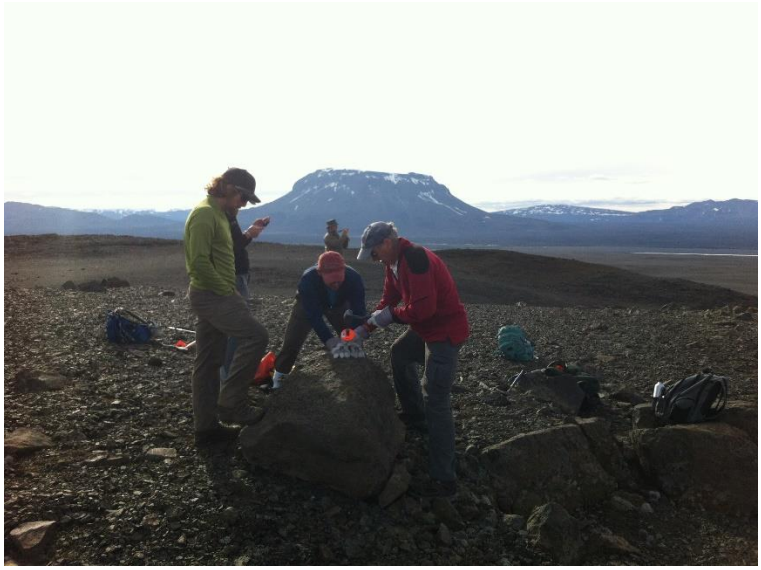

Figure 98. Chiseling a rock sample from a boulder erratic on the summit of Arnardalsalda, across from Mt. Herðubreið. Note researchers collecting inclination and GPS data in the background (photo by author).

Figure 99. Boulder erratic surface after sample collection. Red circle shows chiseled rock area. Erratic is in the boulder field at the Upptyppingar cataract (photo by author).

We sent our rock samples for analysis at PRIME Lab (Purdue Rare Isotope Measurement Laboratory) at Purdue University, and we expect to receive results in May 2016. After the lab reports the ^{36}Cl concentrations, our final step is to calculate exposure age by accounting for cosmogenic nuclide "production rate," which depends on elevation and latitude (Cockburn and Summerfield, 2004; Licciardi et al., 2008; Davies, 2014). Generally, cosmogenic nuclide production rates increase with increasing elevation and latitude (Licciardi et al., 2008). Baynes (2012) and Baynes et al. (2015b) measured ^{3}He concentrations on bedrock surfaces in the Jökulsárgljúfur and Ásbyrgi canyons to reconstruct jökulhlaup timing along the Jökulsá á Fjöllum. Their results from Jökulsárgljúfur clustered around two dates: about 5 ka and 2 ka. They concluded that these dates corresponded to two major jökulhlaups, which eroded bedrock through knickpoint retreat and exposed the current surfaces to cosmic rays. These dates corroborate tephrochronological evidence suggesting a major flood around 2000 BP and a series

of floods between 8000 and 4000 BP (Baynes et al., 2015b). Baynes et al. (2015b) also sampled an "eroded notch" in the rim of Ásbyrgi, which yielded a date of roughly 9 ka, suggesting that Ásbyrgi was carved by a catastrophic jökulhlaup at this time, but that subsequent floods did not reach the canyon.

Howard et al. (2012) proposed carrying out cosmogenic nuclide dating on boulder erratics in the Herðubreið channel reach to determine age of deposition. Boulder erratics up to several meters in diameter perch on ridges and hill summits, some hundreds of meters above the valley floor (Figures 100-101). Few geomorphologic processes are powerful enough to transport such large particles to such high elevations, save for glaciers and megafloods. We assume that glacial or jökulhlaup transport exposed a fresh rock surface and that cosmogenic nuclide dating will tell us the date the boulder was deposited. If boulders date to older than roughly 10.3 ka BP, they were likely deposited by glaciers. If they date to younger than 10.3 ka BP, however—after the study area had been deglaciated—they were likely deposited by megafloods.

Figure 100. Boulder erratics on the eastern flank of Mt. Herðubreið above 500 masl—higher than the flood inundation elevation modeled by Alho et al. (2005) (Howard, unpublished, 2013).

Figure 101. Boulder erratics on the summit of Ferjufjall (558 masl), above Alho et al.'s (2005) modeled inundation elevation. Boulder in front is approximately 1 m wide. White arrow denotes flow direction; black arrow shows hyaloclastite outcrop (Howard, unpublished).

Howard (unpublished, 2013) sampled seven boulder erratics in the Herðubreið channel reach and obtained two to three cosmogenic nuclide dates for each sample (Figures 102-103). Four boulders—samples HR003, HR004, HR005, and HR006—lie at elevations between 550 and 600 masl—within Alho et al.'s (2005) modeled inundation area for a peak flow discharge of 0.9 x 106 m3 s-1. Cosmogenic dates range from 5930—1570 BP. This corroborates previous flood chronology, suggesting that multiple floods occurred between roughly 1500 and 6000 BP (Howard, unpublished, 2013).

A fifth boulder erratic—HR002—yielded an exposure age between 12180—9180 BP. These dates average to before deglaciation in the region around 10.3 ka BP, suggesting that the boulder was glacially deposited. The boulder is located just outside of Howard et al.'s (2012) modeled inundation area, however, so we do not know definitively if it lies above the modeled

floodwaters; nonetheless, its elevation (750 masl) exceeds Howard et al.'s (2012) highest observed trimline (670 m) in the Herðubreið stretch, supporting a glacial origin.

Thus far, Howard's (unpublished, 2013) boulder dates fit with Alho et al.'s (2005) smaller flood model. Two sampled erratics, however, break this trend and support Howard et al.'s (2012) modeled larger peak discharge. HR001—collected at the base of Mt. Herðubreið at an elevation of 600—650 masl—dated between 6990 and 4930 BP. HR007—situated just above 600 masl—yielded an age range of 7470—5590 BP. These two erratics are situated above the reach of floodwaters according to Alho et al.'s (2005) model, but within the inundation area of Howard et al.'s (2012) model of a larger peak flow discharge. Their date ranges firmly situate them post-deglaciation, leaving one prime suspect for their transportation and deposition: jökulhlaups. This evidence supports Howard et al.'s (2012) estimated peak discharge of 2.2 x 10^7 m^3 s^{-1}—the largest known flood on Earth. Only the very oldest dates in this range, however, match with Howard et al.'s (2012) predicted timeframe for this catastrophic flood (9000—7100 BP).

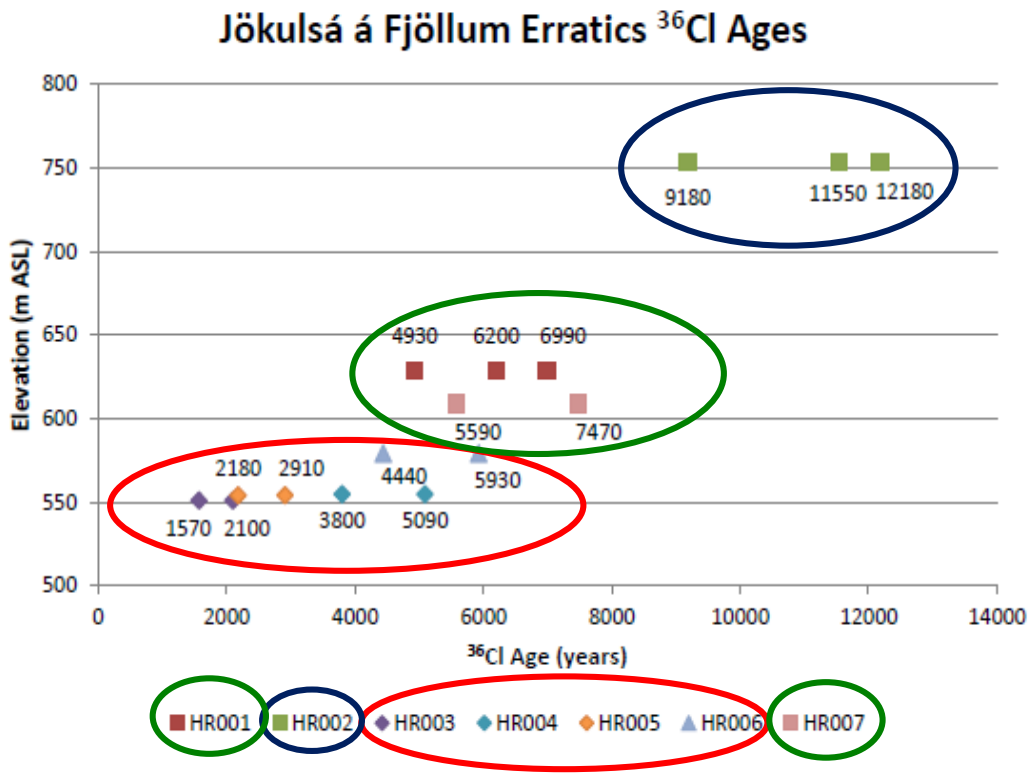

Figure 102. Cosmogenic nuclide exposure dates reported from seven boulder erratics sampled by Howard. Colored circles correspond to sampling locations in Figure 103 (modified from Howard, unpublished, 2013).

Figure 103. Locations of boulder erratics sampled for cosmogenic nuclide exposure dating by Howard (unpublished, 2013); mapped on Howard et al.'s (2012) inundation map of a 2.2 x 10^7 m^3 s^{-1} peak discharge flood. Black line delineates inundation area of Alho et al.'s (2005) modeled 0.9 x 10^6 m^3 s^{-1} peak discharge flood. Colored circles correspond with dates in Figure x. Numbers match number in sample code (e.g. 2 = HR002) (modified from Howard et al., 2012).

Our team sampled 8 boulder erratics in August 2015 to expand this data set in order to test Howard et al.'s (2012) hypothesis. Samples are undergoing cosmogenic nuclide 36Cl dating at PRIME Lab, and we expect to receive results in May 2016. We targeted sampling sites that were inundated according to Howard et al.'s (2012) larger flood model, but above the reach of Alho et al.'s (2005) modeled flood. Of particular interest was Arnardalsalda (648 masl), which was not inundated according to Alho et al.'s (2005) model, but was inundated up to about 640 masl under Howard et al.'s (2012) model (Howard, unpublished, 2013). We sampled boulders at several elevations on Arnardalsalda, including the summit.

We also expanded sample collection to channel reaches that were not modeled by Howard et al. (2012), such as at Upptyppingar, where we sampled boulders above the spillway and in the boulder run-up to the cataract. These dates will serve as paleostage indicators to expand our HEC-RAS flood model, while also providing insight into the formation of these newly reported geomorphologic features.

CRITIQUES OF COSMOGENIC NUCLIDE EXPOSURE DATING

Cosmogenic nuclide dating is an essential tool for dating jökulhlaup geomorphologic features along the Jökulsá á Fjöllum, but—like any method—the technique has several sources of error. First, we assume that jökulhlaup or glacial transport exposes a fresh rock surface that begins to accumulate cosmogenic nuclides as soon as it is exposed. In the case of a megaflood, a boulder likely tumbled along the bottom as bedload or collided with other particles in the flow, chipping off its outer layer and exposing a fresh surface. If the boulder was ice-rafted during a jökulhlaup, we assume that it was shielded from cosmic rays while encased in ice, only beginning to accumulate cosmogenic nuclides after deposition and ice melt. If the boulder was

glacially transported, we assume that its outer layer was scoured off as it was dragged along the glacier bed, with the fresh surface beginning to accumulate cosmogenic nuclides when the glacier receded from the study area around 10.3 ka BP. In the case of bedrock, we assume that bedload in floodwaters or glaciers scoured the top layer off the bedrock surface, exposing fresh rock to cosmic rays.

These assumptions, however, leave room for error. Abrasion may not remove the entire rock layer in which cosmogenic nuclides accumulated during prior exposure. These "inherited" cosmogenic nuclides result in an overestimated exposure date (Cockburn and Summerfield, 2004; Davies, 2014).

Age overestimation is one source of error in cosmogenic nuclide dating; but age underestimation is another. Exposure ages assume that a rock surface has been accumulating cosmogenic nuclides since it was exposed to the atmosphere. However, the surface could have eroded since initial exposure, stripping off cosmogenic nuclides and thus underestimating deposition age. Iceland's central highlands are blasted with strong winds, which often carry black basalt sand (as well as tephra, pumice, and other aeolian sediments). This sandblasting creates ventifaction on many boulders, which could remove accumulated cosmogenic nuclides. Fluvial or aeolian erosion could also strip cosmogenic nuclides off flood-sculpted bedrock surfaces, thus underestimating jökulhlaup age.

Burial can also result in an underestimation of surface exposure dates. Iceland's dynamic landscape changes quickly and rocks can be rapidly buried or exhumed—for example, through freeze-thaw processes or tectonic rifting (Carrivick et al., 2013). Most of the study area is covered by snow for much of the year, and aeolian sediment constantly shifts across the surface.

These covers shield rock from cosmic rays, underestimating surface exposure age (Cockburn and Summerfield, 2004; Davies, 2014).

To minimize these sources of error, scientists select erratics according to several criteria, which we also used to choose our samples: 1) boulders that have not moved or rolled since deposition (e.g. large rocks or rocks on flat, stable surfaces); 2) boulders that are not shadowed by topographic shielding or covered by vegetation or snow; 3) large boulders that are unlikely to have been exhumed or buried; and 4) boulders that do not show evidence of recent erosion (Cockburn and Summerfield, 2004; Davies, 2014; Howard, personal communication, 2015).

PART III: FRAMEWORK FOR FUTURE RESEARCH

CHAPTER 11: FUTURE LINES OF INQUIRY

Previous research has built a solid framework for reconstructing a timeline of Holocene jökulhlaups along the Jökulsá á Fjöllum and determining the magnitude of the largest flood in the channel. Researchers generally agree on a skeleton timeline: by around 10.3 ka BP, the ice sheet had receded from Iceland's central highlands. Since deglaciation, numerous jökulhlaups have surged down the Jökulsá á Fjöllum channel, dramatically altering the landscape. The two largest floods likely occurred around 9000—7100 BP and 2500—2000 BP; and at least 16 smaller floods occurred in the intervening years (Waitt, 2002; Howard et al., 2012).

Flood magnitude, however, is a more contentious point. Alho et al. (2005) estimated that the largest Holocene jökulhlaup along the channel had a peak discharge of 0.9×10^6 m^3 s^{-1}; but Howard et al. (2012) found evidence suggesting a flood with a peak discharge of 2.2×10^7 m^3 s^{-1}, which would make this the largest known flood on Earth. The Jökulsá á Fjöllum flows through a dynamic landscape that has been buffeted by myriad geologic processes throughout the Holocene: from the retreat of the ice sheet to fluvial and megaflood incision in the bedrock channel; and from tectonic rifting and lava flows to aeolian sandblasting of rock surfaces. This amalgamation of processes has modified jökulhlaup geomorphologic evidence, complicating reconstruction of flood events along the channel.

Previous studies have relied on geomorphologic evidence, hydraulic modeling, tephrochronology, and cosmogenic nuclide exposure dating to estimate flood magnitude, extent, and timing. However, there are additional lines of evidence we can use to glean better insight into jökulhlaup history along the Jökulsá á Fjöllum and test Howard et al.'s (2012) hypothesis of

the largest known flood on Earth. This section sets up a framework for future research to answer these questions. It draws on several new lines of evidence that have been used to investigate other jökulhlaups, but have not yet been applied to study Icelandic paleofloods. Each line of evidence represents one piece of the puzzle; our goal is to collect all of the pieces and fit them together to reconstruct Holocene jökulhlaup history along the Jökulsá á Fjöllum.

Expanded Geomorphologic Evidence and Cosmogenic Nuclide Exposure Dating

In order to reconstruct a timeline of Holocene jökulhlaups along the Jökulsá á Fjöllum, we must collect geomorphologic evidence and cosmogenic nuclide dates along the entire length of the channel. This data will allow us to construct a hydraulic model spanning the length of the river, from its exit at Vatnajökull to its mouth at the Arctic Ocean. The more data we collect, the more comprehensive the model will be. We can then return to the field to check our model's accuracy by comparing it with geomorphologic field evidence.

Submarine Evidence of Jökulhlaups

A jökulhlaup discharging millions of cubic meters of water per second would have picked up and transported an enormous quantity of sediment as it surged over 200 km from Vatnajökull to the Arctic Ocean. Although some of this material was deposited in low-energy areas along the flood route, most of it was likely transported all the way to the ocean (Carrivick et al., 2013; Timothy Beach, personal communication, 2016). Studies in other regions have examined submarine jökulhlaup deposits, potentially offering insight into applying this line of evidence to study paleofloods along the Jökulsá á Fjöllum.

Jökulhlaup-transported sediment enters the ocean as hyperpycnal flow—meaning that its density is higher than that of the ocean—and settles quickly, creating enormous submarine sediment fans

called turbidites (Baker and Bunker, 1985; Baker, 2002). The high velocity of the floods often propels these turbidity currents far out to sea (Baker, 2002). Jökulhlaups can also trigger decreases in ocean salinity and increased rates of sediment accumulation (Andrews, 2005). Offshore evidence is reported for jökulhlaups draining off the southern coast of Iceland, as well as from Lake Missoula, Lake Agassiz, and glaciers in Alaska. No literature exists, however, on jökulhlaup evidence in marine sediment cores off the island's northern coast—specifically near the mouth of the Jökulsá á Fjöllum. A search of the Site Survey Data Bank (SSDB)—the online database of the International Ocean Discovery Program (IODP)—also yielded no data on marine sediment cores drilled near the river mouth, marking a significant research gap (International Ocean Discovery Program (IODP), 2015). We can examine megaflood evidence from other submarine environments to determine how to sample and interpret marine sediment cores offshore of the Jökulsá á Fjöllum's mouth. These cores could yield valuable insight into jökulhlaup timing and magnitude.

Jökulhlaups in Southern Iceland

Although marine jökulhlaup evidence has not been reported off Iceland's northern coast, researchers have collected marine sediment cores off the island's southwestern shore that show an increased rate of sediment accumulation, possibly due to jökulhlaup deposition. Sediment deposition rate is determined by radiocarbon dating, usually of foraminifera (Andrews, 2005). In addition to rapid deposition, marine sediment cores also show evidence of decreased salinity, measured by the species of foraminifera present in the sediments. While foraminifera from offshore cores in Iceland have mainly been used to interpret paleoclimate and deglaciation

history, they could provide valuable clues to Holocene jökulhlaup timing and magnitude along the Jökulsá á Fjöllum (Andrews, 2005).

Maria et al. (2000) examined marine sediment cores offshore of Skeiðarársandur to analyze deposits from the 1996 Grímsvötn jökulhlaup. They found that these deposits were not produced by the eruption itself, but were materials deposited by previous volcanism that were scooped up as floodwaters surged by. Although most of the flood's sediment load had been deposited on the sandur, the amount that reached the ocean was very coarse-grained (mostly sand) and settled out near shore (Maria et al., 2000). Maria et al. (2000) also noted that fine-grained particles such as silt were distributed throughout the ocean instead of settling out of the sediment plume and forming concentrated deposits. Lacasse et al. (1998) and Geirsdóttir et al. (2009) also studied jökulhlaup evidence in marine sediment cores off Iceland's southern coast.

Lake Missoula Floods

Jökulhlaup turbidity currents also exist at the mouth of the Columbia River where glacial Lake Missoula megafloods surged into the Pacific Ocean. Baker (2002) described submarine graded sediment deposits over 100 m thick that are situated roughly 1000 km from the Columbia River's mouth, which were deposited as turbidity currents when the floods entered the ocean. However, he noted that sea level was 60—70 m lower than present at the time of flooding, suggesting that submarine-transported sediment was not propelled quite as far into the ocean (Baker, 2002). Normark and Reid (2003) also charted these turbidity currents across the ocean floor to nearly 1000 km offshore, and dates fit well within the Late Pleistocene window of Lake Missoula megafloods.

Lake Agassiz Floods

Jökulhlaups draining from Lake Agassiz also deposited sediments: largely coarse material such as sand in smaller lakes, and finer particles such as silts and clays in oceans and large lakes (wherever flow velocity slowed enough for these particles to settle out) (Kehew and Lord, 1987; Kehew et al., 2009). Lake Agassiz floods spilled through a series of smaller lakes on their way to the ocean (much like water spilling into neighboring compartments in an ice cube tray). Flow was hyperpycnal when it entered these small lakes, forming turbidity currents. Deposits were generally coarser-grained (mostly sand) and well-sorted, and they became finer with increasing distance from their input point. Most fine-grained particles, however, did not have sufficient time to settle and were swept along by continuing floodwaters (Kehew and Lord, 1987; Kehew et al., 2009). Katz et al. (2011), Rayburn et al. (2009), and Cronin et al. (2012) analyzed foraminifera from sediment cores in the former Champlain Sea, using species presence and shell oxygen isotope concentrations to determine salinity levels and sedimentation rates, thus helping to reconstruct Lake Agassiz flood events draining into the North Atlantic Ocean around the Pleistocene—Holocene transition.

Alaskan Glacial Outburst Floods

Submarine jökulhlaup deposits are also found in Alaska. Willems et al. (2011) examined submarine sedimentation from jökulhlaups (with peak discharges on the magnitudes of 10^4—10^5 $m^3\ s^{-1}$) that drained from glaciers into Disenchantment Bay in southern Alaska. Willems et al. (2011) described possible jökulhlaup sediment deposition scenarios—all of which depended on flow velocity, sediment load, and bathymetry of the depositional site—notably: turbidity currents; submarine debris flows; settling from surface plumes; and "continuous hyperpycnal

plumes." Willems et al. (2011) also noted that Icelandic jökulhlaups—at least those during historic times—usually produce hyperpycnal plumes.

SOURCE OF FLOODWATERS

Regardless of size, most studies concur on the source of jökulhlaups in the Jökulsá á Fjöllum. Waitt (2002) noted that "subglacially erupting basaltic lava can melt 14 times its volume of glacier ice," thus leaving the meltwater "poised for catastrophic escape" in the form of a jökulhlaup. Waitt (2002) identified eruptions from Kverkfjöll volcano—which generated meltwater from both Dyngjujökull and Kverkjökull glaciers—as the source for jökulhlaups in the Jökulsá á Fjöllum. Alho et al. (2005) agreed that Jökulsá á Fjöllum jökulhlaups were triggered by eruptions from Kverkfjöll and Bárðarbunga and that meltwater accumulated from Dyngjujökull and Kverkjökull. Furthermore, Kverkfjöll and Bárðarbunga are the only volcanic systems within the Jökulsá á Fjöllum's subglacial drainage basin (Figure 104).

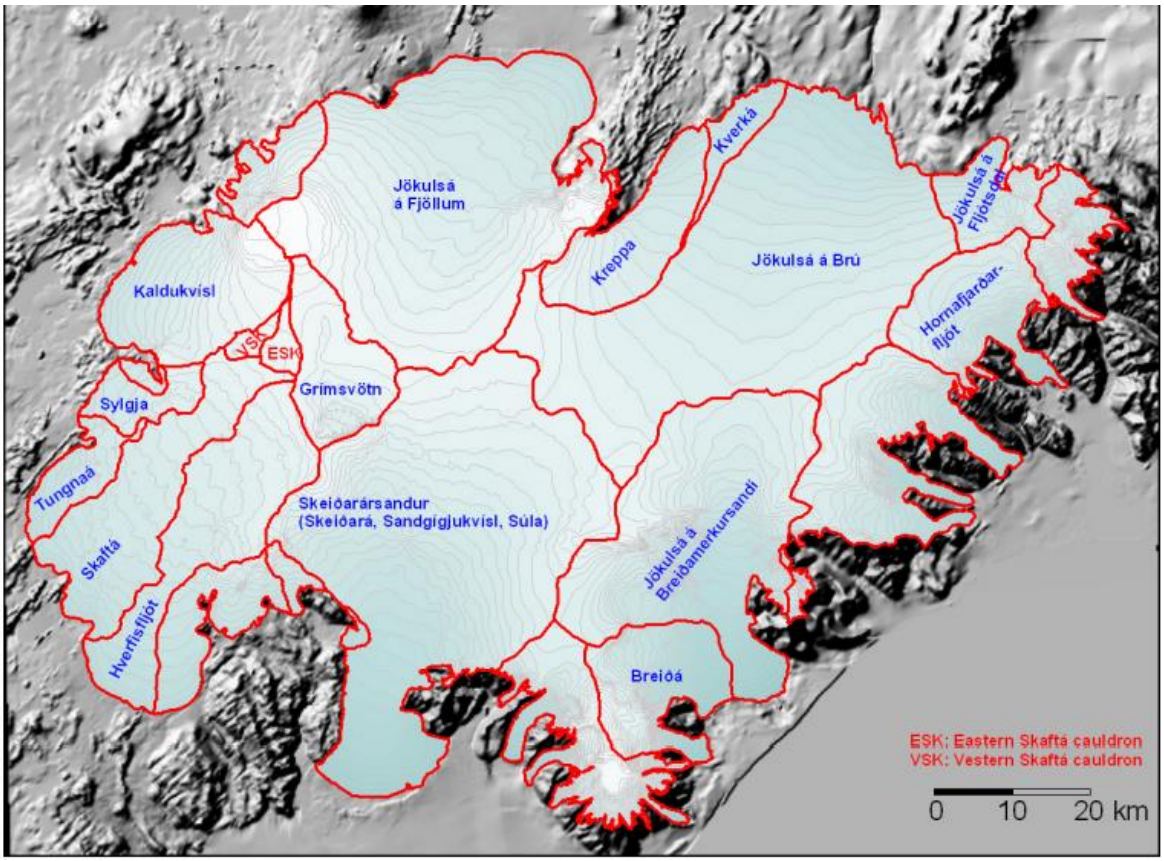

Figure 104. Drainage basins of geothermally-generated meltwater for rivers draining Vatnajökull (Björnsson and Pálsson, 2008).

Yet controversy arises over the size of these megafloods. One of the major criticisms of Howard et al.'s (2012) flood model is that Vatnajökull could not have generated a large enough quantity of water to produce a jökulhlaup with a peak discharge of 2.2×10^7 m^3 s^{-1} (Carrivick et al., 2013). Howard et al. (2012) postulated that a combination of sources was necessary to generate this volume—likely subglacial lakes in the Kverkfjöll and Bárðarbunga calderas as well as marginal lakes formed during ice cap retreat. This section proposes several lines of evidence that have been uninvestigated to date to determine the source of the largest jökulhlaup along the

Jökulsá á Fjöllum, and thus to test Howard et al.'s (2012) hypothesis: ice cap volume and position; subglacial eruption history; and paleolake trimlines.

Ice Cap Volume and Position

In order to determine the source of jökulhlaups along the Jökulsá á Fjöllum, we must reconstruct Vatnajökull's position and volume throughout the Holocene. Studies have tried to reconstruct the ice cap's movement across the landscape by studying moraine deposits (Geirsdóttir et al., 2009; Ingólfsson et al., 2010). Determining glacier extent also helps us to estimate ice cap volume; and quantifying the amount of ice in Vatnajökull allows us to estimate how much meltwater a subglacial eruption could have generated.

In a critique of Howard et al.'s (2012) paper, Carrivick et al. (2013) expressed skepticism that Vatnajökull could have produced a flood with a peak discharge of 2.2×10^7 m^3 s^{-1}. They calculated that a jökulhlaup this large would equate to a water volume of 1529 km^3, which they argued was unlikely given that this value was over half of Vatnajökull's ice volume in 2000 (approximately 3100 km^3, which converts to 2790 km^3 of meltwater) (Carrivick et al., 2013). As another point of comparison, Carrivick et al. (2013) cited Herget's (2005) estimate that the largest Kuray flood had a volume of 695 km^3 (to produce an estimated peak flood discharge of 1×10^7 m^3 s^{-1}). O'Connor (1993) estimated that 4750 km^3 of water drained from Lake Bonneville, reaching a peak discharge of 1×10^6 m^3 s^{-1} (but draining over several weeks).

Six known subglacial lakes lie beneath Vatnajökull (Björnsson, 2002; Björnsson, 2009). The 1996 jökulhlaup from Grímsvötn—which reached a peak discharge of $4.5—5.3 \times 10^4$ m^3 s^{-1}—released 3.2 km^3 of meltwater (Benn and Evans, 2010). Jökulhlaups draining through the Jökulsá á Fjöllum, however, are sourced from a smaller subglacial lake in the Kverkfjöll caldera

or pool in the Bárðarbunga caldera before drainage (Waitt, 2002; Alho et al., 2005; Howard et al., 2012). No studies to date have reported the capacities of these calderas, leaving a significant research gap. This data would provide key insight into the amount of water that could have drained to produce the largest Holocene jökulhlaup.

Marginal lakes have formed at the edges of Vatnajökull throughout the Holocene, and several currently extend off its glaciers, such as the proglacial lake at Skaftafellsjökull (Figure 105). Grænalón is another proglacial lake on the southern edge of Vatnajökull. It has an area of 18 km^2 and a volume of 2 km^3 and has produced jökulhlaups with peak discharges of 2—3 x 10^3 m^3 s^{-1} (Björnsson, 2009). Jökulsárlón—the famous "glacier lagoon" off Vatnajökull's southeastern corner—covers 21 km^2; however, Jökulsárlón is not technically a lake as a narrow channel connects it to the sea (Figure 106) (Schomacker, 2010).

Figure 105. Proglacial lake in front of Skaftafellsjökull (photo by author).

Figure 106. Jökulsárlón—also known as the "glacier lagoon"—is a proglacial lake extending off Vatnajökull's southern side. Icebergs calve off Vatnajökull and fill the lagoon (photo by author).

Although these present-day lakes are far too small to produce a jökulhlaup with the magnitude of Howard et al.'s (2012) modeled flood, marginal lakes may have been considerably larger earlier in the Holocene. They may have emptied in tandem with subglacial lakes in the Bárðarbunga and Kverkfjöll calderas and meltwater from Dyngjujökull and Kverkjökull generated during a subglacial eruption to produce a catastrophic jökulhlaup with Howard et al.'s (2012) estimated peak discharge.

Carrivick et al. (2013, p. 518) rejected Howard et al.'s (2012) estimated peak flood discharge on the grounds that there is no evidence for a source that could generate such an enormous quantity of water, concluding: "We cannot envisage how such a large flood could conceivably have been sourced and triggered from northern Vatnajökull." It is important to note, however, there is also no evidence against a source this large. Harkening back to J Harlen Bretz's Channeled Scabland debate, we must revisit William Morris Davis's "value of

outrageous hypotheses" (Davis, 1926). Rather than confining our interpretation of landforms to familiar geologic processes, we must "…ask by what other outrageous process it is proposed to explain them" (Davis, 1926, p. 468). Reconstructing Vatnajökull's volume and position throughout the Holocene will help determine whether or not the ice cap and marginal lakes could have generated a jökulhlaup as large as that proposed by Howard et al. (2012).

Paleolake Trimlines, Shorelines, and Terraces

A second line of evidence that may provide clues to the source of Holocene jökulhlaups along the Jökulsá á Fjöllum is the reconstruction of trimlines and terraces from marginal paleolakes. Subglacial lake reconstruction is more difficult and may be impossible since Bárðarbunga and Kverkfjöll—the only identified geothermal areas within the Jökulsá á Fjöllum's subglacial drainage basin—are buried beneath hundreds of meters of ice (Björnsson and Pálsson, 2008; Björnsson, 2009).

Marginal lake paleo-shoreline evidence, however, holds potential for jökulhlaup source reconstruction. Lake levels leave distinctive trimlines and/or terraces. No existing publications have investigated this line of evidence for jökulhlaups draining along the Jökulsá á Fjöllum, although Tómasson (2002) used shorelines to reconstruct levels of paleolakes that drained jökulhlaups around 9500 BP in the Hvítá River (which drains the Langjökull ice cap). Numerous studies outside of Iceland have used shoreline evidence to reconstruct paleolakes. Herget (2005) reported trimlines marking lake levels in the Chuja and Kuray Basins (a source for the Kuray megafloods). Trimlines and extent of lake sediment deposits enable estimation of lake depth and extent, and thus lake volume. Lake age can be determined by radiocarbon dating organic material in these deposits (Herget, 2005).

Studies on outburst floods down the Tsangpo River gorge in Tibet also used paleolake shorelines and terraces to reconstruct outburst flood volume and dynamics. Jökulhlaups drained from glacial lakes during the Holocene and carved much of the gorge (Montgomery et al., 2004; Liu et al., 2015). Some studies have dated lake sediments on terraces—which mostly consist of laminated clay and silt, sand, and some pebbles—using OSL (optically stimulated luminescence) (Liu et al., 2015) and radiocarbon dating (Montgomery et al., 2004; Liu et al., 2015) to determine deposition ages and reconstruct lake volume and surface extent.

If we can reconstruct Vatnajökull's northern limits over the course of the Holocene, we will have a better idea of where marginal lakes formed, and thus where we should search for paleo-shorelines and terraces. These lines of evidence would provide clues to lake volume and extent, allowing us to estimate marginal lake contribution to floods and providing another piece of the puzzle to determine the largest Holocene jökulhlaup along the Jökulsá á Fjöllum.

Subglacial Eruption History

As a final line of evidence to determine the source of jökulhlaups along the Jökulsá á Fjöllum, we can reconstruct a timeline of subglacial eruptions beneath Vatnajökull to try to chronologically match flood events with volcanic activity that could have generated enough meltwater to produce a jökulhlaup as cataclysmic as that proposed by Howard et al. (2012). Iceland has a well-documented tephrochronological record that chronicles eruptions throughout the Holocene (Waitt, 2002; Kirkbride et al., 2006). Since Bárðarbunga and Kverkfjöll are the only volcanoes within the Jökulsá á Fjöllum's subglacial drainage area, we must use tephra deposits and lava flows to compile a Holocene record of those eruptions (Björnsson and Pálsson, 2008).

One piece of evidence that supports the claim of a catastrophic jökulhlaup between 9000—7100 BP (as claimed by Waitt (2002), Alho et al. (2005), and Howard et al. (2012)) is the spike in volcanic activity that occurred soon after the ice sheet retreated roughly 10 ka BP (Howard et al., 2012; Carrivick et al., 2013). As the ice sheet receded and thinned, the Earth's surface rebounded. This decrease in overlying pressure triggered volcanic eruptions in an effect similar to uncapping a shaken bottle of soda. Increased volcanic activity lasted for 1000—2000 years (Sigmundsson, 2006), which would place its end around 9000—8000 BP, corresponding with the estimated date of the largest Holocene jökulhlaup. Sigmundsson (2006) stated that "volcanic production was up to 30 times higher than today's rate." Carrivick et al. (2013) cited a similar increase of 20—30 times in north-central Iceland. Furthermore, lava flows spilled across the region throughout the early and mid-Holocene (Jóhannesson and Saemundsson, 1998a,b; Sigmundsson, 2006). This increased geothermal activity likely generated enormous quantities of meltwater beneath the remnant ice cap, possibly resulting in more and/or larger jökulhlaups.

SOILS AND ROFABARDS

Another potential line of evidence for Holocene jökulhlaup reconstruction along the Jökulsá á Fjöllum lies in the soil record along the flood path (Timothy Beach, personal communication, 2016). Megaflood sedimentological deposits have been studied and dated, but there is a dearth of literature on using soils to date jökulhlaup events. The vast majority of the estimated flood path—under both Alho et al.'s (2005) and Howard et al.'s (2012) models—is unvegetated: a barren moonscape crisscrossed by lava flows, columnar basalt, hyaloclastite tuyas, and tephra deposits. However, islands of soils and rofabards are scattered intermittently across the landscape, usually adjacent to rivers or lakes. We can collect sediment cores and use

tephrochronology and radiocarbon dating to determine the oldest soil layer, and thus establish a minimum date of a catastrophic jökulhlaup event. This dangerously assumes, however, that jökulhlaups erased all previous soil deposits; perhaps a small flood occurred that did not erode the entire record, leading to an erroneous interpretation of the most recent flood date.

In August 2015, we collected a sediment core to search for jökulhlaup deposits in the sedimentary record. The area between Arnardalsalda and Þríhyrmngsvatn lake is dissected by tributary streams and small lakes and is partially underlain by wetlands and soils. This is one of the only sections we observed along the Jökulsá á Fjöllum channel (between Kverkfjallarani and Grímsstaðir) that was vegetated. The shores of Þríhyrmngsvatn host a wetland covered by mosses, grasses, and low-lying shrubs (Figure 107).

Figure 107. Left: wetland on the shore of Þríhyrmngsvatn lake. Right: coring site on the lake shore (photos by author).

We took a sediment core in the wetland ~20 m from the lake's southern shore. The top of the core consisted of peat-like soil covered with a surface mat of moss, grass, and small plants. At a depth of 40 cm, the core became crumbly, unconsolidated pumice-gravel mixed with black

sand and a small amount of organics. It was very difficult to drive the corer in and to extrude it, and we abandoned the attempt after 40 cm as we would have needed a larger corer to go deeper.

A number of studies have used lake cores to study paleoclimate and sedimentation rates in Icelandic lakes (such as Larsen et al. (2011); Striberger et al. (2011); and Blair et al. (2015))—although the literature is devoid of studies in the central eastern highlands. Furthermore, no studies have reported using sediment cores to look for jökulhlaup deposits. Mórauðavatn—a lake roughly 10 km west of Þríhyrmngsvatn—may be a promising coring site since it lies in the inundation zone of Howard et al.'s (2012) modeled flood. Unfortunately, we could not ford the river to access the lake. Looking for jökulhlaup evidence in soil profiles and sediment cores is a possible line of future inquiry to reconstruct jökulhlaup history along the Jökulsá á Fjöllum.

CORRELATION WITH CLIMATE EVENTS

A final line of future inquiry could investigate correlations between jökulhlaup events and global climate shifts or sea level rises. No studies to date have reported on this in Iceland. Numerous studies, however, have examined the link between Lake Agassiz megafloods and global climate shifts. Evidence suggests that drainage events through the St. Lawrence Estuary may have delivered enough freshwater into the North Atlantic to lower local ocean salinity and slow down the thermohaline cycle (also known as Atlantic Meridional Overturning Circulation). This may have triggered global cooling events, notably the Younger Dryas (around 13 ka), the Preboreal oscillation (11.5 ka), and the 8.2 ka cooling event (Kehew et al., 2009; Katz et al., 2011; Rayburn et al., 2011; Cronin et al., 2012).

Katz et al. (2011) used paleo-shorelines, estuarine models and bathymetry, and isotopic and foraminifer proxies in sediment cores to determine salinity of the Champlain Sea, a saltwater

inland sea in the Champlain and St. Lawrence Valleys that connected to the North Atlantic Ocean. They found evidence of a significant drop in salinity around 11.5 ka, which corresponds with the onset of the Preboreal oscillation, suggesting a cause-and-effect link between megafloods and climate shifts (Katz et al., 2011).

In another study, Cronin et al. (2012) found evidence linking Younger Dryas cooling to a flood event from Lake Agassiz. Oxygen isotope ratios in foraminifera and ostracodes extracted from sediment cores in the former Champlain Sea pointed to a drop in salinity between 13.1 ka and 12.9 ka, suggesting a large freshwater input. This date closely matches the onset of the Younger Dryas cooling event (around 13 ka), although Cronin et al. (2012) were not convinced that the flood events were significant enough to trigger global cooling (Cronin et al., 2012).

A third study by Rayburn et al. (2011) discovered evidence of freshwater input events in the St. Lawrence Estuary at the beginning of the Younger Dryas. Sedimentation rates, varves, pollen, and foraminifera and ostracodes in sediment cores from the former Champlain Sea reflect both a short period of reduced salinity lasting for less than one year and a longer period of "freshening" lasting for up to a century between 13.2 ka and 12.9 cal ka BP (Rayburn et al., 2011). Rayburn et al. (2011) hypothesized that the first freshwater pulse flowed from smaller glacial Lake Vermont and discharged a total of 0.1 Sv (1×10^5 m^3 s^{-1}) of water, whereas the larger drainage event from Lake Agassiz had a total discharge of 0.30 Sv (3×10^5 m^3 s^{-1}). While stopping short of attributing Younger Dryas cooling to this drainage event, Rayburn et al. (2011) recognized that the timing matched and the link was possible.

These links between Lake Agassiz floods and global climate shifts may offer insight into possible climate effects of Holocene jökulhlaups along the Jökulsá á Fjöllum. The timing of

global and/or regional climate shifts could be compared with jökulhlaup chronology along the channel, potentially revealing climatic effects due to enormous freshwater inputs into the Arctic Ocean—and thus aiding in estimating the water volume and flood magnitude required to trigger those climatic shifts.

CONCLUSION

In his first publication proposing a megaflood origin of eastern Washington's Channeled Scabland, J Harlen Bretz wrote: "…each newly examined scabland tract reawakened a feeling of amazement that such huge streams could take origin from such small marginal tracts of an ice sheet, or that such an enormous amount of erosion, despite high gradients, could have resulted in the very brief time these streams existed" (Bretz, 1923, p. 24). The central-eastern highlands in Iceland inspire a similar sense of awe and kindle an insatiable curiosity about how this complex landscape formed.

Unraveling the myriad geologic processes at work in this dynamic landscape presents a significant challenge. Iceland's central highlands have been sculpted by glacial, fluvial, and aeolian processes. The region is also situated over a tectonic spreading center, adding volcanism to this geomorphologic cocktail. Jökulhlaups have surged down the Jökulsá á Fjöllum river channel throughout the Holocene, leaving behind a suite of megaflood erosional and depositional features. While studies concur that these jökulhlaups were among the largest floods on Earth, a study by Howard et al. (2012) found evidence suggesting a peak flood discharge of 2.2×10^7 m^3 s^{-1} —over a magnitude greater than previously cited peak discharges—which would make this the largest known flood in Earth history.

This project seeks to test Howard et al.'s (2012) hypothesis and, more broadly, to reconstruct a Holocene jökulhlaup timeline along the Jökulsá á Fjöllum. It examines previous research, presents new evidence, and sets up a framework for future research in order to solve this enigmatic puzzle.

While critics argue that a flood of this magnitude was not possible from Vatnajökull, initial field evidence challenges this position. J Harlen Bretz defended his megaflood hypothesis for decades in the face of similar skepticism, eventually prevailing and championing William Morris Davis's "value of outrageous hypotheses" (Davis, 1926). It is imperative to maintain this openness to geologic processes and landscape evolution instead of limiting our interpretation to established principles.

The area along the Jökulsá á Fjöllum incites curiosity at every turn, whether standing on a mountain summit hundreds of meters above the valley floor watching the river wind through a barren moonscape of scoured lava and columnar basalt towers; walking over streamlined hills studded with boulder erratics several meters in diameter; or exploring an ice cave where the Jökulsá á Fjöllum gushes from beneath Vatnajökull. This incredible landscape—molded by so many geologic processes—is a complex puzzle, and it is our goal to assemble the pieces in order to reconstruct a timeline of jökulhlaups along the channel throughout the Holocene—as well as to test the hypothesis of the largest known flood on Earth.

References

Agrawala, S., 2008. Responses to glacier retreat in the context of development planning in Nepal. In: Orlove, B., Wiegandt, E., Luckman, B.H. (Eds.), Darkening Peaks: Glacier Retreat, Science, and Society. University of California Press, Berkeley, CA, pp. 241-248.

Alho, P., 2003. Land cover characteristics in NE Iceland with special reference to jökulhlaup geomorphology. Geografiska Annaler 85 A (3-4), 213-227.

Alho, P., Aaltonen, J., 2008. Comparing a 1D hydraulic model with a 2D hydraulic model for the simulation of extreme glacial outburst floods. Hydrological Processes 22, 1537-1547.

Alho, P., Russell, A.J., Carrivick, J.L., Käyhkö, J., 2005. Reconstruction of the largest Holocene jökulhlaup within Jökulsá á Fjöllum, NE Iceland. Quaternary Science Reviews 24, 2319-2334.

Alho, P., Roberts, M.J., Käyhkö, J., 2007. Estimating the inundation area of a massive, hypothetical jökulhlaup from northwest Vatnajökull, Iceland. Natural Hazards 41, 21-42.

Andrews, J.T., 2005. Late Quaternary marine sediment studies of the Iceland shelf—palaeoceanography, land/ice sheet/ocean interactions, and deglaciation: a review. In: Caseldine, C., Russell, A., Harðardöttir, J., Knudsen, Ó. (Eds.), Iceland—Modern Processes and Past Environments. Elsevier, Amsterdam, pp. 5-24.

Árnadóttir, T., Lund, B., Jiang, W., Geirsson, H., Björnsson, H., Einarsson, P., Sigurdsson, T., 2009. Glacial rebound and plate spreading: results from the first countrywide GPS observations in Iceland. Geophysical Journal International 177, 691-716.

Arnalds, Ó., 2000. The Icelandic ‘rofabard’ soil erosion features. Earth Surface Processes and Landforms 25, 17-28.

Arnalds, Ó., 2004. Volcanic soils of Iceland. Catena 56, 3-20.

Arnalds, A., 2005a. Approaches to landcare—a century of soil conservation in Iceland. Land Degradation and Development 16, 113-125.

Arnalds, Ó., 2005b. Icelandic soils. In: Caseldine, C., Russell, A., Harðardöttir, J., Knudsen, Ó. (Eds.), Iceland—Modern Processes and Past Environments. Elsevier, Amsterdam, pp. 309-318.

Arnalds, Ó., 2008. Soils of Iceland. Jökull 58, 409-421.

Arnalds, Ó., Barkarson, B.H., 2003. Soil erosion and land use policy in Iceland in relation to sheep grazing and government subsidies. Environmental Science & Policy 6, 105-113.

Arnalds, Ó., Gretarsson, E., 2004. Icelandic Soils. Retrieved 10 May 2015, from http://www.rala.is/desert/2-1.html.

Arnalds, Ó., Gísladóttir, F.O., Sigurjonsson, H., 2001. Sandy deserts of Iceland: an overview. Journal of Arid Environments 47, 259-371.

Auriac, A., Spaans, K.H., Sigmundsson, F., Hooper, A., Schmidt, P., Lund, B., 2013. Iceland rising: solid Earth response to ice retreat inferred from satellite radar interferometry and visocelastic [sic] modeling. Journal of Geophysical Research: Solid Earth 118, 1331-1344.

Bain, C., Averbuck, A., 2015. Iceland, 9th ed. Lonely Planet Publications. (384 pp.).

Baker, V.R., 1973. Paleohydrology and sedimentology of Lake Missoula flooding in eastern Washington. Special Paper 144. Geological Society of America, Boulder, CO. (79 pp.).

Baker, V.R., 1978a. Large-scale erosional and depositional features of the Channeled Scabland. In: Baker, V.R. (Ed.), 1981, Catastrophic Flooding: The Origin of the Channeled Scabland. Dowden, Hutchinson & Ross, Stroudsburg, PA, pp. 276-310.

Baker, V.R., 1978b. Paleohydraulics and hydrodynamics of Scabland floods. In: Baker, V.R. (Ed.), 1981, Catastrophic Flooding: The Origin of the Channeled Scabland. Dowden, Hutchinson & Ross, Stroudsburg, PA, pp. 255-275.

Baker, V.R. (Ed.), 1981. Catastrophic Flooding: The Origin of the Channeled Scabland. Dowden, Hutchinson & Ross, Stroudsburg, PA. (360 pp.).

Baker, V.R., 2002. High-energy megafloods: planetary settings and sedimentary dynamics. In: Martini, I.P., Baker, V.R., Garzón, G. (Eds.), Flood and Megaflood Processes and Deposits: Recent and Ancient Examples. Special Publications of the International Association of Sedimentologists. Blackwell Science, Oxford, pp. 3-15.

Baker, V.R., 2009a. Channeled Scabland morphology. In: Burr, D.M., Carling, P.A., Baker, V.R. (Eds.), Megaflooding on Earth and Mars. Cambridge University Press, Cambridge, pp. 65-77.

Baker, V.R., 2009b. Overview of megaflooding: Earth and Mars. In: Burr, D.M., Carling, P.A., Baker, V.R. (Eds.), Megaflooding on Earth and Mars. Cambridge University Press, Cambridge, pp. 1-12.

Baker, V.R., 2009c. The Channeled Scabland: a retrospective. Annual Review of Earth and Planetary Sciences 37, 393-411.

Baker, V.R., Bunker, R.C., 1985. Cataclysmic late Pleistocene flooding from glacial Lake Missoula: a review. Quaternary Science Reviews 4, 1-41.

Baker, V.R., Twidale, C.R., 1991. The reenchantment of geomorphology. Geomorphology 4(2), 73-100.

Baker, V.R., Benito, G., Rudoy, A.N., 1993. Paleohydrology of late Pleistocene superflooding, Altay Mountains, Siberia. Science 259, 348-350.

Baynes, E., 2012. Quantifying extreme bedrock erosion during Icelandic megafloods: field report. University of Edinburgh School of Geosciences. (18 pp.).

Baynes, E.R.C., Attal, M., Dugmore, A.J., Kirstein, L.A., Whaler, K.A., 2015a. Catastrophic impact of extreme flood events on the morphology and evolution of the lower Jökulsá á Fjöllum (northeast Iceland) during the Holocene. Geomorphology 250, 422-436.

Baynes, E.R.C., Attal, M., Niedermann, S., Kirstein, L.A., Dugmore, A.J., Naylor, M., 2015b. Erosion during extreme flood events dominates Holocene canyon evolution in northeast Iceland. Proceedings of the National Academy of Science 112(8), 2355-2360.

Benito, G., 1997. Energy expenditure and geomorphic work of the cataclysmic Missoula flooding in the Columbia River Gorge, USA. Earth Surface Processes and Landforms 22, 457-472.

Benn, D.I., Evans, D.J.A., 2010. Glaciers & Glaciation, 2nd ed. Hodder Education, London. (802 pp.).

Björnsson, H., 2002. Subglacial lakes and jökulhlaups in Iceland. Global and Planetary Change 35, 255-271.

Björnsson, H., 2009. Jökulhlaups in Iceland: sources, release and drainage. In: Burr, D.M., Carling, P.A., and Baker, V.R. (Eds.), Megaflooding on Earth and Mars. Cambridge University Press, Cambridge, pp. 50-77.

Björnsson, H., Pálsson, F., 2008. Icelandic glaciers. Jökull 58, 365-386.

Blair, C.L., Geirsdóttir, A., Miller, G.H., 2015. A high-resolution multi-proxy lake record of Holocene environmental change in southern Iceland. Journal of Quaternary Science 30(3), 281-292.

Bretz, J.H., 1923. The Channeled Scablands of the Columbia Plateau. In: Baker, V.R. (Ed.), 1981, Catastrophic Flooding: The Origin of the Channeled Scabland. Dowden, Hutchinson & Ross, Inc., Stroudsburg, PA, pp. 20-52.

Bretz, J. H., 1928. The Channeled Scabland of eastern Washington. In: Baker, V.R. (Ed.), 1981, Catastrophic Flooding: The Origin of the Channeled Scabland. Dowden, Hutchinson & Ross, Inc., Stroudsburg, PA, pp. 88-119.

Bretz, J.H., 1978. Introduction. In: Baker, V.R. (Ed.), 1981, Catastrophic Flooding: The Origin of the Channeled Scabland. Dowden, Hutchinson & Ross, Stroudsburg, PA, pp. 18-19.

Burr, D., McEwen, A., 2002. Recent extreme floods on Mars. In: Snorasson, A., Finnsdóttir, H.P., Moss, M., The Extremes of the Extremes: Extraordinary Floods. Proc. of a Symp., Reykjavik, IAHS Publication 271, Wallingford, Oxfordshire, UK, pp. 101-106.

Byers, A.C., McKinney, D.C., Byers, E.A., 2015. Post-earthquake assessment: Imja, Tsho Rolpa, and Thulagi glacial lakes in Nepal. United States Agency for International Development (USAID) Technical Report. USAID, Washington, D.C. (65 pp.).

Carling, P.A., Kirkbride, A.D., Parnachov, S., Borodavko, P.S., Berger, G.W., 2002. Late Quaternary catastrophic flooding in the Altai Mountains of south-central Siberia: a synoptic overview and an introduction to flood deposit sedimentology. In: Martini, I.P., Baker, V.R., Garzón, G. (Eds.), Flood and Megaflood Processes and Deposits: Recent and Ancient Examples. Special Publications of the International Association of Sedimentologists. Blackwell Science, Oxford, pp. 17-35.

Carling, P.A., Burr, D.M., Johnsen, T.F., Brennand, T.A., 2009a. A review of open-channel megaflood depositional landforms on Earth and Mars. In: Burr, D.M., Carling, P.A., and Baker, V.R. (Eds.), Megaflooding on Earth and Mars. Cambridge University Press, Cambridge, pp. 33-49.

Carling, P.A., Herget, J., Lanz, J.K., Richardson, K., Pacifici, A., 2009b. Channel-scale erosional bedforms in bedrock and in loose granular material: character, processes and implications. In: Burr, D.M., Carling, P.A., and Baker, V.R. (Eds.), Megaflooding on Earth and Mars. Cambridge University Press, Cambridge, pp. 13-32.

Carling, P.A., Martini, P., Herget, J., Borodavko, P., Parnachov, S., 2009c. Megaflood sedimentary valley fill: Altai Mountains, Siberia. In: Burr, D.M., Carling, P.A., and Baker, V.R. (Eds.), Megaflooding on Earth and Mars. Cambridge University Press, Cambridge, pp. 243-264.

Carey, M., 2008. The politics of place: inhabiting and defending glacier hazard zones in Peru's Cordillera Blanca. In: Orlove, B., Wiegandt, E., Luckman, B.H. (Eds.), Darkening Peaks: Glacier Retreat, Science, and Society. University of California Press, Berkeley, CA, pp. 229-240.

Carr, M.H., 1979. Formation of Martian flood features by release of water from confined aquifers. Journal of Geophysical Research 84, 2995-3007.

Carrivick, J.L., 2007. Hydrodynamics and geomorphic work of jökulhlaups (glacial outburst floods) from Kverkfjöll volcano, Iceland. Hydrological Processes 21, 725-740.

Carrivick, J.L., 2009. Jökulhlaups from Kverkfjöll volcano, Iceland: modelling transient hydraulic phenomena. In: Burr, D.M., Carling, P.A., and Baker, V.R. (Eds.), Megaflooding on Earth and Mars. Cambridge University Press, Cambridge, pp. 273-289.

Carrivick, J.L., Rushmer, L.E., 2006. Understanding high-magnitude outburst floods. Geology Today 22(2), 60-65.

Carrivick, J.L., Russell, A.J., Tweed, F.S., 2004a. Geomorphological evidence for jökulhlaups from Kverkfjöll volcano, Iceland. Geomorphology 63, 81-2002.

Carrivick, J.L., Russell, A.J., Tweed, F.S., Twigg, D., 2004b. Palaeohydrology and sedimentary impacts of jökulhlaups from Kverkfjöll, Iceland. Sedimentary Geology 172, 19-40.

Carrivick, J.L., Tweed, F.S., Carling, P., Alho, P., Marren, P.M., Staines, K., Russell, A.J., Rushmer, E.L., Duller, R., 2013. Discussion of 'Field evidence and hydraulic modeling of a large Holocene jökulhlaup at Jökulsá á Fjöllum channel, Iceland' by Douglas Howard, Sheryl Luzzadder-Beach and Timothy Beach, 2012. Geomorphology 201, 512-519.

Cenderelli, D.A., Cluer, B.L., 1998. Depositional processes and sediment supply in resistant-boundary channels: examples from two case studies. In: Tinkler, K.J., Wohl, E.E. (Eds.), Rivers Over Rock: Fluvial Processes in Bedrock Channels. American Geophysical Union, Washington, D.C., pp. 105-131.

Church, J.A., White, N.J., 2011. Sea-level rise from the late 19th to the early 21st century. Surveys in Geophysics 32, 585-602.

Cockburn, H.A.P., Summerfield, M.A., 2004. Geomorphological applications of cosmogenic isotope analysis. Progress in Physical Geography 28(1), 1-42.

Costa, J.E., 1988. Floods from dam failures. In: Baker, V.R., Kochel, R.C., Patton, P.C. (Eds.), Flood Geomorphology. John Wiley & Sons, New York, pp. 439-463.

Cronin, T.M., Rayburn, J.A., Guilbault, J.-P., Thunell, R., Franzi, D.A., 2012. Stable isotope evidence for glacial lake drainage through the St. Lawrence Estuary, eastern Canada, ~13.1—12.9 ka. Quaternary International 260, 55-65.

Davis, W.M., 1926. The value of outrageous geological hypotheses. Science 63(1636), p. 463-468.

Davies, B., 2014. Cosmogenic nuclide dating. Retrieved 11 May 2015, from http://www.antarcticglaciers.org/glacial-geology/dating-glacial-sediments-

2/cosmogenic_nuclide_datin/.

Dyhouse, G.R., Hatchett, J., Benn, J., 2003. Floodplain Modeling Using HEC-RAS, 1st ed. Haestad Press, Waterbury, CT. (696 pp.).

Fleming, K., Martinec, Z., Wolf, D., 2007. Glacial-isostatic adjustment and the viscosity structure underlying Vatnajökull ice cap, Iceland. Pure and Applied Geophysics 164, 751-768.

Geirsdóttir, A., Eiríksson, J., 1994. Growth of an intermittent ice sheet in Iceland during the late Pliocene and early Pleistocene. Quaternary Research 42, 115-130.

Geirsdóttir, Á., Hardardóttir, J., Sveinbjörnsdóttir, Á.E., 2000. Glacial extent and catastrophic meltwater events during the deglaciation of Southern Iceland. Quaternary Science Reviews 19, 1749-1761.

Geirsdóttir, Á., Miller, G.H., Andrews, J.T., 2007. Glaciation, erosion, and landscape evolution of Iceland. Journal of Geodynamics 43, 170-186.

Geirsdóttir, Á., Miller, G.H., Axford, Y., Ólafsdóttir, S., 2009. Holocene and latest Pleistocene climate and glacier fluctuations in Iceland. Quaternary Science Reviews 28, 2107-2118.

Global Volcanism Program, 2013. Volcanoes of the World, v. 4.4.3. Venzke, E. (ed.). Smithsonian Institution. Retrieved 3 May 2016 from http://volcano.si.edu. http://dx.doi.org/10.5479/si.GVP.VOTW4-2013.

Greipsson, S., 2012. Catastrophic soil erosion in Iceland: impact of long-term climate change, compounded natural disturbances and human driven land-use changes. Catena 98, 41-54.

Guðmundsson, M.T., 2005. Subglacial volcanic activity in Iceland. In: Caseldine, C., Russell, A., Harðardöttir, J., Knudsen, Ó. (Eds.), Iceland—Modern Processes and Past Environments. Elsevier, Amsterdam, pp. 127-151.

Gudmundsson, M.T., Högnadóttir, T., 2007. Volcanic systems and calderas in the Vatnajökull region, central Iceland: Constraints on crustal structure from gravity data. Journal of Geodynamics 43, 153-169.

Gudmundsson, M.T., Larsen, G., Höskuldsson, Á., Gylfason, Á.G., 2008. Volcanic hazards in Iceland. Jökull 58, 251-268.

Hannesdóttir, H., Björnsson, H., Pálsson, F., Aðalgeirsdóttir, G., Guðmundsson, Sv., 2015. Changes in the southeast Vatnajökull ice cap, Iceland, between ~1890 and 2010. The Cryosphere 9, 565-585.

Herget, J., 2005. Reconstruction of Pleistocene ice-dammed lake outburst floods in the Altai Mountains, Siberia. Special Paper 386. Geological Society of America, Boulder, CO. (118 pp.).

Howard, D.A., unpublished results, 2013. Response to "Discussion of 'Field evidence and hydraulic modeling of a large Holocene jökulhlaup at Jökulsá á Fjöllum channel, Iceland' by Douglas Howard, Sheryl Luzzadder-Beach, and Timothy Beach, 2012."

Howard, D.A., 2008. Quantitative hydrologic and hydraulic models for jökulhlaup-type outflow channels on Mars: application of Earth analogues, comparative geomorphology, and remote sensing. Ph.D. Thesis, George Mason University, Fairfax, Virginia. (202 pp.).

Howard, D.A., Luzzadder-Beach, S., Beach, T., 2012. Field evidence and hydraulic modeling of a large Holocene jökulhlaup at Jökulsá á Fjöllum channel, Iceland. Geomorphology 147-148, 73-85.

Hubbard, A., Sugden, D., Dugmore, A., Norddahl, H., Pétursson, H.G., 2006. A modelling insight into the Icelandic Last Glacial Maximum ice sheet. Quaternary Science Reviews 25, 2283-2296.

Huggel, C., Haeberli, W., Kääb, A., 2008. Glacial hazards: perceiving and responding to threats in four world regions. In: Orlove, B., Wiegandt, E., Luckman, B.H. (Eds.), Darkening Peaks: Glacier Retreat, Science, and Society. University of California Press, Berkeley, CA, pp. 68-80.

Icelandic Meteorological Office (IMO), 2015. Bárðarbunga update. Retrieved 5 April 2015, from http://en.vedur.is/earthquakes-and-volcanism/articles/nr/2947.

Icelandic Meteorological Office (IMO), 2016. Hydrology. Retrieved 4 May 2016, from http://en.vedur.is.

Ingólfsson, Ó., Norðdahl, H., Schomacker, A., 2010. Deglaciation and Holocene glacial history of Iceland. In: Schomacker, A., Krüger, J., Kjær, K.H. (Eds.), The Mýrdalsjökull Ice Cap, Iceland: Glacial Processes, Sediments and Landforms on an Active Volcano. Elsevier, Amsterdam, pp. 51-68.

Intergovernmental Panel on Climate Change (IPCC), 2014. Climate Change 2014: Impacts, Adaptation, and Vulnerability. 5th Assessment Report. Retrieved 4 May 2016, from http://www.ipcc.ch.

International Ocean Discovery Program (IODP), 2015. Site Survey Data Bank. Retrieved 3 May 2016, from http://ssdb.iodp.org/about.php.

International Soil Reference and Information Centre (ISRIC), 2015. Leptosols. Retrieved 10 May

2015, from
http://www.isric.org/sites/default/files/major_soils_of_the_world/set4/lp/leptosol.pdf.

Jóhannesson, H., Saemundsson, K., 1998a. Geological Map of Iceland. 1:500 000. Bedrock Geology. Icelandic Institute of Natural History, Reykjavík (2nd edition).

Jóhannesson, H., Saemundsson, K., 1998b. Geological Map of Iceland. 1:500 000. Tectonics. Icelandic Institute of Natural History, Reykjavík (1st edition).

Katz, B., Najjar, R.G., Cronin, T., Rayburn, J., Mann, M.E., 2011. Constraints on Lake Agassiz discharge through the late-glacial Champlain Sea (St. Lawrence Lowlands, Canada) using salinity proxies and an estuarine circulation model. Quaternary Science Reviews 30, 3248-3257.

Kehew, A.E., Lord, M.L., 1987. Glacial-lake outbursts along the mid-continent margins of the Laurentide ice-sheet. In: Mayer, L., Nash, D. (Eds.), Catastrophic Flooding. Allen & Unwin, Boston, MA, pp. 95-120.

Kehew, A.E., Lord, M.L., Kozlowski, A.L., Fisher, T.G., 2009. Proglacial megaflooding along the margins of the Laurentide Ice Sheet. In: Burr, D.M., Carling, P.A., Baker, V.R. (Eds.), Megaflooding on Earth and Mars. Cambridge University Press, Cambridge, pp. 104-127.

Kharin, G.S., Eroshenko, D.V., 2010. The evolution of Cenozoic explosive volcanism: the Iceland Plume. Journal of Volcanology and Seismology 4(5), 310-333.

Kirkbride, M.P., Dugmore, A.J., Brazier, V., 2006. Radiocarbon dating of mid-Holocene megaflood deposits in the Jökulsá á Fjöllum, north Iceland. The Holocene 16(4), 605-609.

Knudsen, Ó., Russell, A.J., 2002. Jökulhlaup deposits at the Ásbyrgi Canyon, northern Iceland: sedimentology and implications for flow type. In: Snorasson, A., Finnsdóttir, H.P., Moss, M., The Extremes of the Extremes: Extraordinary Floods. Proc. of a Symp., Reykjavik. IAHS Publication 271, Wallingford, Oxfordshire, UK, pp. 107-112.

Kristmannsdóttir, H., Björnsson, A., Pálsson, S., Sveinbjörnsdóttir, Á.E., 1999. The impact of the 1996 subglacial volcanic eruption in Vatnajökull on the river Jökulsá á Fjöllum, North Iceland. Journal of Volcanology and Geothermal Research 92, 359-372.

Lacasse, C., Carey, S., Sigurdsson, H., 1998. Volcanogenic sedimentation in the Iceland Basin: influence of subaerial and subglacial eruptions. Journal of Volcanology and Geothermal Research 83, 47-73.

Larsen, Guðrún, 2010. Katla: tephrochronology and eruption history. In: Schomacker, A., Krüger, J., Kjær, K.H. (Eds.), The Mýrdalsjökull Ice Cap, Iceland: Glacial Processes, Sediments and Landforms on an Active Volcano. Elsevier, Amsterdam, pp. 23-49.

Larsen, D.J., Miller, G.H., Geirsdóttir, A., Thordarson, T., 2011. A 3000-year varved record of glacier activity and climate change from the proglacial lake Hvítárvatn, Iceland. Quaternary Science Reviews 30, 2715-2731.

Licciardi, J.M., Denoncourt, C.L., Finkel, R.C., 2008. Cosmogenic ^{36}Cl production rates from Ca spallation in Iceland. Earth and Planetary Science Letters 267, 365-377.

Liu, W., Lai, Z., Hu, K., Ge, Y., Cui, P., Zhang, X., Liu, F., 2015. Age and extent of a giant glacial-dammed lake at Yarlung Tsangpo gorge in the Tibetan Plateau. Geomorphology 246, 370-376.

Magilligan, F.J., Gomez, B., Mertes, L.A.K., Smith, L.C., Smith, N.D., Finnegan, D., Garvin, J.B., 2002. Geomorphic effectiveness, sandur development, and the pattern of landscape response during jökulhlaups: Skeiðarársandur, southeastern Iceland. Geomorphology 44, 95-113.

Maizels, J., 1997. Jökulhlaup deposits in proglacial areas. Quaternary Science Reviews 16, 793-819.

Malin, M.C., Eppler, D.B., 1981. Catastrophic floods of the Jökulsá á Fjöllum, Iceland. Reports of Planetary Geology Program—1981, NASA Technical Memorandum 84211. Government Printing Office, Washington, D.C., pp. 272-273.

Maria, A., Carey, S., Sigurdsson, H., Kincaid, C., Helgadóttir, G., 2000. Source and dispersal of jökulhlaup sediments discharged to the sea following the 1996 Vatnajökull eruption. Geological Society of America Bulletin 112(10), 1507-1521.

Marren, P.M., 2002. Criteria for distinguishing high magnitude flood events in the proglacial fluvial sedimentary record. In: Snorasson, A., Finnsdóttir, H.P., Moss, M., The Extremes of the Extremes: Extraordinary Floods. Proc. of a Symp., Reykjavik. IAHS Publication 271, Wallingford, Oxfordshire, UK, pp. 237-241.

Marren, P.M., Schuh, M., 2009. Criteria for identifying jökulhlaup deposits in the sedimentary record. In: Burr, D.M., Carling, P.A., and Baker, V.R. (Eds.), Megaflooding on Earth and Mars. Cambridge University Press, Cambridge, pp. 225-242.

Marren, P.M., Russell, A.J., Rushmer, E.L., 2009. Sedimentology of a sandur formed by multiple jökulhlaups, Kverkfjöll, Iceland. Sedimentary Geology 213, 77-88.

Mikhail, A., 2015. Ottoman Iceland: a climate history. Environmental History 20, 262-284.

Montgomery, D.R., Hallet, B., Yuping, L., Finnegan, N., Anders, A., Gillespie, A., Greenberg, H.M., 2004. Evidence for Holocene megafloods down the Tsangpo River gorge, southeastern Tibet. Quaternary Research 62, 201-207.

Montgomery, D.R., 2012. Dirt: The Erosion of Civilizations. University of California Press, Berkeley, CA. (285 pp.).

Norðdahl, H., Pétursson, H.G., 2005. Relative sea-level changes in Iceland: new aspects of the Weichselian deglaciation of Iceland. In: Caseldine, C., Russell, A., Harðardöttir, J., Knudsen, Ó. (Eds.), Iceland—Modern Processes and Past Environments. Elsevier, Amsterdam, pp. 153-203.

Normark, W.R., Reid, J.A., 2003. Extensive deposits on the Pacific Plate from Late Pleistocene North American glacial lake outbursts. Journal of Geology 111(6), 617-637.

O'Connor, J.E., 1993. Hydrology, hydraulics, and geomorphology of the Bonneville Flood. Special Paper 274. Geological Society of America, Boulder, CO. (83 pp.).

O'Connor, J.E., Grant, G.E., Costa, J.E., 2002. The geology and geography of floods. In: House, P.K., Webb, R.H., Baker, V.R., Levish, D.R. (Eds.), Ancient Floods, Modern Hazards: Principles and Applications of Paleoflood Hydrology. Water Science and Application 5. American Geophysical Union, Washington, DC, pp. 359-385.

Pagli, C., Sigmundsson, F., Lund, B., Sturkell, E., Geirsson, H., Einarsson, P., Árnadóttir, T., Hreinsdóttir, S., 2007. Glacio-isostatic deformation around the Vatnajökull ice cap, Iceland, induced by recent climate warming: GPS observations and finite element modeling. Journal of Geophysical Research 112, B08405.

Pardee, J.T., 1942. Unusual currents in glacial Lake Missoula, Montana. In: Baker, V.R. (Ed.), 1981, Catastrophic Flooding: The Origin of the Channeled Scabland. Dowden, Hutchinson & Ross, Inc., Stroudsburg, PA, pp. 169-181.

Preusser, H., 1976. The Landscapes of Iceland: Types and Regions. Doctoral Thesis. Dr. W. Junk b.v., The Hague, Netherlands. (363 pp.).

Rayburn, J.A., Cronin, T.M., Franzi, D.A., Knuepfer, P.L.K., Willard, D.A., 2011. Timing and duration of North American glacial lake discharges and the Younger Dryas climate reversal. Quaternary Research 75, 541-551.

Richardson, K., Carling, P.A., 2005. A Typology of sculpted forms in open bedrock channels. Special Paper 392. Geological Society of America, Boulder, CO. (108 pp.).

Riel, B., Milillo, P., Simons, M., Lundgren, P., Kanamori, H., Samsonov, S., 2015. The collapse of Bárðarbunga caldera, Iceland. Geophysical Journal International 202, 446-453.

Robinson, Z.P., Fairchild, I.J., Russell, A.J., 2008. Hydrogeologic implications of glacial landscape evolution at Skeiðarársandur, SE Iceland. Geomorphology 97, 218-236.

Rudoy, A.N., 2002. Glacier-dammed lakes and geological work of glacial superfloods in the Late Pleistocene, Southern Siberia, Altai Mountains. Quaternary International 87, 119-140.

Runólfsson, S., 1987. Land reclamation in Iceland. Arctic and Alpine Research 19(4), 514-517.

Russell, A.J., Knudsen, Ó. 2002. The effects of glacier-outburst flood flow dynamics on ice-contact deposits: November 1996 jökulhlaup, Skeiðarársandur, Iceland. In: Martini, I.P., Baker, V.R., Garzón, G. (Eds.), Flood and Megaflood Processes and Deposits: Recent and Ancient Examples. Special Publications of the International Association of Sedimentologists. Blackwell Science, Oxford, pp. 67-83.

Russell, A.J., Fay, H., Marren, P.M., Tweed, F.S., Knudsen, Ó., 2005. Icelandic jökulhlaup impacts. In: Caseldine, C., Russell, A., Harðardöttir, J., Knudsen, Ó. (Eds.), Iceland—Modern Processes and Past Environments. Elsevier, Amsterdam, pp. 153-203.

Russell, A.J., Roberts, M.J., Fay, H., Marren, P.M., Cassidy, N.J., Tweed, F.S., Harris, T., 2006. Icelandic jökulhlaup impacts: implications for ice-sheet hydrology, sediment transfer and geomorphology. Geomorphology 75, 33-64.

Sagan, C., 1980. Cosmos. Carl Sagan Productions, Inc., Ballantine Books Trade Paperbacks, New York. (396 pp.).

Schomacker, A., 2010. Expansion of ice-marginal lakes at the Vatnajökull ice cap, Iceland, from 1999 to 2009. Geomorphology 119, 232-236.

Sigmundsson, F., 1991. Post-glacial rebound and asthenosphere viscosity in Iceland. Geophysical Research Letters 18(6), 1131-1134.

Sigmundsson, F., 2006. Iceland Geodynamics: Crustal Deformation and Divergent Plate Tectonics. Springer-Praxis Publishing Ltd, Chichester, UK. (209 pp.).

Sigurdsson, H., Jóhannesson, H., Larsen, G., 1995. Iceland Geology: a Field Guide. Geological Society of America and Volcano Tours 1995 Excursion. (39 pp.).

Sjöberg, L.E., Pan, M., Erlingsson, S., Asenjo, E., Arnason, K., 2004. Land uplift near Vatnajökull, Iceland, as observed by GPS in 1992, 1996 and 1999. Geophysical Journal International 159, 943-948.

Striberger, J., Björck, S., Ingólfsson, O., Kjær, K.H., Snowball, I., Uvo, C.B., 2011. Climate variability and glacial processes in eastern Iceland during the past 700 years based on varved lake sediments. Boreas 40, 28-45.

Sturkell, E., Einarsson, P., Sigmundsson, F., Geirsson, H., Ólafsson, H., Pedersen, R., de Zeeuw-van Dalfsen, E., Linde, A.T., Sacks, S.I., Stefánsson, R., 2006. Volcano geodesy and magma

dynamics in Iceland. Journal of Volcanology and Geothermal Research 150, 14-34.

Sveinsson, R., 1953. A Memorandum on Soil Erosion and Reclamation: Problems in Iceland. Chief State Soil Conservation Service, Gunnarsholt, Iceland. (60 pp.).

Teller, J.T., Clayton, L., 1983. An introduction to glacial Lake Agassiz. In: Teller, J.T., Clayton, L. (Eds.), Glacial Lake Agassiz. Special Paper 26. Geological Association of Canada, St. John's, Newfoundland, Canada, pp. 3-5.

Thoma, M., Wolf, D., Neumeyer, J., 2001. Inverting land uplift near Vatnajökull, Iceland, in terms of lithosphere thickness and viscosity stratification. In: Sideris, M.G. (Ed.), Gravity, Geoid, and Geodynamics 2000. International Association of Geodesy Symposia 123. Springer, Berlin, pp. 97-102.

Þórðarson, Þ., 2005. Environmental and climatic effects from atmospheric SO_2 mass-loading by Icelandic flood lava eruptions. In: Caseldine, C., Russell, A., Harðardöttir, J., Knudsen, Ó. (Eds.), Iceland—Modern Processes and Past Environments. Elsevier, Amsterdam, pp. 205-219.

Thordarson, T., Larsen, G., 2007. Volcanism in Iceland in historical time: Volcano types, eruption styles and eruptive history. Journal of Geodynamics 43, 118-152.

Thordarson, T., Höskuldsson, Á., 2008. Postglacial volcanism in Iceland. Jökull 58, 197-228.

Tómasson, H., 2002. Catastrophic floods in Iceland. In: Snorasson, A., Finnsdóttir, H.P., Moss, M., The Extremes of the Extremes: Extraordinary Floods. Proc. of a Symp., Reykjavik, IAHS Publication 271, Wallingford, Oxfordshire, UK, pp. 121-126.

Turcotte, D.L., Schubert, G., 2002. Geodynamics, 2nd ed. Cambridge University Press, New York. (456 pp.).

Tweed, F.S., Russell, A.J., 1999. Controls on the formation and sudden drainage of glacier-impounded lakes: implications for jökulhlaup characteristics. Physical Geography 23(1), 79-110.

Waitt, R.B., 2002. Great Holocene floods along Jökulsá á Fjöllum, north Iceland. In: Martini, I.P., Baker, V.R., Garzón, G. (Eds.), Flood and Megaflood Processes and Deposits: Recent and Ancient Examples. Special Publications of the International Association of Sedimentologists. Blackwell Science, Oxford, pp. 37-51.

Ward, A.D., Trimble, S.W., 2004. Environmental Hydrology, 2nd ed. CRC Press, Boca Raton, FL. (475 pp.).

Wiegandt, E., Lugon, R., 2008. Challenges of living with glaciers in the Swiss Alps, past and

present. In: Orlove, B., Wiegandt, E., Luckman, B.H. (Eds.), Darkening Peaks: Glacier Retreat, Science, and Society. University of California Press, Berkeley, CA, pp. 33-48.

Willems, B.A., Powell, R.D., Cowan, E.A., Jaeger, J.M., 2011. Glacial outburst flood sediments within Disenchantment Bay, Alaska: Implications of recognizing marine jökulhlaup deposits in the stratigraphic record. Marine Geology 284, 1-12.

Wohl, E., 1998. Bedrock channel morphology in relation to erosional processes. In: Tinkler, K.J., Wohl, E.E. (Eds.), Rivers Over Rock: Fluvial Processes in Bedrock Channels. American Geophysical Union, Washington, D.C., pp. 133-151.